OUTPUT-ONLY SYSTEM IDENTIFICATION USING BLIND SOURCE SEPARATION

Ph.D. THESIS

by

SMITA KALONI

DEPARTMENT OF EARTHQUAKE ENGINEERING
INDIAN INSTITUTE OF TECHNOLOGY ROORKEE
ROORKEE - 247 667 (INDIA)
JULY, 2018

OUTPUT-ONLY SYSTEM IDENTIFICATION USING BLIND SOURCE SEPARATION

A THESIS

Submitted in partial fulfilment of the requirements for the award of the degree

of

DOCTOR OF PHILOSOPHY

in

EARTHQUAKE ENGINEERING

by

SMITA KALONI

DEPARTMENT OF EARTHQUAKE ENGINEERING
INDIAN INSTITUTE OF TECHNOLOGY ROORKEE
ROORKEE - 247 667 (INDIA)
JULY, 2018

INDIAN INSTITUTE OF TECHNOLOGY ROORKEE
ROORKEE

CANDIDATE'S DECLARATION

I hereby certify that the work which is being presented in the thesis entitled **"OUTPUT-ONLY SYSTEM IDENTIFICATION USING BLIND SOURCE SEPARATION"** in partial fulfilment of the requirements for the award of the Degree of Doctor of Philosophy and submitted in the Department of Earthquake Engineering of the Indian Institute of Technology Roorkee, Roorkee is an authentic record of my own work carried out during a period from July, 2014 to July, 2018 under the supervision of Dr. Manish Shrikhande, Professor, Department of Earthquake Engineering, Indian Institute of Technology Roorkee, Roorkee.

The matter presented in this thesis has not been submitted by me for the award of any other degree of this or any other Institute.

(SMITA KALONI)

This is to certify that the above statement made by the candidate is correct to the best of my knowledge.

Date: July, 2018 **(Manish Shrikhande)**
Supervisor

The Ph.D. Viva-Voce Examination of Ms. Smita Kaloni, Research Scholar, has been held on .....

Chairman, SRC **Signature of External Examiner**

This is to certify that the student has made all corrections in the thesis.

Signature of Supervisor **Head of the Department**

Date

Abstract

The increasing complexity of engineering structures has raised the requirement of continuous monitoring for their proper functioning. Structural health monitoring needs reliable response measurements, robust system identification algorithm for its analysis to assess the state of the structure. The process involves postulation of a model for the structural system followed by the estimation of the model parameters based on the analysis of output and/or input data. With advancement in communication technology and affordable computing, the vibration-based system identification techniques have been receiving attention to this end. Earlier approaches to structural system identification were based on minimization of the prediction error of the response of identified model. Direct estimation of the system parameters in physical space (namely, stiffness, mass and damping) has also been studied within prediction error minimization framework, or within Bayesian framework. Other methods for system identification in modal space based on the estimation of frequency response functions in frequency domain, or impulse response functions in time domain have also been developed. Various single input single output, single input multi output, multi input multi output based modal identification techniques have been developed in the past. However in come cases the input excitation are not known or difficult to measure, (e.g. ambient vibration excitation) output only system identification are used where only response measurements are available for estimation of system parameters.

We focus on output-only modal identification in this work. Random decrement (RD) technique, natural excitation technique (NExT), stochastic subspace identification (SSI) and frequency domain decomposition (FDD) are some of the most commonly used output-only modal identification procedures. The random decrement, natural excitation and stochastic subspace identification techniques are not suitable for identification of base excitation problems where all response measurements include a component of base motion. Frequency domain decomposition often leads to several spurious modes which are often very difficult to distinguish from true structural modes. Recently, blind source separation (BSS) procedures based on certain statistical properties of signals have been used for modal identification.

The objective of BSS procedure is to extract the source components or modal responses from the measured data for further estimation of modal parameters such as natural frequencies, modal damping and mode shapes. Statistical BSS procedures like independent component analysis (ICA), second order blind identification (SOBI), complexity pursuit (CP) and their derivatives involve identification of modal responses within a scaling factor. Because of this scaling of modal response, the estimation of mode shapes is a complex affair in these procedures. Moreover, these procedures are sensitive to the algorithmic parameters as well as the assumptions about the statistical properties of the signals considered for source separation are not always valid.

Motivated with the limitations of statistical-BSS based procedure, a non-statistical time-frequency based synchrosqueezed transform (SST) procedure for BSS is proposed in this study. It is shown that using acceleration measurements there is a greater chance of identifying higher modes than with displacement/velocity measurements. The decomposition of recorded response time histories in the time-frequency plane improves the quality of identification and allows extraction of modal components (sources) in true strength/intensity to the extent of their contribution in making up the total response. This allows for developing a simple procedure for estimation of mode shapes and modal damping, which avoids tedious computations required for other formulations. The mode shapes are estimated from the ratios of the extracted harmonic components from the response measured at different floors. A simplified procedure of estimation of modal damping is proposed. Due to decaying ground motion amplitudes towards the end of an event, the tail portions of the recorded response primarily comprise of free vibration response and a simple curve fitting of an exponentially decaying envelope to the tail portion of extracted modal source provides the estimate of modal damping. For validating the performance of proposed modal identification several example (for different building model and different earthquake excitation) cases have been considered.

This study, focusses on modal identification and tracking changes thereof as damage indicator. In vibration based damage identification techniques a prior knowledge of modal parameters is required, to serve as a benchmark for comparison. Often, the lack of availability of this type of data can make a method impractical for certain applications. To address this issue a moving time window based damage identification procedure is proposed. Modal identification is performed in a number of non-overlapping time intervals by using synchrosqueezed transform based blind identification scheme. The time windows are selected based on the energy distribution of the signal in the time-frequency plane. As the

window moves forward, the changes in modal parameters of the structure are tracked to detect changes in the state of structure. The change in flexibility of the structure is tracked by using a rank-1 update reduced rank approximation. Numerical simulation studies are presented on UCLA Factor Building for different earthquake events to demonstrate the validity of the proposed method.

Acknowledgements

To begin with, I would like to express my sincere thanks and gratitude to my supervisor, Prof. Manish Shrikhande, for his inspirational guidance and support. He has been a wonderful mentor and has provided me with the right attitude and impetus, needed to complete this dissertation in time.

I would also like to pay my heartiest gratitude to Prof. Yogendra Singh, Prof. Pankaj Agarwal, Prof. B. K. Mishra, and Prof. A. K. Mathur for their valuable suggestions and encouragement during various stages of this work.

Support provided by the faculty and the staff of Earthquake Engineering Department during the period of four years is greatly acknowledged.

I am thankful to the authority of NIT Uttarakhand for granting me great opportunity for pursuing Ph.D. from such an esteemed institute. I am also thankful to my colleagues at the Department Civil Engineering, NIT Uttrakhand for their constant support during this period.

I would like to thank my friends Shweta Bajaj, Chhavi, Neha Kumari, Jyoti Shukla, Ankita Bisht, Khyati Tamta, Deepti Ranjan Majhi, and Gautham Reddy for their wonderful company during my stay at IIT Roorkee.

No words are adequate to express my gratitude towards my parents Mrs. Pushpa Kaloni and Mr. K. N. Kaloni. Special thanks is reserved for my mother who has given me immense strength and moral support to pursue my dreams and aspirations. I would like to dedicate this work to her.

I am also thankful to my siblings Manoj, Vineeta, and Nidhi for their consistent support and encouragement.

I am grateful to my parents-in-law Mrs. Mithilesh Tiwari and Mr. M. N. Tiwari for their emotional support and encouragement. I am also thankful to my brother-in-law Vimalendu for his emotional support.

Last but not the least, I would like to thank my husband Satyendu for his wonderful companionship. He has always been the source of motivation and without his unwavering emotional support, this work would have never been crystallized.

Smita Kaloni

Contents

List of Figures

List of Tables

Chapter 1

Introduction

1.1 System Identification

The complexity of civil engineering structures is increasing on account of the technological advancements, evolution of new materials, functional requirements and contemporary architectural trends. Several challenging projects have been executed in India (for example, The 42 (268 m), One Avighna Park (266 m), Kalisindh Thermal Power Station Cooling tower (202 m)), and beyond (Burj Khalifa (828 m), Shanghai Tower(632 m), Taipei 101 (508 m)). Maintenance of such complex systems is a major challenge and an early detection of damage/deterioration in any structural element is crucial for a satisfactory performance of the system. Vibration based system identification holds a lot of potential for a structural health monitoring system to alert the maintenance team.

The response of structures under dynamic excitation depends on its dynamic characteristics, namely, natural frequencies, mode shapes, and damping. These dynamic (or modal) characteristics are in turn governed by the physical properties such as mass/inertia, stiffness and energy dissipation. System identification is an inverse problem to ascertain the structural (physical or, modal) parameters from the analysis of the system response (output) along with (or, without) the information about the excitation (input). Results of system identification study can be used for different purposes, such as, validation and/or calibration of an analytical/finite element model, condition assessment and to detect possible damages following extreme loading events (wind storms, earthquakes, etc.). Earlier approaches to structural system identification were based on minimization of the prediction error of the response of identified model. Direct estimation of the system parameters in physical space (namely, stiffness, mass and damping) has also been studied within prediction error minimization framework, or within Bayesian framework. Other methods for system

identification in modal space based on the estimation of frequency response functions in frequency domain, or impulse response functions in time domain have also been developed. An extensive overview of these procedure are presented in [70, 71, 51, 3, 81, 58, 7, 78, 5]. Often it is not possible to measure the input excitation and one has to work only with the response/output data. Several output only identification techniques have been developed in the past operating either in time or frequency domains. Some of the commonly used time domain procedures are random decrement technique (RD) [50], natural excitation technique (NExT) [52], eigensystem realization algorithm (ERA) [53], stochastic subspace identification (SSI) [108]. The most popular frequency domain procedure is frequency domain decomposition (FDD) [15]. A few wavelet-based techniques [103, 65, 118] have been proposed for refining the input data for use in the aforementioned techniques. Non-uniqueness of the identified system model is a problem with most of these procedures. Typically, one begins with the identification of a sufficiently higher order model and monitor the stability of the identified parameters as the order of assumed model is gradually reduced. The quality of the identification results is generally poor for nonstationary signals. A wavelet-based Hilbert-Huang transform (HHT) technique has also been used in modal identification for nonstationary signals [113, 114]. Intrinsic mode functions (IMF) have been extracted by using HHT from the measured response data by an iterative empirical mode decomposition (EMD) procedure [44]. However, the iterative empirical mode decomposition process does not guarantee extraction of modal response and the process is also vulnerable to numerical instabilities, particularly for higher modes.

Recently, statistical signal processing framework like proper orthogonal decomposition (POD) [57], and blind source separation (BSS) [42, 23, 8] has been used in structural dynamics. Proper orthogonal decomposition is a data compression technique to reduce the number of independent components while preserving variance as much as possible. Further, the derived orthogonal components may not correspond to modal responses as the process does not involve any constraint from the dynamics of structure. Contrary to this BSS has been used as a promising tool for output-only modal identification in last decade [119, 58, 85, 120, 37, 38, 39, 92, 91]. Unlike other output-only modal identification methods, the BSS-based procedures do not require any prior assumption about the model order. The blind source separation involves separation of a set of independent signals from their mixture without any prior information about the mixing process. The separation of independent sources from the observed mixtures is achieved by optimizing some statistical measure of the underlying process with techniques like independent component analysis

(ICA) [23, 46], second-order blind identification (SOBI) [8] and complexity pursuit (CP) [116]. There are a few challenges in putting these blind source separation techniques to use. First, these procedures are based on certain idealizations about the statistical properties of the signals which may not always hold for all types of signals; second, the results are often found sensitive to the choice of algorithmic parameters; and third, the independent source components are identified only within a scaling factor of true sources, *i.e.*, if $s_i(t)$ is a source then the BSS process will extract a proportional source $\alpha_i s_i(t)$.

One of the most significant applications of system identification in structural engineering is the health monitoring and damage detection. Worldwide the efforts are directed towards development of an automated structural health monitoring system for issuing timely alerts for maintenance. We propose a new blind source separation scheme in a non-statistical framework by using the wavelet-based synchrosqueezed transform (SST) [27, 11, 106] for modal identification. The primary objective is to minimize the subjectivity in the data processing for structural system identification and health monitoring.

1.2 Damage Detection

The structural systems are evolving into increasingly more complex forms with various types of claddings obstructing the physical access for regular inspection and maintenance. With increasing size and scale of structural systems coupled with difficulty in accessing structural members, the conventional methods of visual inspection and the use of various non-destructive techniques are impractical. A need is therefore felt for a quick and automated screening system to monitor the health of structural system. Some damage identification procedures have evolved over time where structural characteristics are inferred from analysing its vibration response data and are known as vibration-based system identification techniques.

Damage in a structure manifests as deterioration and degradation of strength and/or permanent deformations following inelastic excursions. Inelastic deformations lead to reduction in the secant stiffness of the structure and this stiffness degradation can be tracked as an indicator of the damage. In this study, the stiffness degradation following damage is used as an indicator of the damage. Any changes in the system stiffness imprints the changes in modal properties, namely, natural frequencies, mode shapes and modal damping. Therefore damage in a structural system is identified by tracking changes in either the stiffness, or modal parameters of the system. In 1993 Rytter [90] divided the damage

identification methodology into four levels detection, localization, quantification and prognosis. The scope of the study is limited to damage detection. Several damage identification techniques have been proposed in the past. The classification is mainly based on the type of recorded data used, and/or the processing used to identify the damage. Some of the commonly used vibration based procedures are based on measure of shift in natural frequencies [94], changes in mode shapes [110] and mode shape curvature [80], change in strain energy [31] and changes in flexibility matrix [79]. Apart from these, model updating procedures are also sometimes used for damage identification [122, 69, 97]. One of the main challenges in vibration-based damage detection procedures is the need of a reference set of information corresponding to the undamaged state of the structure against which the identified parameters are compared to detect any deviations. Many a times availability of a detailed finite element model of the healthy structure, or some data set(s) from the undamaged structure is presumed. Often, the lack of availability of this type of data renders the entire exercise impractical [32]. There is, therefore, a need for developing processes where only vibration data from a single event/experiment is adequate for the purpose of damage detection. We address this issue by studying the evolution of identified modal parameters in different time windows of a vibration record.

1.3 Aims and Objectives

The present study is aimed at developing a vibration-based modal identification procedure which can be used with relatively smaller stretches of data to facilitate moving window analysis of the identified modal parameters for the purpose of damage detection. The main objectives of the current undertaking are as follows:

- To formulate the problem of modal identification of earthquake excited systems by using blind source separation process;
- To develop a non-iterative and robust scheme for identifying independent modal sources. We make use of wavelet based synchrosqueezed transform for this purpose;
- To extract information about modal damping from the separated modal components from the response of earthquake excited systems; and
- To develop a moving time window based damage detection scheme.

1.4 Organization of Thesis

The present thesis is organized in six chapters as follows:

Chapter 1 introduces the problem statement and outlines the broad contours of the objectives of the study.

Chapter 2 presents a contextual framework for the problem statement with a background discussion on the system/modal identification techniques with particular emphasis on blind source separation (BSS) methods.

Chapter 3 introduces the concept of synchrosqueezed transform (SST), followed by the development of a new synchrosqueezed transform based modal identification method for earthquake excited systems.

Chapter 4 presents a validation exercise for the SST based modal identification scheme. A numerical study is carried out on three degree of freedom system, followed by an experimental and numerical case study on UCLA Factor building.

Chapter 5 deals with the problem of damage detection using the SST based modal identification. A case study of UCLA factor building is considered. The damage identification is carried out in moving time windows.

Chapter 6 summarizes the developements and findings of this study and recommendations for possible extensions.

Chapter 2

Literature Review

2.1 System Identification

System identification is the process of modelling the underlying physical system based on the analysis of a set of input-output or only output data. Initially, the concept of system identification was used in the context of control systems engineering and later developed as a diagnostic tool for condition monitoring of equipment and machinery. With the developments in sensor, computing and storage technologies, its potential for preventive maintenance of large scale structural systems was recognized by the structural engineering community and the field of structural health monitoring has been under constant evolution for the last few decades. The motivation for the use of system identification in structural engineering comes from two basic needs. First, to have reliable information of the structure as constructed and its dynamic properties for improving the predictive capabilities of the analytical models. Second, to monitor the health of the structure in view of age related degradation, or following adverse environmental loading [64].

For civil engineering structures, system identification refers to either identification of physical parameters (mass, damping, and stiffness), or the parameters in modal space, namely, natural frequencies, mode shapes and modal damping. The modal identification is a relatively more stable process than the identification of physical parameters which often poses problems of ill-conditioning and non-uniqueness. Since the modal parameters are governed by the physical parameters of the structural system, those can be used for structural health monitoring, damage detection, and modal updating purposes [71, 29]. For specified physical properties like mass, stiffness, and damping the modal parameters are defined by the generalized eigenvalue problem of free vibration. Considering the undamped

free vibration problem given by Eq. (2.1):

$$\mathbf{M}\ddot{\mathbf{x}}(t) + \mathbf{K}\mathbf{x}(t) = \mathbf{0} \tag{2.1}$$

where, $\mathbf{M}$ and $\mathbf{K}$ respectively represent the mass and stiffness matrices, and $\ddot{\mathbf{x}}$ and $\mathbf{x}$ denote the acceleration and displacement response. The normal modes can be determined by exploring the possibility of existence of synchronous simple harmonic motion as a solution which leads to the generalized eigenvalue problem defined by Eq. (2.2):

$$(\mathbf{K} - \lambda\mathbf{M})\boldsymbol{\phi} = \mathbf{0} \tag{2.2}$$

where, λ represents the eigenvalue, square of the natural frequency and $\boldsymbol{\phi}$ represents the associated eigenvector, or the mode shape vector. There exist n such eigenpairs for an n degree of freedom system. The free vibration of damped system is given by Eq. (2.3)

$$\mathbf{M}\ddot{\mathbf{x}}(t) + \mathbf{C}\dot{\mathbf{x}}(t) + \mathbf{K}\mathbf{x}(t) = \mathbf{0} \tag{2.3}$$

and the associated eigenvalue problem is given by:

$$\left(\lambda^2\mathbf{M} + \lambda\mathbf{C} + \mathbf{K}\right)\phi = \mathbf{0} \tag{2.4}$$

where, $\mathbf{C}$ is the damping matrix, λ represents the eigenvalue and $\boldsymbol{\phi}$ is the associated eigenvector of the quadratic eigenvalue problem (QEP) [100]. The solution of quadratic eigenvalue problem is much more demanding in comparison to the linear eigenvalue problem of undamped systems as defined by Eq. (2.2). Usually for the small/moderate inherent damping in the structural system, the classical damping model suffices and the normal modes of the undamped system can be used to decouple the system of equations in mode superposition analysis. We assume the classical damping model in this study. The forced vibration of a damped system is described by Eq. (2.5):

$$\mathbf{M}\ddot{\mathbf{x}}(t) + \mathbf{C}\dot{\mathbf{x}}(t) + \mathbf{K}\mathbf{x}(t) = \mathbf{f}(t) \tag{2.5}$$

where, $\mathbf{f}(t)$ is the external excitation. The dynamic response of the system is determined by the solution of governing equation of motion, either in time domain or in frequency domain (for linear systems). Typically, the mode superposition is employed in the case of linear system behaviour for economic computations. The reliability of the results obviously depend on how faithful the model parameters are to the physical system. Since it is difficult to independently verify the physical parameters of the analytical model, namely, inertia, damping and stiffness properties, the dynamic properties in modal space are determined from experimental observations. The physical parameters are calibrated against these observations to improve the fidelity of the analytical model as a predictive tool. The experimental modal analysis (EMA) is therefore a crucial link in the process of model verification.

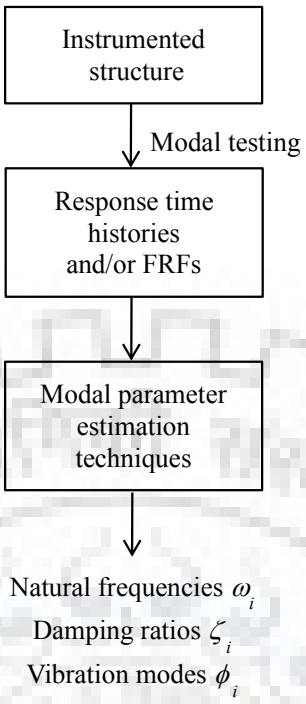

Fig. 2.1. Experimental modal analysis procedure

2.2 Experimental Modal Analysis

The experimental modal analysis is aimed at determining the modal parameters of the structure subjected to a monitored excitation [30]. Both dynamic responses and input excitations are used for identification of modal parameters. The EMA procedure comprises of two steps (i) the testing of the structure to obtain the required raw data (input excitation and response), (ii) the analysis of data to estimate the modal parameters of the structural system. Sometimes an additional step of sanity check is required to weed out the spurious information. The scheme of experimental modal analysis is shown in Fig. 2.1.

2.2.1 Structural Testing

A lot of careful planning is required for setting up the test for experimental modal analysis [105]. The structural testing comprises three stages, namely, the excitation, sensing, and the data acquisition and data processing. The system response characteristics are governed by the excitation characteristics, and therefore, the choice of the excitation is of vital importance in the experimental modal analysis. The impact hammer, or shaker/vibration generator is usually used for forced vibration testing else, the structural response is recorded for the ambient environmental and operating loads on the structure. The impact hammer procedure is simple, but the magnitude and distribution of excitation energy is quite limited

and is not sufficient to excite large structures and hence, its application is limited only to the small, lightly damped systems. For large structures, vibration generators or shakers are used. A shaker allows the application of a variety of input excitation within a frequency range such as a constant harmonic, sine sweep, random waveform, etc. In some situations the input excitation is unquantifiable such as ambient/environmental disturbance, wind loads, traffic-induced vibrations, etc. and the modal parameters are estimated using only the output response data. Such procedures are called as output-only system identification or operation modal analysis (OMA).

Apart from the excitation, the other critical components of structural testing are sensors—type and their placements, signal conditioning and data acquisition. The choice of sensor depends on response quantity to be measured, operating frequency and amplitude ranges, resolution, and triggering system. The signal conditioning and data acquisition needs to account for the accurate analog to digital conversion, anti-aliasing filter, synchronization across different data channels, background recording noise, etc. The effective utilization of the recorded response data also depends on the number and placement of sensors in the structure. Some guidelines have been recommended in the past in this regard [55, 25, 98, 41]. The sanitized data is then processed for identifying system parameters — either in physical space, or in modal space. We consider modal identification in this study on account of its robustness.

2.2.2 Modal Parameter Estimation

The modal system identification was initially developed as a tool for validating analytical models in aerospace engineering and for condition monitoring of machines. The ideas were subsequently applied to civil engineering systems for model validation and health monitoring with easy availability of computing power and networked storage for large data. Over the years, several algorithms and procedures have evolved for the experimental determination of modal properties with specific objectives and/or constraints. The user needs to first examine the suitability of a particular procedure for the application at hand before planning the instrumentation and tests. The EMA procedures are formulated either in time domain, or in frequency domain. Although frequency domain methods are more intuitively appealing, time domain methods are generally preferred owing to better resolution and fidelity. Other classification is based on the basis of availability (or, non-availability) of a specified model structure for parametric (or, non-parametric) identification of modal properties. Non-parametric methods lead directly to the modal properties and are referred to

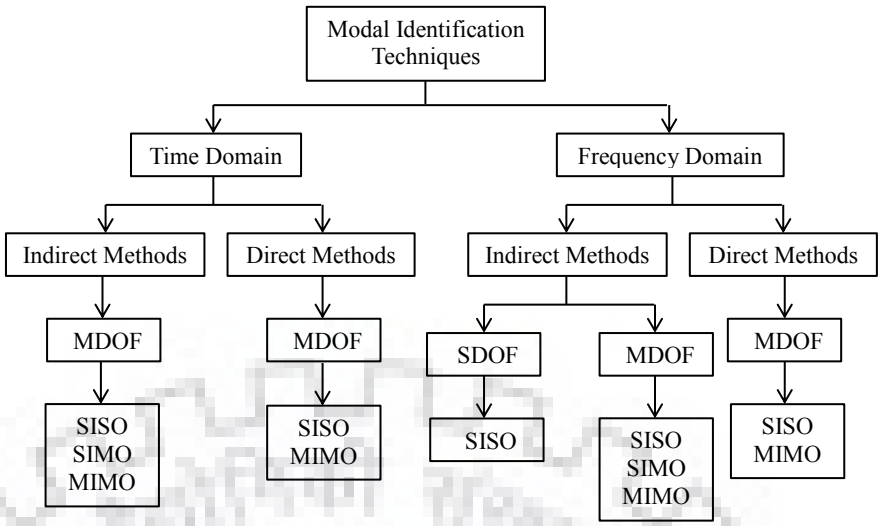

Fig. 2.2. Classification of experimental modal identification techniques

as the direct methods, while the parametric methods identify the structure of a time series model and the properties in modal space are derived therefrom and therefore are classified as indirect modal identification methods. Another classification of the EMA procedures is based on the excitation and measurement type, namely, single input-single output (SISO), single input-multiple output (SIMO), and multiple input-multiple output (MIMO). The classification of experimental modal identification procedures is summarised in Fig. 2.2. Some important time domain EMA procedures are complex exponential algorithm (CE) for single input single output (SISO) systems [102], least square complex exponential (LSCE) algorithm for single input multiple output SIMO systems [16], Ibrahim time domain (ITD) for SIMO systems [48], poly-reference complex exponential (PRCE) [109], and eigensystem realization algorithm [53] for MIMO systems. Maia provides a comprehensive review of experiment modal identification procedures [71]. All of the modal identification procedures mentioned above are based on the analyses of a set of measured input and output data. However, in some cases it is difficult to measure the input excitation like the wind-induced vibrations in high rise buildings, traffic-induced vibrations of bridges, etc., output only identification techniques are used. We discuss these output-only procedures in some detail.

2.3 Output-only System Identification

When the input/excitation can not be measured (or, not known) modal parameters can be identified from the analysis of the system response data only and the process is referred

to as the output-only identification, or the operational modal analysis (OMA). The basic assumption for OMA procedures is that the excitation sources are broadband, uncorrelated and distributed over the entire structure. The output-only identification techniques are classified according to domain of operation, *i.e.*, time or frequency. Apart from these, some procedures are based on the signal characteristics in time-frequency plane.

2.3.1 Time Domain Techniques

The output-only system identification in time domain has received a lot of attention in past because of their potential to achieve fine resolution in spectral representation. Early efforts were based on autoregressive (AR) time series models [70], which were found suitable for civil engineering structure under ambient vibrations for estimation of modal damping. However, these models are very sensitive to choice of window length, sampling rate, and signal to noise ratio [13]. Identification of impulse response function (IRF) (or, free vibration response) from the measured vibration response data provides information about the natural frequency and damping. The random decrement (RD) technique, or the natural excitation technique (NExT) is used for estimating the free vibration response from measured vibration response data. These estimates of impulse response functions are subsequently used as input Markov parameters for other modal identification methods such as Ibrahim time domain, or eigensystem realization algorithm. Stochastic subspace identification is another time domain technique for identifying a state-space model of the system from the analyses of vibration response data.

Random Decrement Technique

Random decrement (RD) a signal processing technique for analysing the dynamic response of structure under ambient excitation [22, 21]. The objective of RD is to identify the free response known as random decrement functions from the recorded vibration response data. The RD technique is based on the on the idea that the random component of the response can be averaged out to estimate the free vibration (or impulse response) of the structural system. The response of any system to random excitation consists of two parts: first, the deterministic part (response to initial displacement and\or velocity), the second random part being the response to random excitation. By considering the average of a number of samples of the same random vibration response, the random part of the response will average out, leaving the deterministic of free vibration part of the response. To avoid averaging out

the free vibration part of the signal, the samples should start from (i) constant level, (ii) positive slope and zero level, and (iii) negative slope and zero level to provide the sample free decay step response, free decay positive impulse response and free decay negative impulse response, respectively. For the measured response $y(t)$ the free vibration decay response may be obtained by averaging the segment of system response time histories as:

$$\hat{h}(\tau) = \frac{1}{N} \sum_{n=1}^{N} y(t_n + \tau) \tag{2.6}$$

where, t_n denotes the first time instant when the response crosses the chosen threshold. The RD technique has been developed in association with time domain modal identification methods, like the Ibrahim time domain method (ITD) [49] or the eigensystem realisation algorithm (ERA) [53] for modal identification.

Natural Excitation Technique

The natural excitation technique (NExT)[52] is an output only system identification technique of structure under ambient excitation. The natural excitation technique is designed for estimation of free vibration response or impulse response from the recorded forced vibration response data. In the case of white noise excitation, the cross-correlation between any two response time histories recorded at different locations are given by linear combination of damped sinusoids and each sinusoid has a damped natural frequency and damping ratio that is equal to one of the corresponding fundamental mode [9]. Based on the similarities in mathematical expression of the response cross-correlation and impulse response function due to input white excitation, cross correlation of the response signals is used as the impulse response function or free decay function in case of NExT procedure. Most commonly the ERA is combined with the Natural Excitation Technique (NExT) to identify modal parameters from ambient vibration measurements.

Stochastic Subspace Identification

The stochastic subspace identification procedure deals with the processing of recorded response data without estimating the impulse response function (Markov parameters). The state matrix is estimated from the measured response data by projecting data into covariance subspace and estimating a minimum order state matrix therefrom. The eigenvalues and eigenvectors are then estimated by solving the standard eigenvalue problem with the estimated state matrix [108, 100].

2.3.2 Frequency Domain Techniques

Earliest frequency domain procedures were based on the peak picking (PP) method. Natural frequencies are obtained from the peaks of Fourier amplitude spectrum, or frequency response function [24, 107]. A more robust technique, namely, frequency domain decomposion, based on the decomposition of power spectra is very commonly used in structural system identification.

Frequency Domain Decomposition

Frequency domain decomposition (FDD) [14, 15] deals with the decomposition of the power spectral density of a multi degree of freedom (MDOF) system as sum of contributions from modal responses by using singular value decomposition (SVD) of power spectral density matrices (PSD). The mode shapes can be extracted from the singular vectors of the decomposition at a frequency which maximizes the corresponding singular value. The spurious modes are detected by keeping track of the modal assurance criterion (MAC) between the identified mode shape and one from a suitable analytical model.

2.4 Techniques Based on Time-Frequency Distribution

Considering that the vibration signals contain useful information in both time and frequency-domains, a joint characterization in the time-frequency plane allows a simultaneous view at both representations. The short time Fourier transform (STFT) and spectrogram, wavelet transform, etc. are the primary tools in joint time-frequency representations [103, 59, 60, 61]. Another time-frequency based approach for modal identification is Hilbert-Huang transform (HHT), wherein the vibration signature is decomposed into a sum of constituent intrinsic mode functions (IMF) through an iterative sifting process followed by applying Hilbert transform on each of these IMFs [44, 112, 113, 114]. All operational modal analysis procedures discussed above pre-suppose the existence of a model structure in some form or the other to which the modal identification from recorded response data is predicated. Most of the time the problem is resolved by assuming a sufficiently higher order model and examining consistency of the identified modal parameters as the model order is reduced gradually. The process is thus vulnerable to producing some spurious modes which are artefacts of numerical process and have little relation to the dynamics of the structure. Out of all these procedures the random decrement, natural excitation and stochastic subspace identification techniques are not suitable for identification of base excitation problems where all response

measurements include a component of base motion. The requirement of information about the model structure is obviated in a model free procedure like blind source separation (BSS) which we discuss next.

2.5 Blind Source Separation

The blind source separation (BSS) is a powerful signal processing tool which involves separation of a set of independent signals (sources) from their mixture. The BSS problem is identical to cocktail party problem, where several speakers are present in a room speaking at the same time, and the available microphones record the mixture of speaker's voices. The objective is to segregate the voices (independent sources) from the recorded mixture. Similarly, in BSS problem individual source components (speakers' voices) are estimated from the observed data (the recorded mixture of voices) without any information of the mixing pattern. The only information available is that the sources are originating from different physical process. The BSS technique has found application in several fields ranging from communications engineering [17], biomedical application [73, 56], differentiating pure tones and sharp-pointed resonance [6], machine condition monitoring [87, 82, 86] to damage detection [119] and modal identification [119, 58, 85, 120, 37, 38, 39, 92, 91, 93].

2.5.1 The BSS Model

The simplest BSS problem is stated as:

$$\mathbf{x}(t) = \mathbf{A}\mathbf{s}(t) \tag{2.7}$$

where, $\mathbf{x}(t)$ is the vector of observed output, $\mathbf{s}(t)$ is the vector of source signals, and $\mathbf{A}$ is the mixing matrix. The BSS model for noisy data is stated as:

$$\mathbf{x}(t) = \mathbf{A}\mathbf{s}(t) + \mathbf{n}(t) \tag{2.8}$$

where, $\mathbf{n}(t)$ represents the measurement noise. The BSS model is illustrated in Fig 2.3. The mixing of sources can be the static (instantaneous mixing) or convolutive mixing. The mixing process is generally considered as static to simplify source separation process. The convolutive mix can be transformed into static mix by a linear transformation, and therefore, we discuss the instantaneous mixing of source components. The separation of sources from the mixture without any idea of the process is achieved by establishing a basic framework based on independence of sources. Since the BSS problem comprises of two unknowns in a

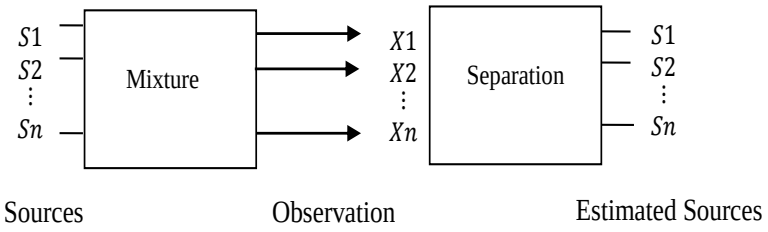

Fig. 2.3. Basic blind source separation framework

product form ($\mathbf{As}(t)$), indeterminacies related to the amplitude and the order of the sources will remain in the results: (i) The effect of scalar α on the source component is balanced by multiplying the column of mixing matrix with $\frac{1}{\alpha}$, thus the variance of the source cannot be determined, and (ii) the permutation of the columns of mixing matrix can be balanced by a permutation of source order. Therefore, the order of sources can not be determined uniquely.

Among various BSS procedures, independent component analysis (ICA) and second-order blind identification (SOBI) have received more attention. The ICA and SOBI procedures are multivariate statistical methods, and unknown variables are entirely based on the statistical relationship between the sources and observed data. The ICA procedure is a higher order statistics technique whereas the SOBI procedure exploits the second order statistics.

2.5.2 Independent Component Analysis

The ICA procedure is considered as an efficient iterative method for separation of sources from the observed data [54]. Apart from statistical independence, another assumption of ICA model is the non-Gaussianity of the source. The ICA is based on the principle of the central limit theorem. Therefore by maximising the non-Gaussianity of the sources, independent components are separated from the observed mixture. Let us consider,

$$\mathbf{y}(t) = \mathbf{W}\mathbf{x}(t) \tag{2.9}$$

where, $\mathbf{W}$ is the inverse of the mixing matrix $\mathbf{A}$. The model can also be expressed as:

$$\mathbf{y}(t) = \mathbf{W}\mathbf{x}(t) = \mathbf{Z}\mathbf{s}(t) \tag{2.10}$$

where, $\mathbf{Z} = \mathbf{W^T A}$. According to central limit theorem $\mathbf{Zs}(t)$ will be more Gaussian than any of the individual sources. Thus by maximising the non-Gaussianity of $\mathbf{Zs}(t)$ or equivalently $\mathbf{Wx}(t)$ the independent source components $\mathbf{s}(t)$ are estimated. The non-Gaussianity of the random variable in ICA procedure is obtained by considering higher order moments,

such as kurtosis or negentropy etc. The independent components can also be estimated by exploiting the mutual information minimisation theory of random variables. Once the independent sources are estimated from observed data, the mixing matrix is estimated. In ICA procedure, the observed data $\mathbf{x}(t)$ are processed by centering to obtain zero mean data followed by the whitening operation to transform the centered data to a new set whose components are uncorrelated and have unit variance.

2.5.3 Second Order Blind Identification

The second popular technique for blind identification is the second order blind identification (SOBI). The SOBI method [8] is based on the second-order statistics (i.e., autocorrelation) and the assumptions that sources are stationary and uncorrelated. The SOBI method involves the orthogonal decomposition of the covariance kernel to extract individual sources and is generally implemented as a three-step process: (i) pre-whitening, which involves the linear transformation of the observed data such that the whitened data are uncorrelated with unit variance, (ii) the orthogonalization, applied to diagonalize the time-lagged covariance matrix $\mathbf{R}_x^w(\tau)$ of whitened data, and (iii) to find a unitary transform for the whitening matrix $\mathbf{W}$, such that $\mathbf{U} = \mathbf{WA}$.

$$\begin{aligned} \mathbf{R}_x^w(\tau) &= \mathbf{W}E[\mathbf{x}(t)\mathbf{x}^T(t+\tau)]\mathbf{W}^H \\ &= \mathbf{WA}\mathcal{E}[\mathbf{s}(t)\mathbf{s}^T(t+\tau)]\mathbf{A}^T\mathbf{W}^T \\ &= \mathbf{U}\mathbf{R}_s(\tau)\mathbf{U}^T \end{aligned} \tag{2.11}$$

where, $E[\cdot]$ denotes the mathematical expectation operator. The unitary transformation diagonalizes the whitened covariance matrix $\mathbf{R}_x^w(\tau)$. The desired unitary matrix can be estimated from the eigenvalue decomposition of the time-lagged whitened covariance matrix. The mixing matrix can be then estimated from the relationship between whitening matrix and the estimated unitary matrix. The independent sources can be subsequently estimated from the measured data and pseudo-inverse of the mixing matrix.

2.6 Modal Identification using Blind Source Separation

The blind source separation has been extensively used for modal identification in recent times on account of its potential for a robust identification technique as it does not require any prior information about the model structure. The process can be implemented within

a framework of generic assumptions about the data. The vibration response, however, is a convolutive mix and the BSS procedure for static mixture is applicable in the modal space, wherein the vibration response is given as the linear combination of modal responses.

2.6.1 Modal Identification

Let us consider an n degree of freedom linear mechanical system defined by Eq. (2.5):

$$\mathbf{M}\ddot{\mathbf{x}}(t) + \mathbf{C}\dot{\mathbf{x}}(t) + \mathbf{K}\mathbf{x}(t) = \mathbf{f}(\mathbf{t}) \tag{2.12}$$

where, $\mathbf{M}, \mathbf{C}$ and $\mathbf{K}$ are the mass, damping and the stiffness matrices, $\mathbf{x}$ denotes the displacement response, $\mathbf{f}$ is the excitation, and a dot indicates time derivative. The dynamic response of the mechanical system in time domain can be defined in terms of impulse response function given as:

$$\mathbf{x}(t) = \mathbf{h}(t) * \mathbf{f}(t) \tag{2.13}$$

where, $\mathbf{h}(t)$ denotes matrix of impulse response functions and $*$ represents the convolution operator. In view of difficulties in handling convolutive mixtures, Kerschen *et* al. proposed the concept of virtual sources based on the modal expansion theorem [58]. Accordingly, the response is defined as:

$$\mathbf{x}(t) = \mathbf{\Phi}\mathbf{q}(t) = \sum_{i=1}^{n} \boldsymbol{\phi}_i q_i(t) \tag{2.14}$$

where, $\mathbf{q}(t)$ denotes modal coordinates, and $\mathbf{\Phi}$ is the mode shape matrix. The modal coordinates may be considered as statistically independent, if the ratios of system natural frequencies are not integers [58, 84]. The similarity between Eq.(2.14) and the BSS statement Eq.(2.7) may be noted with modal coordinates ($\mathbf{q}(t)$) being source components ($\mathbf{s}(t)$) regardless of the number and type of the physical excitation, and the mode shape matrix ($\mathbf{\Phi}$) being the mixing matrix, $\mathbf{A}$. The other modal parameters (natural frequencies and modal damping) are identified from post-processing of the identified sources. The modal frequencies values are estimated from the peak picking method applied to identified source components. The damping values are estimated from half power bandwidth method or the identified source components are transformed into a free decaying signal using the natural excitation techniques (NExT) [52]. This additional step, however, degrades the quality of damping estimates [58, 84]. The procedure for estimation of modal parameters using BSS techniques is presented through flow chart in Fig 2.4. Initially, the independent component analysis (ICA) was applied for modal identification using virtual source concept [58, 85] for free and forced vibration response of mechanical system. A fairly good correspondence

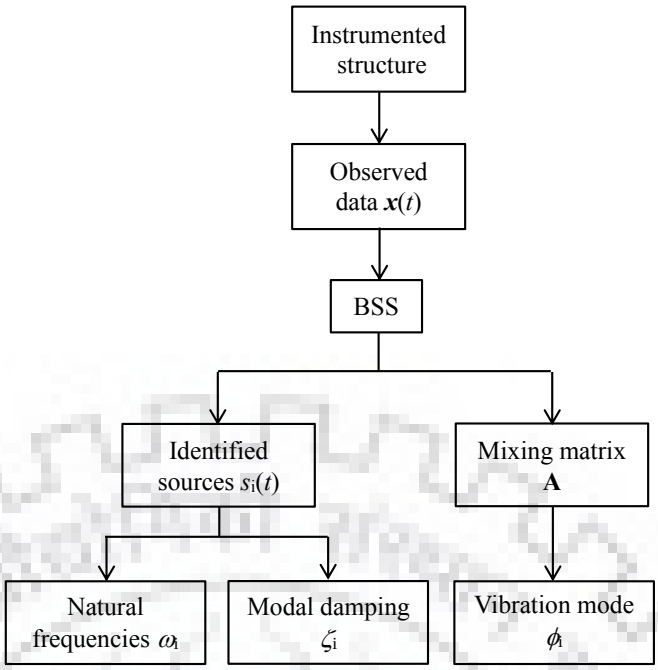

Fig. 2.4. Estimation of modal parameters using BSS

was observed between the vibration modes and mixing matrix for lightly damped system. For the damping value greater than 1% ICA procedure reported performance degradation. Some modifications to ICA procedure were suggested in conjunction with short time Fourier transform (STFT) to address the nonstationarity of the response time histories [115]. In comparison to ICA procedure, SOBI has been more popular in modal system identification mainly because of two reasons: (i) it exploits the temporal structure of the signal for estimation of individual sources component,and (ii) working with second-order statistics is numerically easier in comparison to higher order statistics. The SOBI formulation relies on the stationarity of covariance structure, and the results begin to deteriorate in the presence of non-stationarity. However, unlike ICA, SOBI procedure performs satisfactorily for lighter to moderate damping [85, 120]. The SOBI procedure sometimes predicts spurious modes which do not correlate with structural modes of vibration [84]. Prior knowledge of noise covariance is one of the pre-requisites of SOBI procedure, it may not always be possible to have this information. The sensitivity to non-stationarity has been addressed up to some extent by analysing the time series in time windows [75]. An extended SOBI algorithm known as modified cross-correlation (MCC) makes use of several time windows in the formation of covariance matrices, by considering the auto and cross-correlation of the measurements as Markov parameters [38]. The modified cross-correlation technique differs from SOBI only in two aspects (i) the SOBI techniques work in the response (observed) data whereas the MCC works on the correlation at all time lags of the response (observed) data. The main

idea behind this is that in case of SOBI procedure, information of noise statistics is needed a priori and acquiring it is almost an impossible task; therefore, correlation of observed data is considered to eliminate the noise components, and (ii) in MCC diagonalisation procedure involves covariance matrices obtained from multiple non-overlapping windows instead of time lagged covariance matrices as in case of SOBI to address the issue of nonstationarity. The SOBI procedure has been further extended to wavelet-based modified cross correlation (WMCC) [37]. For signals with lower energy modes, and noisy data wavelet transform is used for the separation of sources [63, 121]. The procedure of estimation of sources through WMCC involves the pre-processing of correlation of response data using stationary wavelet transform for obtaining time-invariant wavelet coefficients followed by diagonalization of several time-lagged non-overlapping windows for the estimation of mixing matrix and source components. For nonstationary response, covariance matrices have been obtained from several trimmed overlapping windows, followed by joint-approximate diagonalisation (JAD) of these matrices for modal parameter estimation [92]. The diagonalization process in all of these SOBI and variants involve two problem-specific parameters: window length and time lag, which are often hard to determine. These parameters are the function of the degree of the non-stationarity present in the system [12].

Recently a generalization of the ICA procedure, called *complexity pursuit* (CP) [45] has been proposed for modal identification [116, 117, 118]. The complexity pursuit based BSS overcomes some of the limitations of the ICA procedure, namely, the assumption of independent nature of source components, and presence of at least one Gaussian source component. The CP procedure consists of estimating source component from the temporal structure of the signals and does not require any additional condition of Gaussian distribution of sources. The estimation of source components through CP is based on Stone's theorem [104], wherein the simplest (non-dispersive) constituents (sources) are sequentially extracted from a recorded mixture. In structural dynamics problems, these extracted constituents—represent the modal response to a scale factor— are obtained by minimising a measure of the complexity of recorded signals. The detail theoretical study on CP based BSS for modal identification was further carried out by Antoni *et* al. [5]. The simulation shows that CP is not superior to SOBI in the general case and suffers performance issue in the presence of closely spaced modes and complex modes. Antoni et al. proposed a generalized CP approach [5] where the simplest (non-dispersive) constituents (sources) are sequentially extracted from a recorded mixture using an arbitrary number of filters. However, the problem of scaling issues of extracted modal components remains unaddressed.

2.6.2 Outstanding Issues in BSS based Modal Identification

The output-only modal identification procedures hold potential for evolving into robust automated system for online monitoring of systems subjected to environmental loading. Based on the review presented above, following issues have been identified for developing robust BSS based procedures.

Formulation for Base Excited System For earthquake excited structural systems, the strong motion recording comprise the total acceleration at a point while the equation of motion is formulated in terms of the motion relative to the base motion and the modal expansion is in reference to the relative displacement response.

Scaling of Identified Sources One of the major problem associated with BSS based on ICA, SOBI, CP and their variants is that the independent sources are identified within a scaling factor. This causes problems in identification of mode shapes and necessitates use of specialized techniques for the purpose.

Dependency on Algorithmic Parameters The diagonalisation process in SOBI and its variants involve two problem-specific parameters, namely, window length and time lag, and the results are sensitive to the choice of these parameters.

Non-stationarity The SOBI procedure is based on the assumption of stationarity of the sources, which is not true most of the times.

Iterative Nature The ICA and CP procedures are iterative procedures for estimation of source components from the observed data. The iterative procedure does not always guarantee extraction of exact components and also increases the computational load.

Spurious Modes The SOBI procedure introduces spurious mode due to numerical processing. The separation of spurious modes from the genuine modes requires further processing.

Pre-processing of Data The ICA and SOBI procedures require a number of pre-processing steps like the whitening, centring, correlation of input data, wavelet transforms, etc.

Noisy Data The study on noise contaminated data has not received much attention.

Based on the problems mentioned above, we develop a simplified BSS based modal identification in a non-statistical framework using synchrosqueezed transform (SST). The SST is an adaptive procedure, which facilitates the separation of harmonics from the vibration signature.

Chapter 3

Modal Identification Using Blind Source Separation

3.1 Background

Identification and quantification of the constituents comprising a multi-component signal is a classical problem of signal processing. The process of separation of constituents from the measured data without any information of the mixing process is known as blind source separation. The source separation procedures are generally categorized into two classes depending upon their application domain, statistical and non-statistical. Statistical signal processing based blind modal identification technique has received attention in past one decade [58, 74, 37, 92]. In non-statistical category empirical mode decomposition procedure has been used [44]. In recent years a new non-statistical synchrosqueezed transform (SST) technique has been developed as source separation tool [27, 111, 106, 11] which offers fine resolution in the time-frequency plane. For earthquake like signals where all constituents of time series are well localised in time and frequency plane, synchrosqueezed transform provide an effective alternative for source separation. In this study synchrosqueezed transform has been used for blind modal identification. The details are given in next sections.

3.2 The Synchrosqueezed Transform

Synchrosqueezing technique was initially introduced in the context of audio signal processing [28] and further analysed as an alternative to empirical mode decomposition algorithm [27]. The synchrosqueezed transform (SST) is a wavelet based time-frequency analysis tool that

can identify different harmonic components from a time series comprising several harmonics [47]. SST procedure has been used in different areas including speech recognition [27], geophysics [43], atmospheric and climate studies [106, 11], medical data analysis [27], fault diagnosis [67, 66, 34] and damping estimation[76, 77]. Let us consider a signal $y(t)$ as:

$$y(t) = \sum_{i=1}^{m} s_i(t) \tag{3.1}$$

with each source component, known as intrinsic mode type function (IMT), is like $s_i(t) = A_i(t)\cos\theta_i(t)$, and m is the number of components in $y(t)$, A_i and $\theta_i(t)$ respectively are the instantaneous amplitude and (slowly varying) phase of the ith component. Knowing the signal $y(t)$, the source separation problem deals with estimation of its constituents components $s_i(t)$. For noise corrupted data the Eq. (3.1) can be modified as:

$$y(t) = \sum_{i=1}^{m} s_i(t) + n(t) \tag{3.2}$$

where, and $n(t)$ is the measurement noise.

3.3 Synchrosqueeezed Transform Procedure

Synchrosqueezed transform (SST) allows the estimation of harmonics present in a time series. The SST has the ability to provide the sharper representation of signal in time-frequency plane by reallocating the coefficients of continuous wavelet transform to time frequency plane by applying synchrosqueezing operation. The signal can be then reconstructed by allowing transformation from time frequency plane. Synchrosqueezed transform for estimation of individual source components is a three step process: (i) computation of wavelet transform, (ii) synchrosqueezing operation to map the wavelet transform coefficients from the time-scale plane to the time-frequency plane, and (iii) reconstruction of the time-domain signal from its synchrosqueezed transform.

3.3.1 Continuous Wavelet Transform

The continuous wavelet transform (CWT) provides the time frequency information of any signal $y(t)$ and is defined as [26]:

$$W_y(a,b) = \frac{1}{\sqrt{a}} \int y(t)\psi^* \left(\frac{t-b}{a}\right)\, dt \tag{3.3}$$

where $W_y(a,b)$ is known as continuous wavelet transform coefficient, $\psi^*(t)$ is the complex conjugate of the mother wavelet $\psi(t)$. The CWT represents the inner product between

the signal $y(t)$ and a scaled version of the complex conjugate of the mother wavelet $\psi(t)$. The parameters a and b control the scale and time-shift of the transform process. The instantaneous frequency $\omega(a,b)$ of the signal y for any point in time-scale plane (a,b) for which $W_y(a,b) \neq 0$ is given by [28, 27]:

$$\omega(a,b) = \begin{cases} \frac{-i}{W_y(a,b)} \frac{\partial[W_y(a,b)]}{\partial b}; & |W_y(a,b)| \neq 0 \\ \infty; & |W_y(a,b)| = 0 \end{cases} \tag{3.4}$$

The synchrosqueezing operation is performed on the wavelet transform to map the wavelet coefficients from time-scale plane to time-frequency plane.

3.3.2 Synchrosqueezing of CWT Coefficients

The synchrosqueezing operation is defined as the mapping of CWT coefficients from time-scale plane to the time-frequency plane, *i.e.*, $(b,a) \rightarrow (b, \omega(a,b))$. The continuous wavelet transform provides a "blurred" representation of signal in time-frequency plane. To obtain the sharper representation of signal synchosqueezing operation is applied.

Let us assume that the CWT coefficient $W_y(a,b)$ is evaluated at discrete values of the scale parameter, a_k, with $(\Delta a)_k = a_k - a_{k-1}$ and its synchrosqueezed transform $T_y(\omega, b)$ is determined at the centre ω_l of the frequency interval $[\omega_l - \frac{\Delta\omega}{2}, \omega_l + \frac{\Delta\omega}{2}]$, with $\omega_l - \omega_{l-1} = \Delta\omega$, by adding different contributions [27]:

$$T_y(\omega_l, b) = \frac{1}{\Delta\omega} \sum_{a_k : |\omega(a_k,b) - \omega_l| \leq \frac{\Delta\omega}{2}} W_y(a_k, b) {a_k}^{-3/2} (\Delta a)_k \tag{3.5}$$

This facilitates the refinement of the signal representation in time-frequency plane around frequency, ω_l.

3.3.3 Signal Reconstruction from SST

The original signal can be reconstructed from its synchrosqueezed transform as:

$$y(t) = \Re \left[\frac{1}{C_\psi} \sum_l T_y(\omega_l, b) \right] \tag{3.6}$$

where, $\Re(\cdot)$ denotes the real part of a complex quantity, and the normalizing constant C_ψ is related to the mother wavelet $\psi(t)$ as:

$$C_\psi = \frac{1}{2} \int_0^\infty \frac{\hat{\psi}^*(\xi)}{\xi} \, d\xi \tag{3.7}$$

with $\hat{\psi}(\xi)$ being the Fourier transform of $\psi(t)$ and the superscript $(\cdot)^*$ indicating complex conjugate.

It is possible to extract individual harmonics present in the signal by using an ideal band pass filters with a unit gain in the passband to extract the relevant information from the time-frequency plane which is then transformed to time-domain by using Eq. (3.6). The procedure of estimation of source component using SST procedure is illustrated in Fig. 3.1. The property of reallocation and reconstruction of individual components through the SST is ideally suited for its use as a source separation technique in BSS and offers a viable alternative to ICA, SOBI and CP techniques.

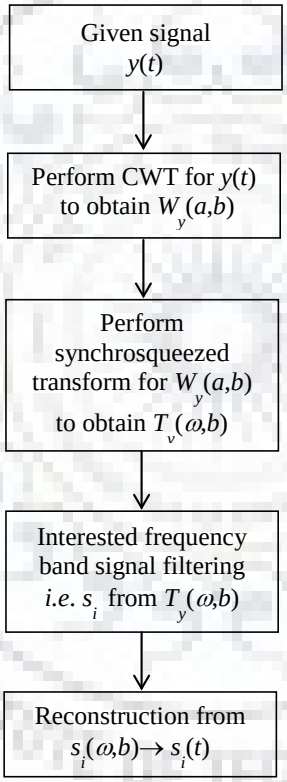

Fig. 3.1. Source separation procedure using synchrosqueezed transform

One important parameter in synchrosqueezed transform is the selection of mother wavelet $\psi(t)$. The mother wavelet is selected such that its Fourier transformation $\hat{\psi}(\xi)$ is concentrated in the absolute value around the positive frequency $\xi = \omega_0$ and is small and rapidly decaying elsewhere. We use Morlet wavelet for estimation of CWT coefficients in this study. The implementation details for discrete time sampled data have been proposed by Thakur *et* al. [106].

3.4 Modal Parameters Estimation using Synchrosqueezed Transform

The estimation of modal parameters from vibration data using BSS schemes is based on the mathematical similarity between the fundamental BSS problem stated in Eq. (2.7) as: $\mathbf{x}(t) = \mathbf{A}\mathbf{s}(t)$ and the modal expansion theorem Eq. (2.14) as: $\mathbf{x}(t) = \mathbf{\Phi}\mathbf{q}(t)$, where $\mathbf{x}(t)$ is the measured response or the response correspond to equation of motion Eq. (2.3), [58, 85, 38]. For base excited structures, such as during earthquake excitation, the equations of motion are formulated in terms of the relative displacement of the mass with respect to the base, whereas the inertial accelerometers used for building instrumentation pickup total acceleration of the point. Therefore, the accelerometer data can not be used directly for modal identification using BSS formulation in its original form and for identifying relative responses from the accelerometer measurements, additional information of ground motion is required. Thus for performing output-only modal identification of base excited structures, the modal expansion theorem needs to be reformulated in terms of total response.

3.5 BSS Formulation for Base Excited Structures

Let us consider vibrations of an n degree of freedom (DOF) system described by the equation of motion as:

$$\mathbf{M}\ddot{\mathbf{x}} + \mathbf{C}\dot{\mathbf{x}} + \mathbf{K}\mathbf{x} = \mathbf{f}(t) \tag{3.8}$$

where, $\mathbf{M}, \mathbf{C}$ and $\mathbf{K}$ are the mass, damping and the stiffness matrices, $\mathbf{x}$ denotes the displacement response, $\mathbf{f}(t)$ is the excitation, and a dot indicates time derivative. The system response can be given by a linear combination of the normal modes of the system as:

$$\mathbf{x}(t) = \mathbf{\Phi}\mathbf{q}(t) = \sum_{i=1}^{n} \boldsymbol{\phi}_i q_i(t) \tag{3.9}$$

where, $\mathbf{q}(t)$ denotes modal coordinates, and $\mathbf{\Phi}$ is the mode shape matrix. Thus the modal expansion of system response Eq. 3.9 is considered analogous to the BSS statement given by Eq. 2.7 as:

$$\mathbf{x}(t) = \mathbf{A}\mathbf{s}(t) \tag{3.10}$$

where, $\mathbf{x}(t)$ is the vector of observed output, $\mathbf{A}$ is the mixing matrix similar to the mode shape matrix $\mathbf{\Phi}$, and $\mathbf{s}(t)$ represents the virtual sources equivalent to modal coordinates $\mathbf{q}(t)$ regardless of the number and type of the physical excitation force. The modal parameters

(natural frequencies and modal damping) are identified from the post-processing of the identified source time histories, and the mode shapes are provided by the columns of the mixing matrix. This is the formulation of BSS in terms of the system response to load directly applied to the structural system and the measured response corresponds to the system response as in the governing equation of motion.

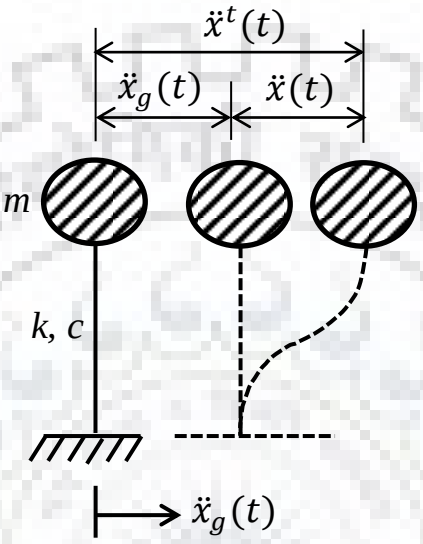

Fig. 3.2. Single degree of freedom system subjected to base excitation

For a base excited structure, such as during earthquake excitation, as shown in Fig. 3.2, the equations of motion are given in terms of the relative displacement of the mass with respect to the base:

$$\mathbf{M}\ddot{\mathbf{x}}(t) + \mathbf{C}\dot{\mathbf{x}}(t) + \mathbf{K}\mathbf{x}(t) = \mathbf{p}_{\text{eff}}(t) \tag{3.11}$$

where $\mathbf{p}_{\text{eff}}(t)$ is the effective force vector, can be written as:

$$\mathbf{p}_{\text{eff}}(t) = -\mathbf{M}\mathbf{R}\ddot{\mathbf{x}}_g(t) \tag{3.12}$$

where $\ddot{\mathbf{x}}_g(t)$ represents the ground acceleration, $\mathbf{R}$ is matrix of rigid body influence coefficients, and $\mathbf{x}(t)$ denotes the displacement of mass-points relative to the base. The solution by mode superposition proceeds with the modal expansion as in Eq. (3.9). However, the relative motion can not be measured directly and the inertial accelerometers used for building instrumentation pickup total acceleration of the point [18]. The governing equation of motion in terms of the total accelerations can be given by:

$$\begin{aligned} \mathbf{M}\left(\ddot{\mathbf{x}}(t) + \mathbf{R}\ddot{\mathbf{x}}_g(t)\right) &= -\mathbf{C}\dot{\mathbf{x}}(t) - \mathbf{K}\mathbf{x}(t) \\ \text{or, } \ddot{\mathbf{x}}^t(t) &= \left(\ddot{\mathbf{x}}(t) + \mathbf{R}\ddot{\mathbf{x}}_g(t)\right) = -\mathbf{M}^{-1}(\mathbf{C}\dot{\mathbf{x}}(t) + \mathbf{K}\mathbf{x}(t)) \end{aligned} \tag{3.13}$$

With the help of modal expansion theorem, we have

$$\ddot{\mathbf{x}}^t(t) = -\mathbf{M}^{-1}(\mathbf{C}\mathbf{\Phi}\dot{\mathbf{q}}(t) + \mathbf{K}\mathbf{\Phi}\boldsymbol{q}(t)) \tag{3.14}$$

Since the damping term is generally negligible in comparison to the restoring force term, we get an approximate relation for total acceleration as:

$$\ddot{\mathbf{x}}^t(t) \approx -\mathbf{M}^{-1}\mathbf{K}\mathbf{\Phi}\mathbf{q}(t) = -\mathbf{\Phi}\left(\mathbf{\Lambda}\boldsymbol{q}(t)\right) \tag{3.15}$$

where, $\mathbf{M}^{-1}\mathbf{K} = \mathbf{\Phi}\mathbf{\Lambda}\mathbf{\Phi}^{-1}$ has been substituted from generalized eigenvalue problem of structural dynamics, and $\mathbf{\Lambda}$ is the diagonal matrix containing eigenvalues. This is now in a form suitable for using BSS with total acceleration measurements, $\ddot{\mathbf{x}}^t(t)$. The weighted modal coordinates are the sources to be identified while the mode shapes can be inferred from the mixing matrix. The weighting of modal coordinates by the respective eigenvalues enhances the energy of higher mode components which helps in the identification of higher modes as well—an important factor for structural health monitoring applications. Further, the modal responses are narrow band due to sharply peaked transfer functions centered at the modal frequencies for lightly damped structural systems.

The structural vibration records receive contributions from several modes of vibration of different frequencies which need to be extracted as virtual sources in the mixture. The harmonic constituents of a vibration signature can be separated by the process of synchrosqueezing transform, band-pass filtering and reconstruction (Eqs. (3.3–3.6)). Thus the recorded vibration signature at any degree of freedom in a structural system can be given by:

$$x_k(t) = \sum_{i=1}^{m} s_{ki}(t) \tag{3.16}$$

where, $x_k(t)$ represents the response of kth degree of freedom, and $s_{ki}(t)$ denotes the ith SST identified component of the kth signal. The estimated independent source components are used for the estimation of modal parameters of n degree of freedom structural system. Considering all dynamic degrees of freedom, we have:,

$$\begin{aligned} x_n(t) &= s_{n1}(t) + s_{n2}(t) + \ldots + s_{nm}(t) \\ \vdots &= \qquad\qquad \vdots \\ x_2(t) &= s_{21}(t) + s_{22}(t) + \ldots + s_{2m}(t) \\ x_1(t) &= s_{11}(t) + s_{12}(t) + \ldots + s_{1m}(t) \end{aligned} \tag{3.17}$$

Considering the modal expansion of the dynamic response with m number of dominant modes, we have:

$$\mathbf{x}(t) = \sum_{i=1}^{m} \boldsymbol{\phi}_i \mathbf{q}_i(t) \tag{3.18}$$

where, $\mathbf{q}_i(t)$ is modal coordinate and $\boldsymbol{\phi}_i$ mode shape vector of ith mode. For n degree of freedom system the modal expansion theorem can be written as:

$$\begin{bmatrix} x_n(t) \\ \vdots \\ x_2(t) \\ x_1(t) \end{bmatrix} = \begin{bmatrix} \phi_{n1} & \phi_{n2} & \dots & \phi_{nm} \\ \vdots & \vdots & \ddots & \vdots \\ \phi_{21} & \phi_{22} & \dots & \phi_{2m} \\ \phi_{11} & \phi_{12} & \dots & \phi_{1m} \end{bmatrix} \begin{bmatrix} q_1(t) \\ \vdots \\ q_2(t) \\ q_m(t) \end{bmatrix} \tag{3.19}$$

Comparing Eqs. (3.17 and 3.19), the one-to-one relationship between the separated harmonic components and the mode shape vectors and modal coordinates can be established.

For base excited structures considering response at all degree of freedom system and its constituent parts obtained from SST:

$$\begin{aligned} \ddot{x}_n^t(t) &= s_{n1}(t) + s_{n2}(t) + \ldots + s_{nm}(t) \\ \vdots &= \vdots \\ x_2^t(t) &= s_{21}(t) + s_{22}(t) + \ldots + s_{2m}(t) \\ x_1^t(t) &= s_{11}(t) + s_{12}(t) + \ldots + s_{1m}(t) \end{aligned} \tag{3.20}$$

where, $\ddot{x}_n^t(t)$ represents the total acceleration response of nth degree of freedom.
The modal expansion equation for base excited n degree of freedom system can be written using Eq. (3.15) as:

$$\begin{bmatrix} \ddot{x}_n^t(t) \\ \vdots \\ \ddot{x}_2^t(t) \\ \ddot{x}_1^t(t) \end{bmatrix} = \begin{bmatrix} \phi_{n1} & \phi_{n2} & \dots & \phi_{nm} \\ \vdots & \vdots & \ddots & \vdots \\ \phi_{21} & \phi_{22} & \dots & \phi_{2m} \\ \phi_{11} & \phi_{12} & \dots & \phi_{1m} \end{bmatrix} \begin{bmatrix} \omega_1^2 q_1(t) \\ \vdots \\ \omega_2^2 q_2(t) \\ \omega_m^2 q_m(t) \end{bmatrix} \tag{3.21}$$

Again if we compare Eqs. (3.20 and 3.21), the identified constituent sources $s_{ni}(t)$ are proportional to the modal response $\omega_i^2 q_i(t), i = 1, 2, ..., m$. Thus for the case of base excitation and acceleration measurements, the SST identified constituent components correspond to modal responses weighted by respective eigenvalues, ω_i^2, and lead to a comparatively better representation of higher modes than displacement/velocity measurements.

3.6 Synchrosqueezed Transform Based Modal Parameter Estimation

From the one-to-one relationship between the element of matrices given by Eq. (3.20) and Eq. (3.21), the source components identified through SST procedure are the true measure

of modal response. Modal parameters namely mode shape, modal damping and natural frequencies are estimated by processing of the identified modal response vectors.

3.6.1 Estimation of Mode Shapes

Assuming the mode shapes to be normalized to unity at nth degree of freedom, it follows that the identified constituent sources $s_{ni}(t)$ are proportional to the modal coordinates $q_i(t)$; $i = 1, 2, ..., m$. The natural frequency and modal damping can be estimated by post-processing of the identified modal coordinates. The mode shapes coefficients at other degree of freedom are estimated as the time average of instantaneous ratios of SST identified modal responses:

$$\phi_{ki} = \underset{t}{\text{mean}} \left(\frac{s_{ki}(t)}{s_{ni}(t)} \right) \tag{3.22}$$

The computation of mode shape coefficients as normalization of response with respect to the one at nth DOF may sometime create numerical error if the response at n DOF is not significant in the mode being identified. Therefore, for numerical robustness, the mode shapes coefficients can be estimated as the time average of instantaneous ratio (normalization) of SST identified sources with respect to the component with maximum energy for that harmonic:

$$\phi_{ki} = \underset{t}{\text{mean}} \left(\frac{s_{ki}(t)}{s_{pi}(t)} \right) \tag{3.23}$$

where, $s_{pi}(t)$ is the source component having maximum energy for ith harmonic, $E_i\,(= \int_0^t (s_{pi}(t))^2\ dt\,)$ out of all degrees of freedom $k = 1, 2, \ldots, n$. For the case of seismic excitation through base motion, the estimated mode shape ordinates have a bias due to the contribution of ground motion component in addition to the structural vibration. This bias ($= \underset{t}{\text{mean}}\,(\ddot{u}_g(t)/s_{pi}(t))$) needs to be removed from the estimated coefficients to get the structural mode shapes. The extracted mode shape coefficients can be further normalized either to unit length, or mass orthonormalized as required. The modal assurance criterion (MAC) [1] is used to measures the correlation between the identified mode shapes with theoretical or reference mode shapes. The modal assurance criteria is defined as:

$$\text{MAC} = \frac{|\ \hat{\boldsymbol{\phi}}^T \boldsymbol{\phi}\ |^2}{\left(\hat{\boldsymbol{\phi}}^T \hat{\boldsymbol{\phi}}\right)\left(\boldsymbol{\phi}^T \boldsymbol{\phi}\right)} \tag{3.24}$$

where, $\hat{\boldsymbol{\phi}}$ and $\boldsymbol{\phi}$ are the estimated and reference mode shape vectors respectively. The MAC value ranges from 1 to 0 with values close to unity representing a good correlation between the identified and reference mode shapes. The other modal parameters (natural frequency and modal damping) are estimated from post-processing of maximum energy

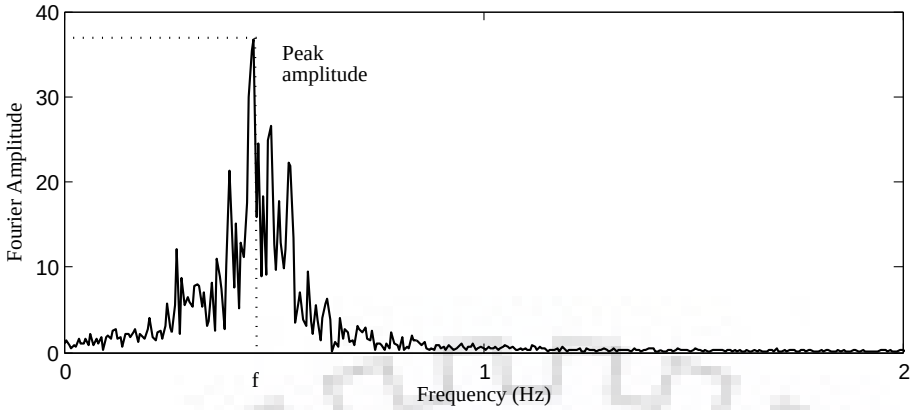

Fig. 3.3. Peak picking method of estimation of natural frequency

source components as modal coordinates. In this study the procedure proposed for mode shape estimation is based on the availability of response measurements at all floor levels. However in case of building instrumentation spatial incompleteness is a major issue. In such cases the missing response time histories can be synthesized either in the frequency domain or in the time domain by using a suitable interpolation scheme. In time domain interpolation, the piecewise cubic Hermite interpolating polynomial (PCHIP) interpolation has been used to estimate the corresponding discrete time sample of response time histories at intermediate floors [99].

3.6.2 Estimation of Natural Frequencies

The estimation of natural frequencies is most straightforward procedure in comparison to other modal parameters. The synchrosqueezed transform provides a sharper representation of the signal in the time-frequency plane. Therefore, the approximate information of the natural frequencies can be extracted from SST plots. However for more accurate and robust measurement peak picking method can be applied to identified modal coordinates. Peak picking method is the simplest procedure of identifying the frequencies of the system where natural frequencies are taken from the observation of the peaks on the Fourier amplitude spectrum of the identified source. The process of estimation of natural frequencies using peak picking method is shown in Fig. 3.3.

3.6.3 Estimation of Modal Damping

Various methods are available for estimation of damping from the structural response to free, forced, or ambient vibration. The commonly used methods are logarithmic decay

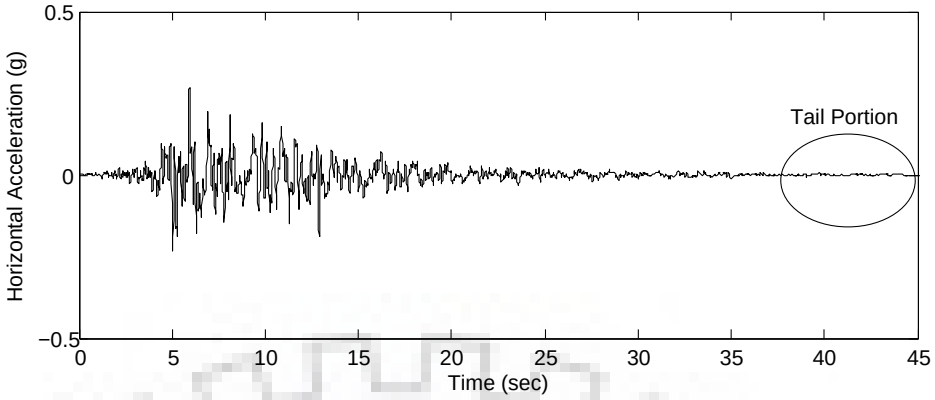

Fig. 3.4. Hector Mine 1999 earthquake ground motion (Horizontal component)

method, half power bandwidth method, and curve fitting method [20]. In the logarithmic decay or free decay method, a pull and release test is conducted to measure the free vibration record. Logarithmic decay method is valid for small oscillation of a lightly damped system. The second commonly used method is half-power bandwidth method which is based on estimation of the system of transfer function from the input-output data pairs. It is difficult to use in case of closely spaced modes. The curve fitting method has been considered as a most reliable method of estimation of modal damping [88]. The curve fitting procedure involves the fitting response time series with exponentially damped harmonic functions. However, for forced excitation cases the shape of the response is unknown therefore curve fitting cannot be applied directly to the measured response. In some of the studies, the measured response has been transformed to free decay response using natural excitation technique (NExT) [52, 50] for further estimation of modal damping.

In BSS based modal identification procedures the modal damping values are estimated through the processing of identified modal coordinates. For free vibration cases, damping values are identified directly by fitting the exponential decay function to the identified modal coordinates. Whereas for forced vibration cases the identified modal coordinates are processed using NExT procedure to convert them into a free vibration decay function for identification of modal damping. Processing of the modal coordinates with NExT procedure increases the computational load as well includes the error in the identified results. In this study, a novel procedure is proposed for identification of modal damping for earthquake excited structures. For typical earthquake excitations, the ground motion amplitudes in the tail portion are very small as shown in Fig. 3.4, and therefore, the system response shall be primarily dominated by the free vibration component. It is, therefore, appropriate

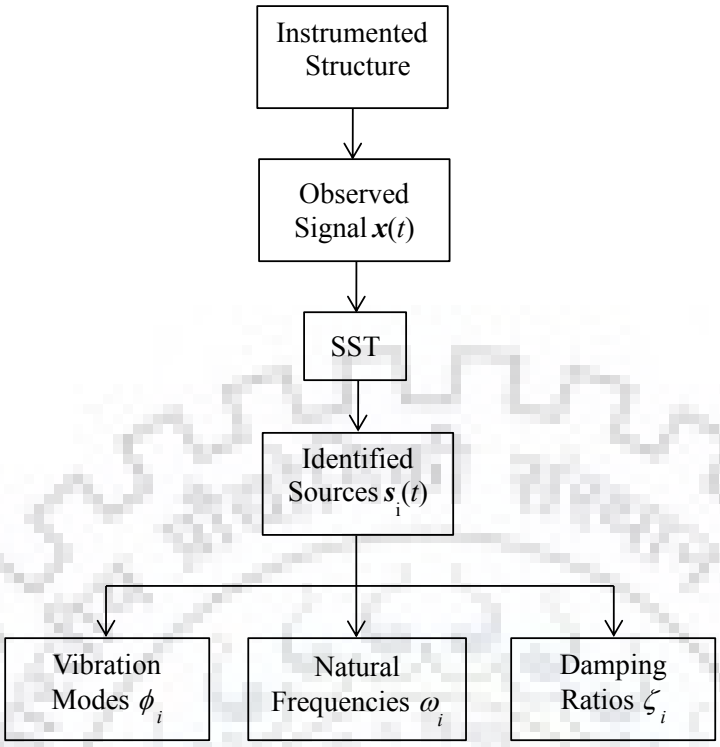

Fig. 3.5. SST-based modal identification

to extract a small stretch of the tail portion of the identified sources as representative of the free vibration response and estimate the modal damping by finding a suitable decay exponent of the envelope. We explore the possibility of fitting an exponential decay function of the form:

$$e(t) = \rho e^{-2\zeta_n \omega_n t} \tag{3.25}$$

to the tail data $y(t) = s^2(t)$, where, $s(t)$ denotes the source identified by SST procedure, ζ_n is the modal damping, ω_n is the natural frequency (in rad/s) for the respective mode, and ρ denotes the initial amplitude of the envelope. Thus this approach provides a simplified procedure for estimation of modal damping from SST identified sources. The complete scheme of SST-based modal identification is shown in Fig. 3.5.

Chapter 4

Validation of SST-Based Modal Identification

To validate the SST based modal identification procedure formulated in the preceding chapter, it is tested on a three degree of freedom shear building model. The results identified from the proposed procedures are compared with the analytical and SOBI identified results. Subsequently, the studies are performed on UCLA Factor Building using the real earthquake data recorded on site. The robustness of the proposed procedure for modal identification with noisy data is studied using analytically computed response of UCLA Factor Building for a suite of three different ground motions.

4.1 Modal Identification of Shear Building Model

A three-degree of freedom shear frame building model, shown in Fig 4.1, is considered for the validation study. The equation of motion for this shear building model may be given as:

$$\mathbf{M}\ddot{\mathbf{x}} + \mathbf{C}\dot{\mathbf{x}} + \mathbf{K}\mathbf{x} = \mathbf{f} \tag{4.1}$$

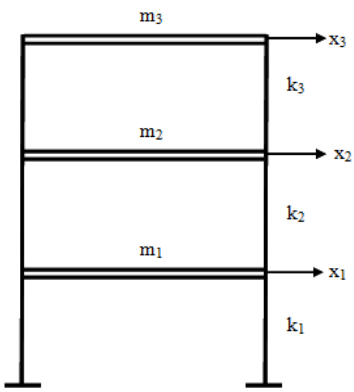

Fig. 4.1. Three DOF-system

where mass $m_1 = m_2 = m_3 = 10$ kg is assumed to be lumped at each floor, $k_1 = k_2 = k_3 = 2$ kN/m are the stiffness of floor columns and c_{ij} are the coefficients so as to give 5% damping in each mode. The building model is subjected to Northridge earthquake (January 17,1994 at 4:30 A.M. UTC) of magnitude: $M_w \sim 6.7$ recorded at Tarzana-Cedar Hill A at sampling frequency of 50Hz. The Tarzana-

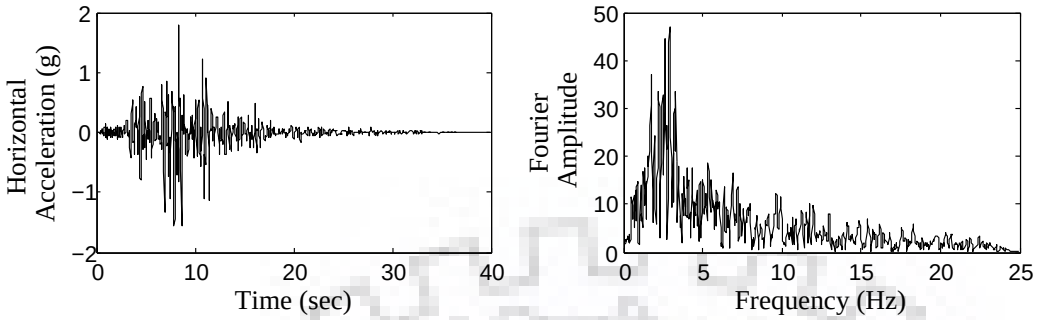

Fig. 4.2. Northridge earthquake ground motion considered for analysis

Cedar Hill A station is located approximately 7 km south of epicentre, receives the peak ground acceleration (PGA) approximately as 1.8g, 1.00g in two horizontal directions and 1.04g in vertical direction. In this numerical study the horizontal component of ground acceleration with peak amplitude of 1.8g is used for the analysis. The details of ground acceleration are shown in Fig. 4.2 [4]. The response $\mathbf{x}(t)$ is obtained by solving Eq. (4.1) using Newmark's constant acceleration method.

4.1.1 Source Separation using SST

As discussed earlier, the SST procedure facilitates the separation of harmonic components present in the signal. The response measurements and corresponding SST plots at all floors are shown in the Fig. 4.3. The fine horizontal lines in the SST plot denote the different frequency components present in the signal. Using SST, source components are separated from measured acceleration data by applying suitable band pass filters. The identified sources corresponding to top floor measurement response are shown in Fig. 4.4 where, (a) shows the total acceleration response at top floor, (b) shows the three source components identified from SST using suitable band pass filters, (c) represents the reconstructed signal as summation of three identified sources $s_1(t)+s_2(t)+s_3(t)$, and (d) represents the measured vs reconstructed response. The three identified signal constitute more than 99% energy of the original signal. Therefore, it can be concluded that the SST is an effective tool for providing the time frequency information of the signal as well as capable of extracting the individual harmonics. In similar fashion the harmonic components are extracted from the responses at remaining two degree of freedom. This shows that the time-frequency based SST is an effective alternative to other statistical BSS procedures. From the mathematical similarity

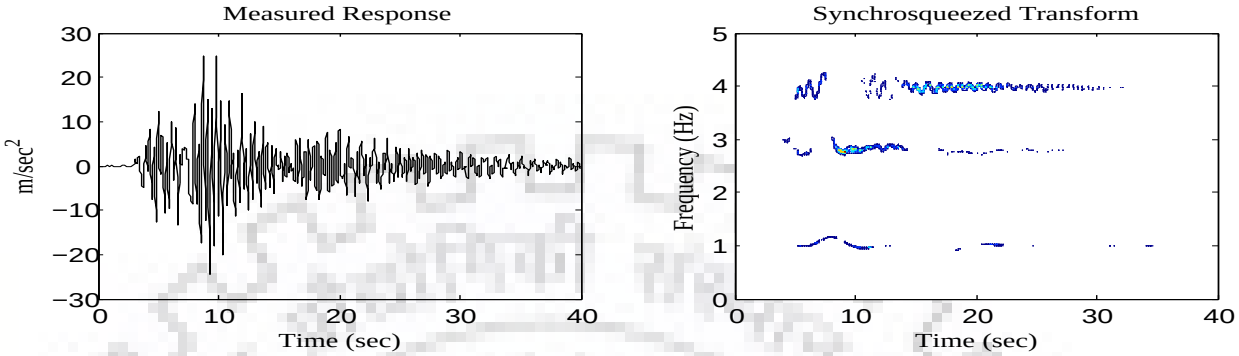

(a) Top floor

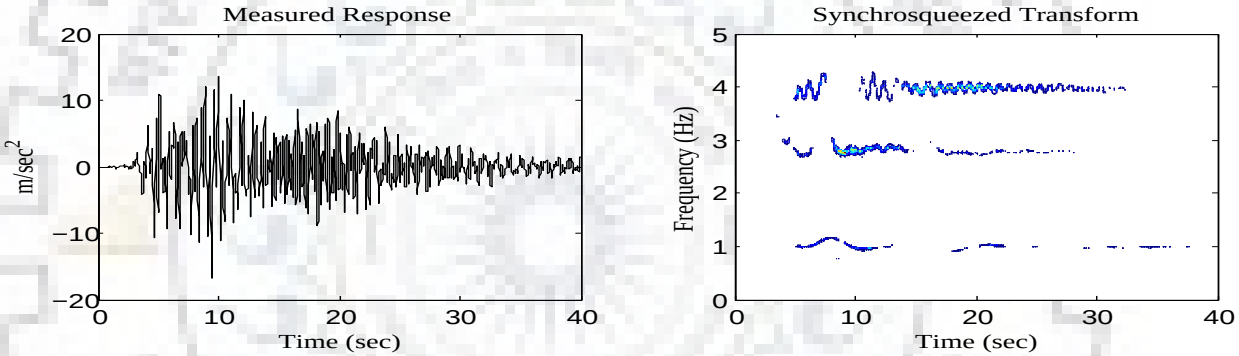

(b) Second floor

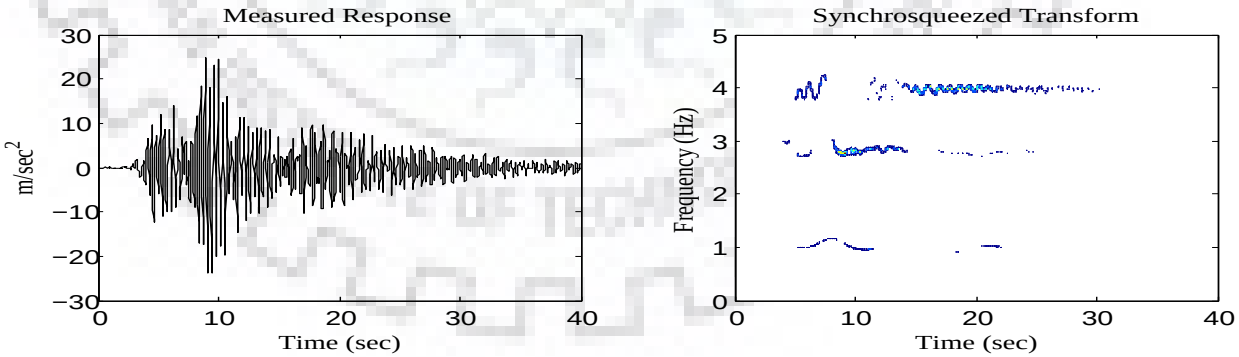

(c) First floor

Fig. 4.3. Acceleration measurements and corresponding SST plots at different floor levels

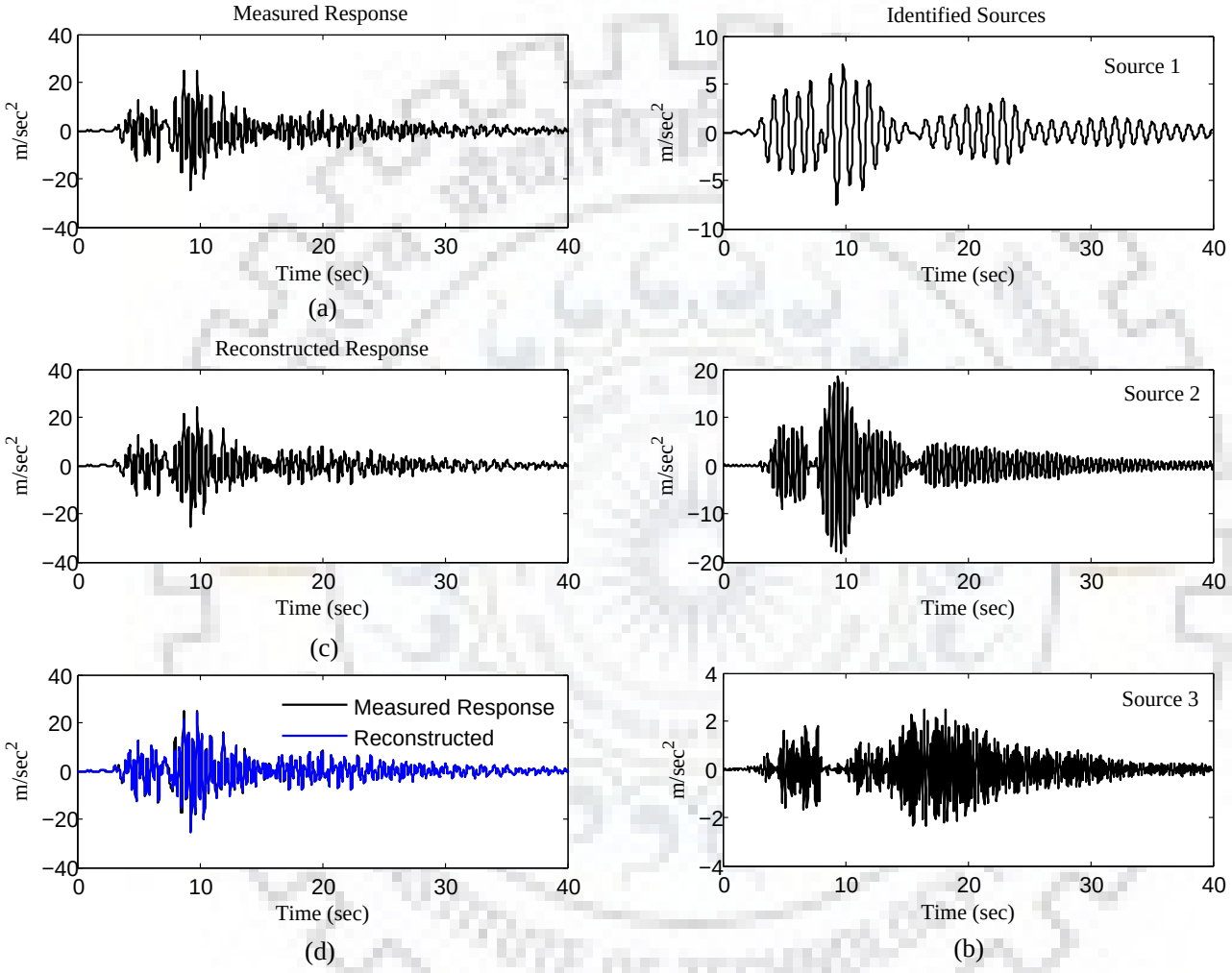

Fig. 4.4. (a) Total acceleration response at top floor, (b) identified source components, (c) reconstructed response from the SST identified sources, and (d) Analytically computed versus reconstructed response at top floor

.

between modal expansion of system response Eq. (3.21) and basic SST definition Eq. (3.20), the SST identified harmonics can be seen as the measure of modal response. To validate this, SST identified source components are compared with the analytical modal responses. The analytical modal coordinates for base excited structures are obtained by using the modal expansion in terms of total acceleration derived in previous chapter (Eq. 3.15) as:

$$\ddot{\mathbf{x}}^t(t) = -\mathbf{\Phi}\left(\mathbf{\Lambda}\boldsymbol{q}(t)\right) \tag{4.2}$$

The modal response contributions are then obtained by scaling the modal coordinate with mode shape coefficient $\phi_{ji}q_i(t)$ for the ith mode response at jth degree of freedom. Figure 4.5 shows the SST identified sources from top floor measured response and analytically obtained modal response.

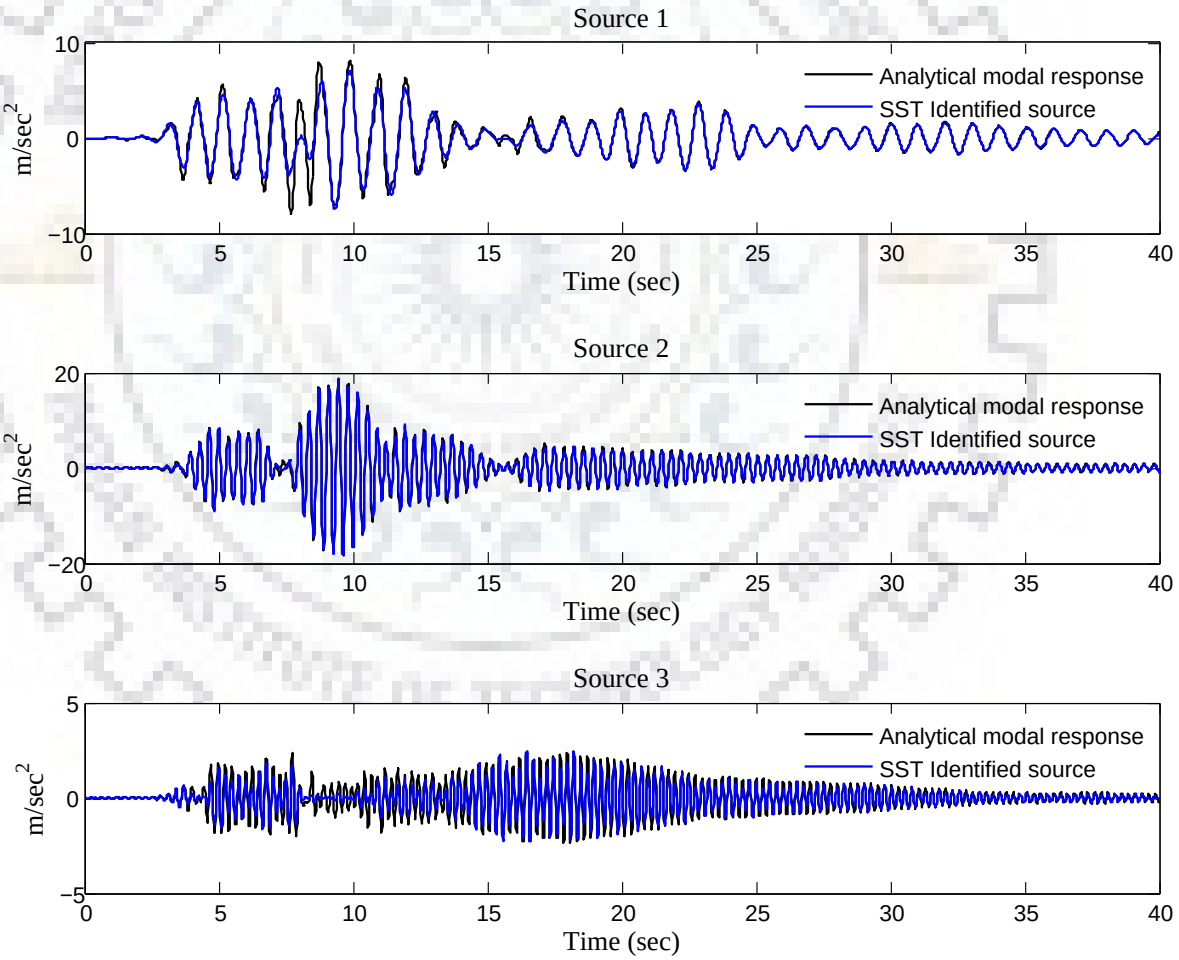

Fig. 4.5. SST identified sources and theoretical modal responses at top floor level

The analytical modal response and SST identified sources are compared using relative error (e) calculated as:

$$e = \sqrt{\frac{\sum_i \left(\hat{s}(t_i) - s(t_i)\right)^2}{\sum_i \hat{s}^2(t_i)}} \times 100\% \tag{4.3}$$

Table 4.1. Relative error between the identified sources and analytical modal responses

Relative error in %			
DOF	Mode 1	Mode 2	Mode 3
3	1.42	1.60	2.20
2	1.51	2.20	2.00
1	1.90	2.21	2.45

where, $\hat{s}(t)$ is the analytical modal response, and $s(t)$ is the SST identified source. The relative error of 1.42%, 1.60% and 2.20% are observed between the first, second, and third SST identified sources and analytical modal responses respectively. Similarly the sources identified at other degree of freedoms are also compared with corresponding analytical modal response vectors. The relative error estimated between the analytical modal responses at each degree of freedom is mentioned in Table 4.1. The smaller value of error shows that the identified sources are measure of modal response to its true strength and the procedure proposed for of estimation of mode shapes (Eq. (3.22)) is suitable using SST identified sources.

4.1.2 Modal Identification Results

The modal parameters, namely, natural frequencies, mode shapes and modal damping are computed using SST based modal identification procedure along with SOBI procedure. The widely used SOBI procedure is used in this study as a point of reference for SST based BSS method. Considering the normalization of mode shape to unity at top floor, the mode shape coefficients at other degree of freedom are obtained as the time average of instantaneous ratio of SST identified sources with respect to top floor sources for that harmonic using Eq. (3.22). The top floor sources components are the maximum energy components. The identified mode shapes are compared with the analytical mode shapes and are shown in Fig. 4.6. The modal assurance criterion (MAC) is used to compute the fidelity of the identified mode shapes with analytical mode shapes. The modal assurance criteria is defined by Eq. (3.24) as:

$$\text{MAC} = \frac{| \hat{\boldsymbol{\phi}}^T \boldsymbol{\phi} |^2}{\hat{\boldsymbol{\phi}}^T \hat{\boldsymbol{\phi}} \; \boldsymbol{\phi}^T \boldsymbol{\phi}} \tag{4.4}$$

where, $\hat{\boldsymbol{\phi}}$ and $\boldsymbol{\phi}$ are the estimated and analytical mode shape vector respectively. The MAC value ranges from 1 (perfect correlation) to 0 (poor correlation). The MAC values estimated

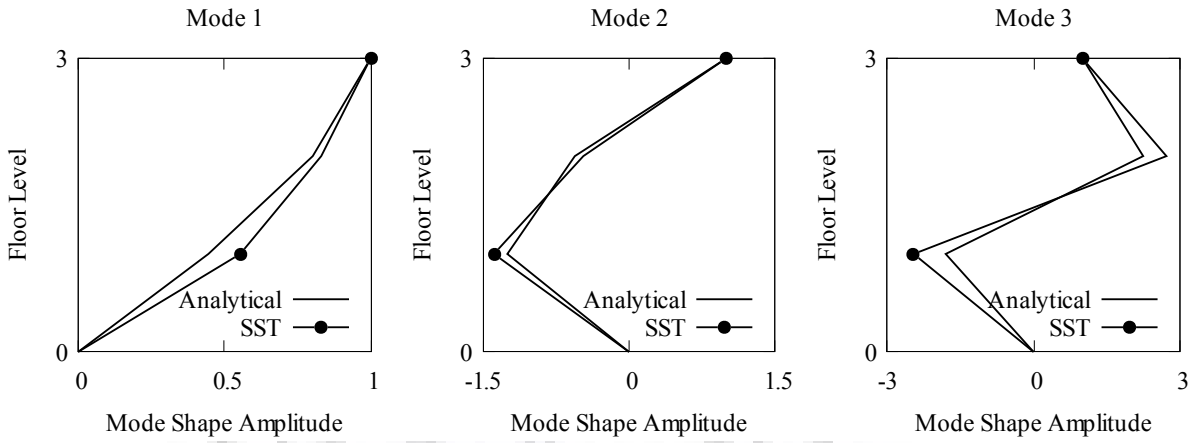

Fig. 4.6. SST identified and analytical mode shapes

Table 4.2. Modal identification results three DOF-system

		Mode 1	Mode 2	Mode 3
Frequencies (Hz)	Theoretical	1.00	2.80	4.06
	SST	1.00	2.75	3.98
	SOBI	1.00	2.75	3.98
MAC	SST	1.00	1.00	0.99
	SOBI	1.00	1.00	0.99
Damping ratio (%)	SST	5.00	4.50	4.80
	SOBI	4.80	4.50	4.30

from SST and SOBI based procedure with theoretical mode shapes are mentioned in Table 4.2. Higher MAC values has been observed between the SST identified and analytical mode shapes. This shows that a simplified procedure as time average of instantaneous ratios of identified sources provides an ideal estimation of mode shapes. When mode shapes are normalized with respect to top floor the sources identified from top floor response are the measure of modal coordinates. The other two modal parameters (natural frequencies and modal damping) are now estimated by processing the identified modal coordinates. The frequency spectrum of the identified modal coordinates are shown in Fig. 4.7. Using the peak picking method, natural frequencies are estimated for each mode. The natural frequencies estimated from SST, SOBI procedure along with theoretical results are mentioned in Table 4.2. The natural frequencies identified from procedure are closer to the theoretical

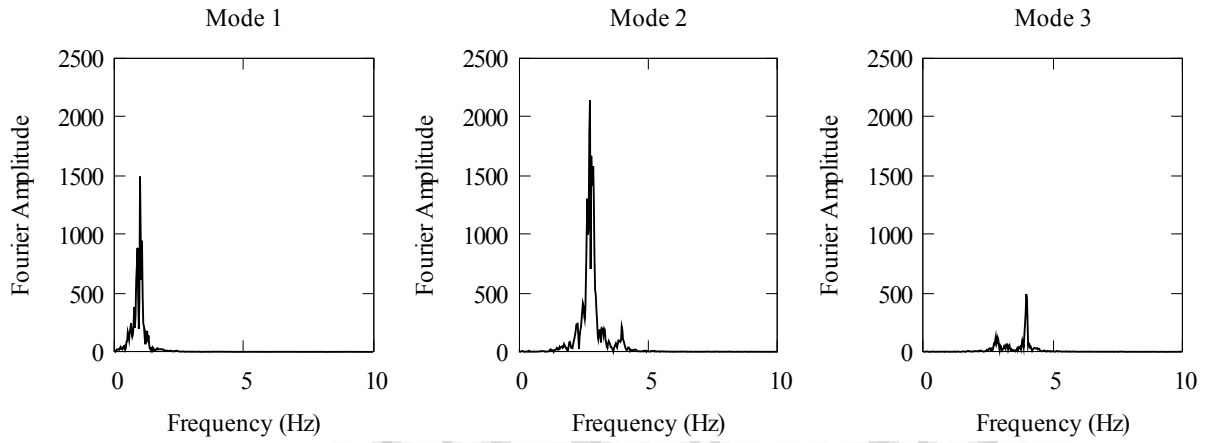

Fig. 4.7. Frequency spectrum of SST identified sources

results as well SOBI identified results.

Lastly, the modal damping values are estimated from the identified modal coordinates using the proposed procedure (see, Section 3.6.3). The modal damping estimates are obtained from both SST and SOBI procedures. Last fifty data points from tail portion are considered for the analysis. Fitting of squared values of data points with exponential decay function are shown in Fig. 4.8 along with the fitting parameters.

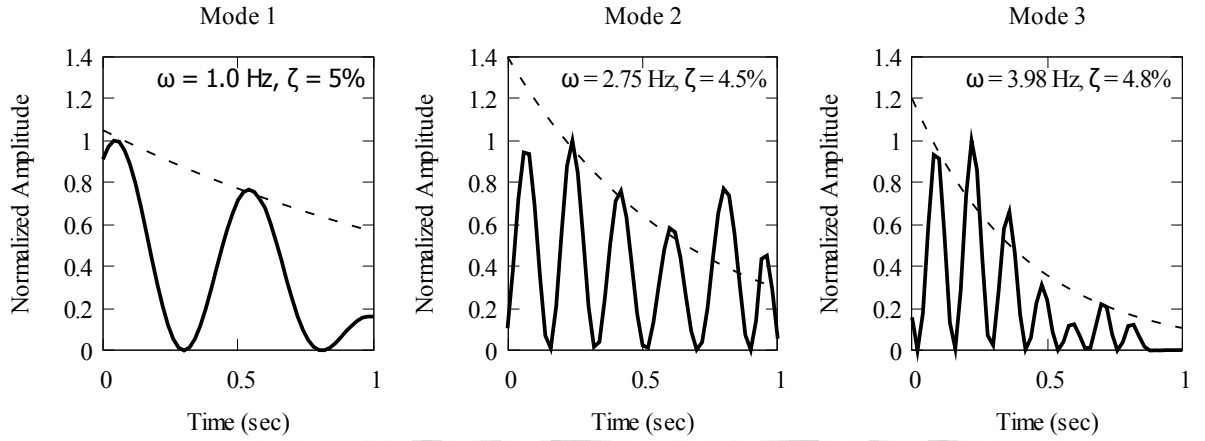

Fig. 4.8. Fitting of SST-based identified tail portion of sources with damped free vibration envelope for three DOF-system

The modal damping estimates are mentioned in Table 4.2. The damping estimates are found to be close to 5%, the assumed modal damping for the model. This shows that by fitting the exponential decay function to tail portion of identified sources provides reasonably good estimates of modal damping for base excitation cases. From the identified results it can be concluded that the proposed procedures provides viable tool for robust estimation of mode shape, natural frequencies and modal damping.

4.2 Modal Identification of UCLA Factor Building from Recorded Data

4.2.1 Building Description

For validation of the proposed SST-based modal identification, we consider the UCLA Doris and Louis Factor building, commonly known as UCLA Factor Building or (UCLAFB). Constructed in late 1970's the UCLAFB accommodates several centres of health and biomedical facilities. The UCLAFB is a fifteen-storey special moment resisting (SMF) steel frame structure. The height of the building above the ground is approximately 66m. There are 12 SMF bays in both the EW and NS directions of the building. Figure 4.9 shows the UCLAFB elevations and the typical floor plan.

Due to a slight projection on the east and west sides of the building, the floor area for floors 10 through 16 increases by 13.5 percent approximate. The building is symmetric about the East-West axis and slightly asymmetric about the North-South axis. Except for some concrete caissons, the structure is supported by concrete spread footing. The building consists of 72 uniaxial forced balanced accelerometers with an on site recording system. Four accelerometers exist at each floor above grade, oriented to record translational motions near the perimeter of the floor (two in each direction). Building has two basement levels, each of the two basement levels has an accelerometer to record translation in two directions, as well as two accelerometers to record vertical responses. Later in 2003 building's sensor network was upgraded to a 24-bit network that continuously records data including numerous small earthquakes. This building is one of the most densely permanently instrumented buildings in North America and has provided a wealth of strong motion recordings over a decade for system identification and health monitoring studies (see, *e.g.*, [101, 37, 38]). However, it has not yet experienced any damaging earthquake so far.

The available recorded structural response data from UCLA Factor Building is used for the validation study. Subsequently, the finite element model of UCLAFB is used for a numerical study for a suite of earthquake ground motions. Finite element platform SAP 2000 is used for the finite element modelling of building [96]. Rayeigh damping model for 2% damping in first and third modes is used in the analysis. To simplify the finite element modelling the building foundation is modeled as fixed base. The building is designed for mass quantities estimated from the architectural drawing and live load is assumed 1.5 kN/m^2 for load calculations. The details of mass quantities of UCLA Factor Building are given

(a) Elevation

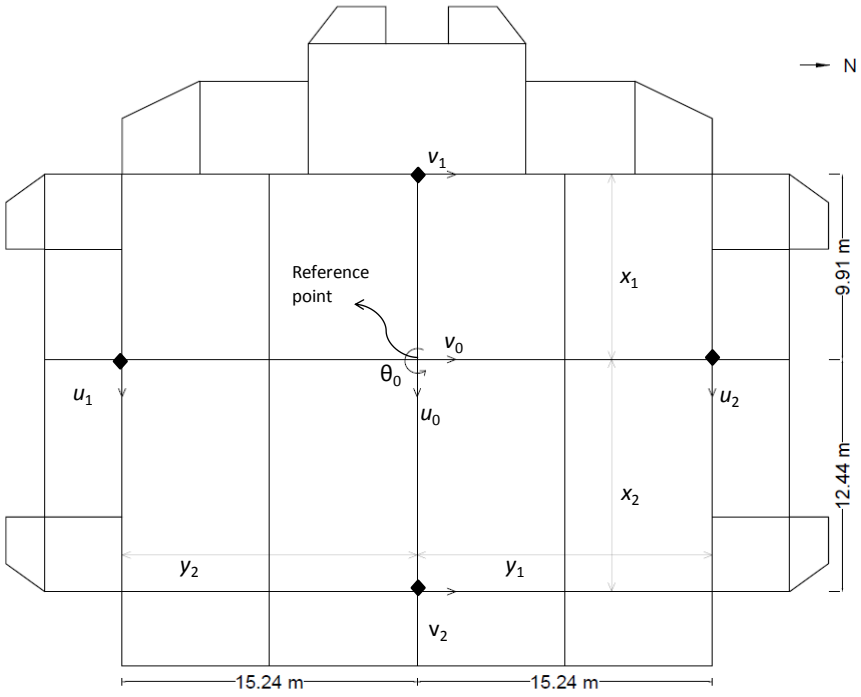

(b) Plan

Fig. 4.9. UCLA Factor building

Table 4.3. Mass quantities UCLA Factor Building

Dead Load		Live load
Floor System	Exterior System	
3.0kN/m^2	1.45kN/m^2	1.5kN/m^2

in Table 4.3. The stiffness of the non structural components is however ignored in finite element modelling [101]. Total acceleration in three in-place directions (two translations and one rotation) are obtained by assuming four uni-axial accelerometers installed at each floor. Using co-ordinate transformations technique the triad of total acceleration data are obtained at reference point assuming rigid diaphragm [101]. For numerical study on UCLAFB, it is assumed that the position of accelerometers is same in all floors and is shown in Fig. 4.9b. The recorded response u_1, u_2, v_1, and v_2 from each floor are used to obtain the storey accelerations in translation directions u_0, v_0, and torsional direction θ_0 at the reference point using the set of following kinematic relation:

$$u_1 = u_0 - y_1\theta_0, \quad u_2 = u_0 - y_2\theta_0, \quad v_1 = v_0 - x_1\theta_0 \quad \text{and} \quad v_2 = v_0 - x_2\theta_0 \tag{4.5}$$

where x and y are the respective coordinates of the assumed accelerometer position from reference point at which the story accelerations are calculated. The set of equations presented in Eq. (4.5) is an over-constrained system where the number of equations are greater than the numbers of unknown and the least-squares solution of these equation is obtained as:

$$\begin{bmatrix} u_0 \\ v_0 \\ \theta_0 \end{bmatrix} = \begin{bmatrix} 1 & 0 & -y_1 \\ 1 & 0 & -y_2 \\ 0 & 1 & -x_1 \\ 0 & 1 & -x_2 \end{bmatrix}^{\dagger} \begin{bmatrix} u_1 \\ u_2 \\ v_1 \\ v_2 \end{bmatrix} \tag{4.6}$$

where, $[\cdot]^{\dagger}$ represents the Moore-Penrose pseudo inverse [100]. Thus the estimated storey acceleration in translation and rotational directions are used for modal identification.

4.2.2 Modal Identification using Recorded Data

In this study, we consider the recorded building response during the 28 September 2004 Parkfield, CA earthquake ($M_w \sim 6.0$) which had epicentre located about 260 km from the UCLAFB. The recorded peak acceleration at the roof level was 0.0025 g in the EW direction. The use of such a small intensity shaking minimizes other influences like, soil-structure

interaction, response of non-structural components, etc. and the performance of the identification algorithm can be judged easily. The same set of data has been used in several other studies providing a good pool of independent results for comparison. The building response has also been computed analytically via a finite element model. The analytically computed building response from finite element model is compared with the recorded response data during the Parkfield earthquake. The total acceleration time histories recorded at the roof, and those computed from finite element model, along EW, NS and torsional directions are shown in Fig. 4.9. A good agreement between these sets of time histories in EW and NS directions affirms the fidelity of the finite element model. However in torsional direction the magnitude of response from analytical model are an order of magnitude lower than those estimated from recordings. Further, the torsional component derived from records seems to be affected by measurement noise as reflected by high frequency jitters.

4.2.3 Comparison of SST, EMD and SOBI Source Separation Procedures

Similar to SST scheme, empirical mode decomposition (EMD) procedure also deals with the decomposition of signal into the numbers of components called intrinsic mode functions (IMFs) using iterative sifting procedure. The first three lowest frequency IMFs in each EW, NS and Torsional direction obtained using EMD procedure from recorded roof response of UCLAFB are shown in Fig. 4.10 along with the BSS estimates from SST and SOBI formulations. The analytically computed modal contributions from the first nine modes (three in each EW, NS and torsional direction) are also shown for comparison. The agreement between identified BSS sources and the modal acceleration from finite element model is very good, the IMF from EMD does not suggest any relationship with the modal characteristics. Further, the source identified by SOBI captures the frequency characteristics reasonably well, but the amplitudes in time-domain are much smaller than the true modal response amplitudes. This is due to the formulation of SOBI which identifies independent sources within a scaling factor. The source identified by SST procedure, on the other hand, retains the fidelity with true modal response in frequency as well as in time-domain amplitude and can, therefore, be used for estimating mode shapes as well —as described earlier in the preceding chapter. The modal response corresponding to torsional modes, however, shows some discrepancies.

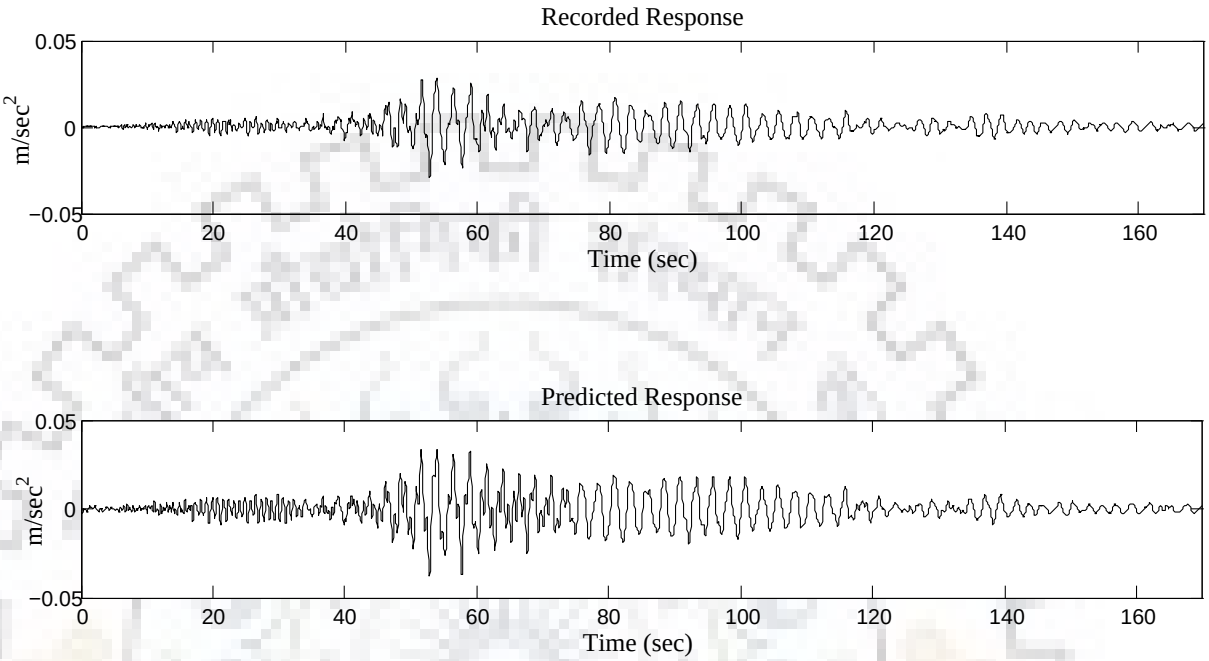

(a) EW-Direction

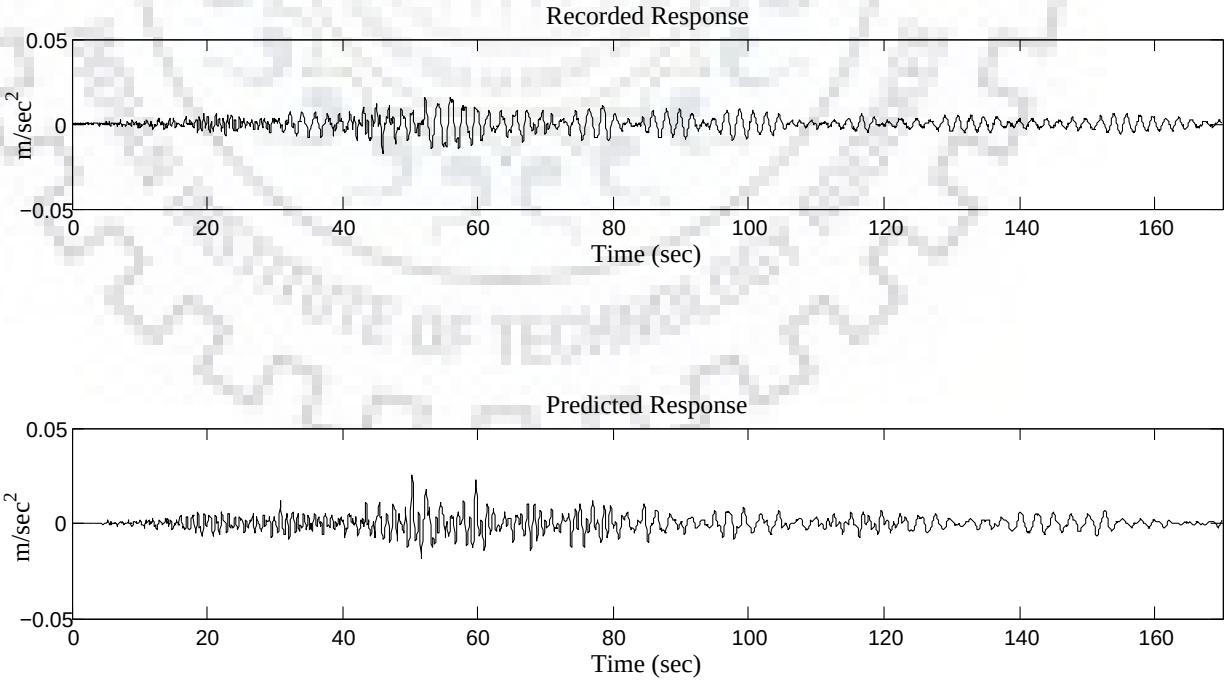

(b) NS-Direction

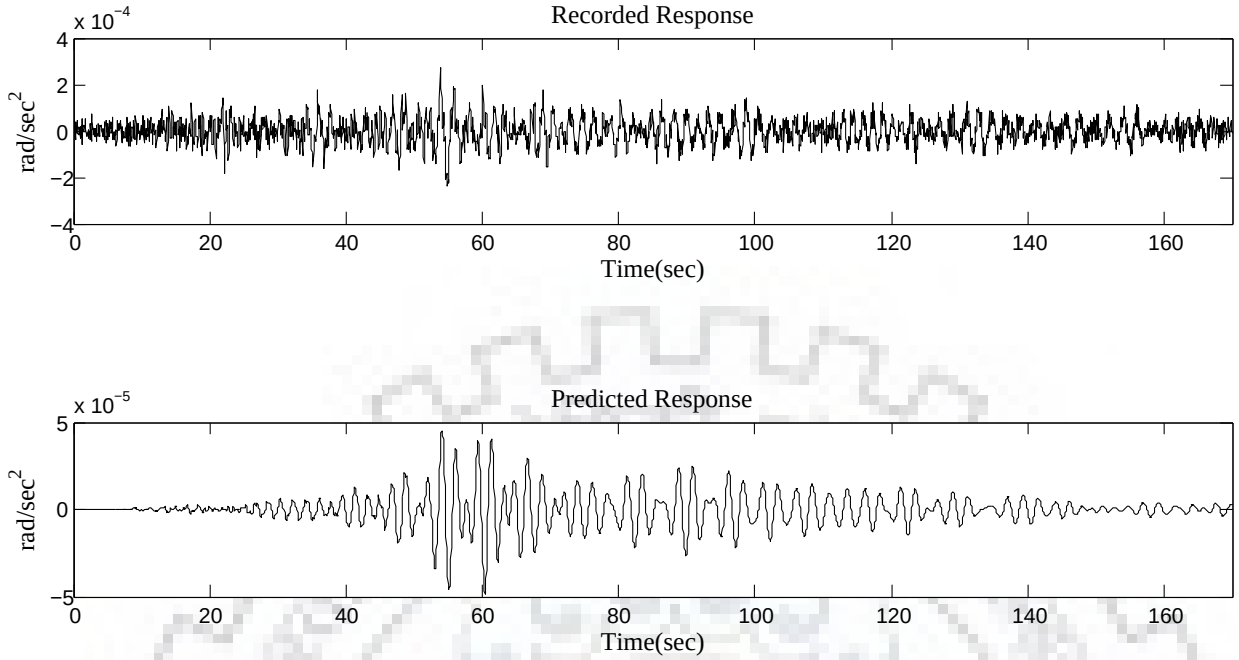

(c) Torsion-Direction

Fig. 4.9. Recorded roof acceleration and prediction from finite element model

4.2.4 Modal Identification Results

SST identified source components represent the modal components in true strength to the extent of their contribution in forming the total response. The mode shapes coefficients are estimated as the time average of instantaneous ratio (normalization) of SST identified sources with respect to the source component of a reference degree of freedom where the mode shape coefficient is assumed to be unity. The natural frequency and modal damping are estimated by post-processing of the identified modal response. The SST based identified modal parameters results are compared with the identified results from BSS based SOBI procedure and the wavelet based modified cross correlation (WMCC) results addressed by [37] on the same dataset. The detailed formulation of WMCC procedure is given in APPENDIX B.

Estimation of Natural Frequencies

The natural frequencies are estimated by the peak-picking method using Fourier transform of the identified sources. The estimated natural frequencies of first five modes, in each EW, NS and torsional direction are tabulated in Table 4.4. The free vibration results of the finite element model are tabulated as *Analytical*, while the SST-based and SOBI-based

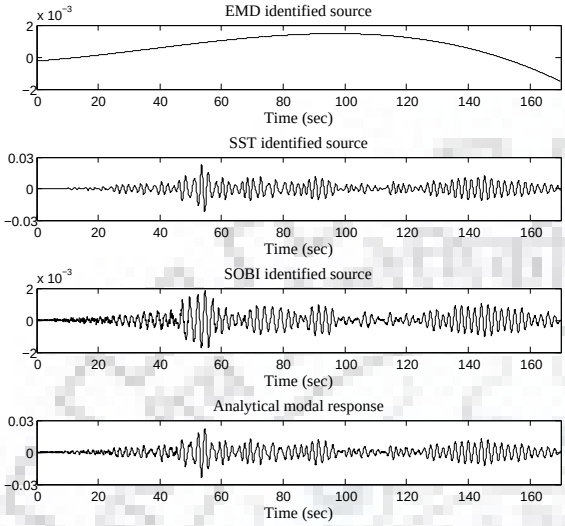

(a) Time domain

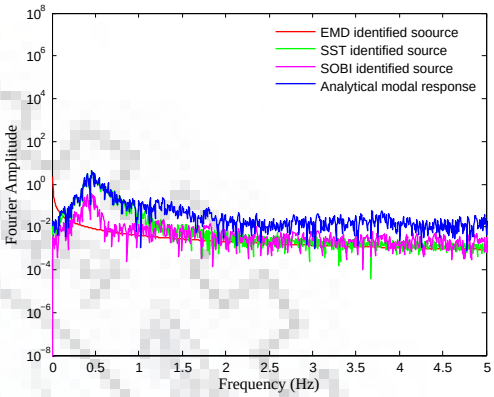

(b) Frequency Domain

Source 1 (EW-Direction)

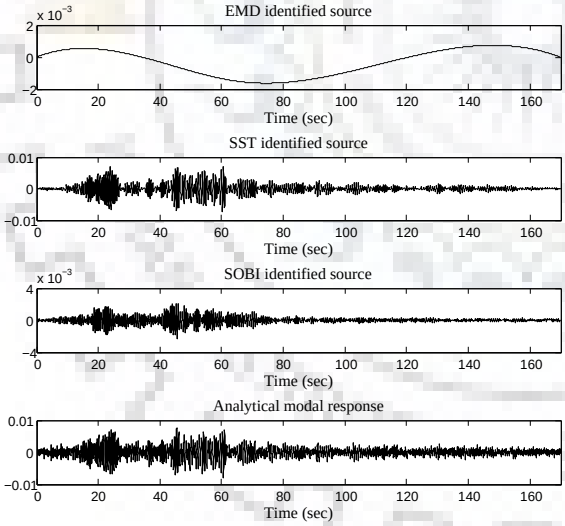

(c) Time domain

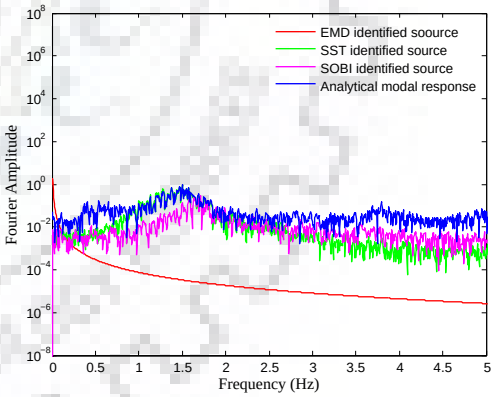

(d) Frequency Domain

Source 2 (EW-Direction)

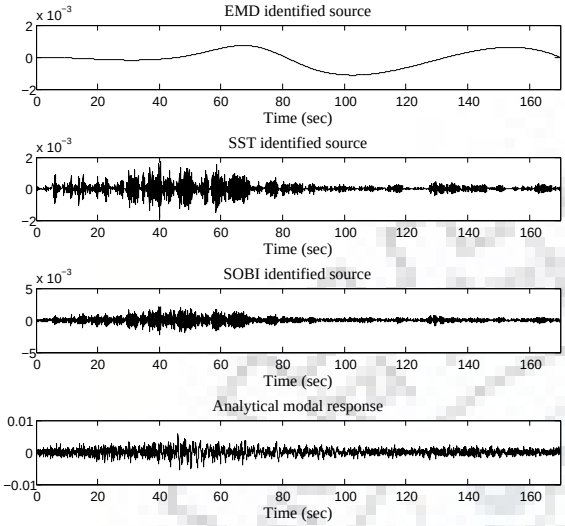

(e) Time domain

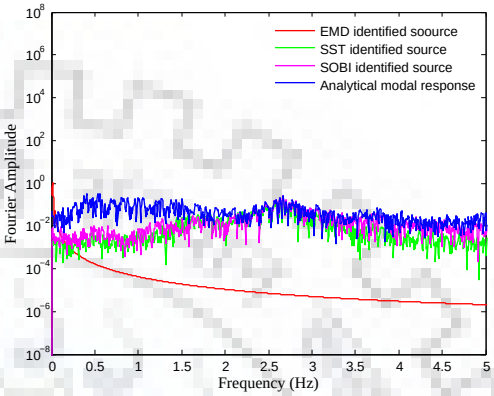

(f) Frequency Domain

Source 3 (EW-Direction)

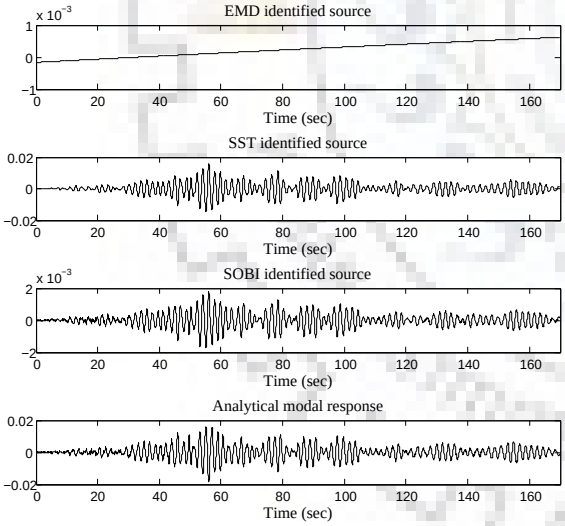

(g) Time domain

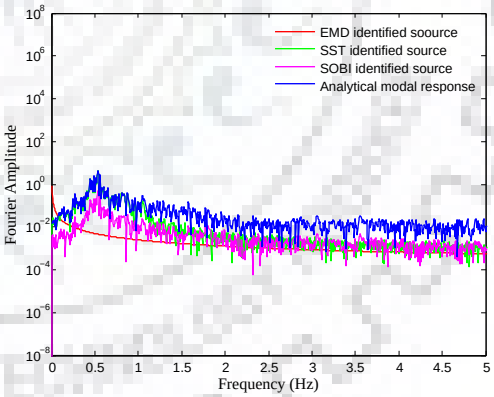

(h) Frequency Domain

Source 1 (NS-Direction)

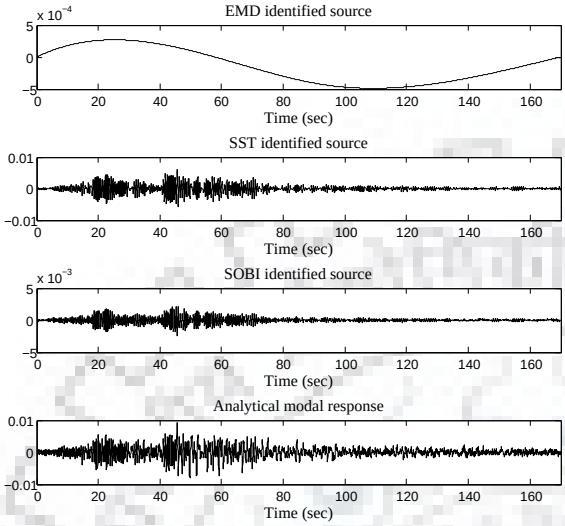

(i) Time domain

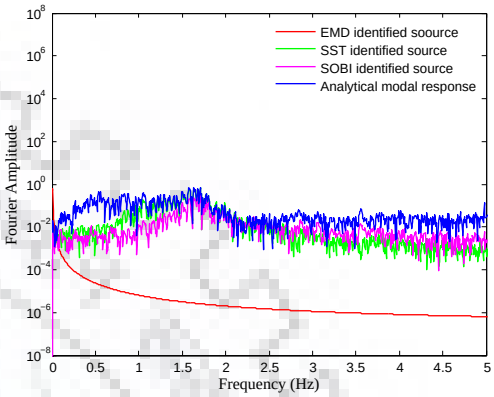

(j) Frequency Domain

Source 2 (NS-Direction)

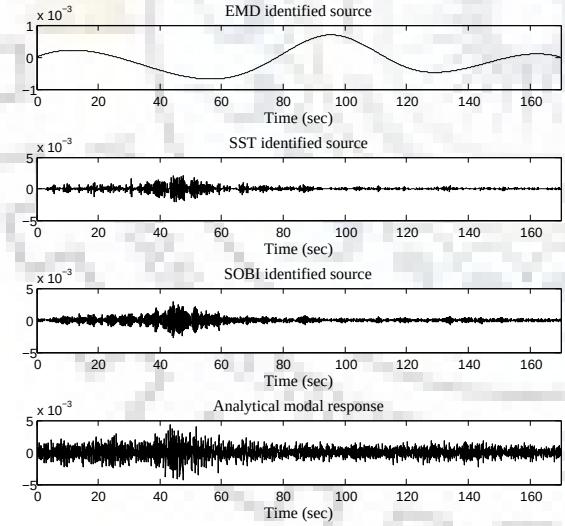

(k) Time domain

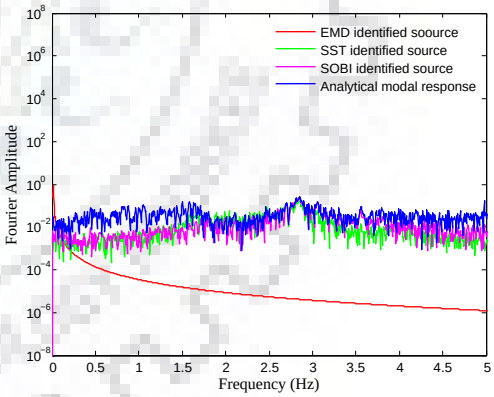

(l) Frequency Domain

Source 3 (NS-Direction)

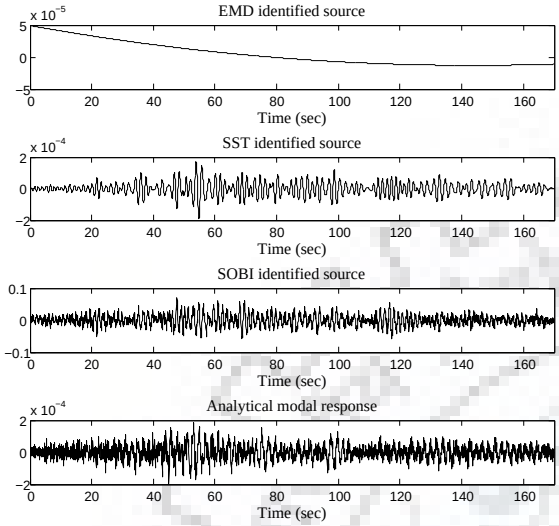

(m) Time domain

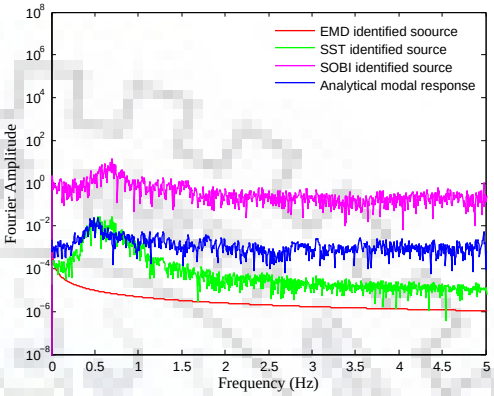

(n) Frequency Domain

Source 1 (Torsion-Direction)

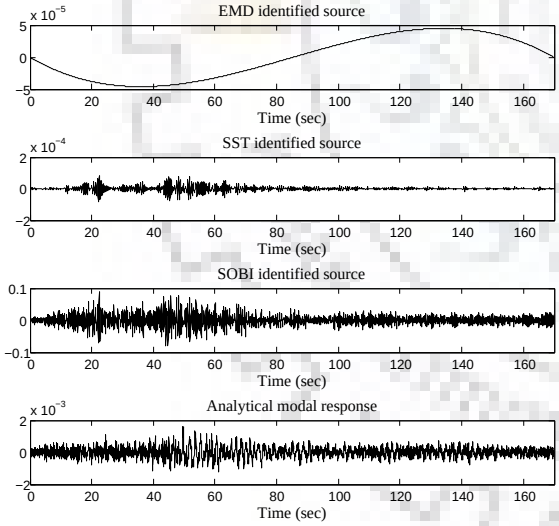

(o) Time domain

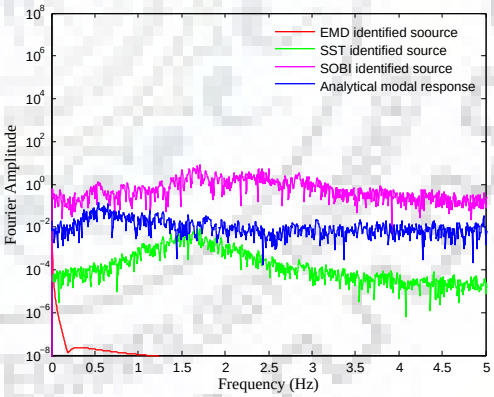

(p) Frequency Domain

Source 2 (Torsion-Direction)

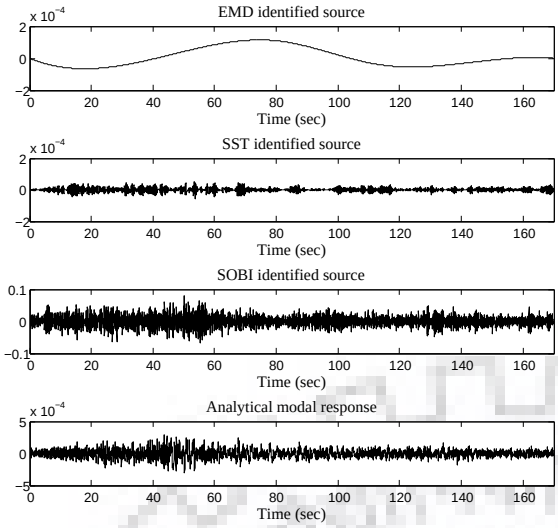

(q) Time domain

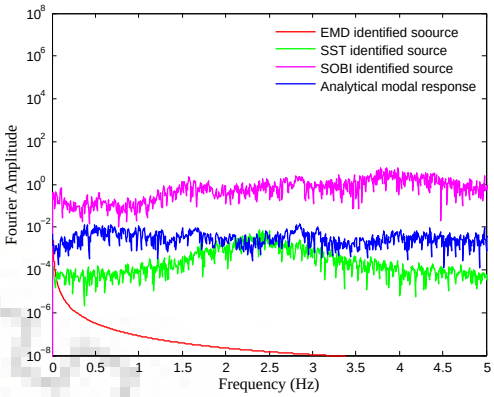

(r) Frequency Domain

Source 3 (Torsion-Direction)

Fig. 4.10. Identified sources from different schemes using roof level response

modal identification results are tabulated under the columns *SST* and *SOBI*, respectively. The WMCC results are adapted from Hazra *et* al. for wavelet based modified cross correlation method using the same dataset [37]. The estimated natural frequencies by different BSS procedures are comparable to each other, and consistently higher than the frequencies predicted by the finite element model. This discrepancy might be due to limitations in the modelling of skeletal structural frame ignoring the stiffness contributions of non-structural components.

Estimation of Mode Shapes

The mode shape vectors are obtained by taking ratios of the sources identified from different floor levels as described in the preceding chapter. The mode shapes are estimated from the identified harmonic components by Eq. (3.22). These identified mode shapes are compared with those obtained from the calibrated finite element model of the UCLAFB and SOBI identified mode shapes. The mode shape plots for first three modes in each EW, NS and torsional direction identified from SST, SOBI and analytically computed mode shapes are shown in Fig. 4.11. The modal assurance criterion (MAC) for the first three modes of finite element model in each EW, NS, and torsional direction with those estimated by the SST-based modal identification and also between SST and SOBI estimates are shown in Table 4.5. The WMCC estimates for mode shapes are not available in the numerical form to facilitate MAC computations. Large MAC values confirm the consistency of estimated

Table 4.4. Natural frequencies (in Hz) of UCLA Factor building from Parkfield earthquake

Mode	Analytical			SOBI			WMCC			SST		
	EW	NS	Tor	EW	NS	Tor	EW	NS	Tor	EW	NS	Tor
1	0.39	0.40	0.56	0.45	0.54	0.65	0.47	0.51	0.68	0.46	0.54	0.70
2	1.16	1.22	1.64	1.49	1.68	2.37	1.5	1.70	2.37	1.50	1.71	2.38
3	1.95	2.13	2.74	2.67	2.85	3.82	2.67	2.88	3.83	2.67	2.85	3.78
4	*	*	*	4.35	4.98	5.19	4.20	4.55	5.00	3.88	4.37	4.59
5	*	*	*	6.24	6.41	7.27	5.31	5.69	6.19	5.32	5.51	5.57

$*$ the finite element model shows local modes after mode # 9.

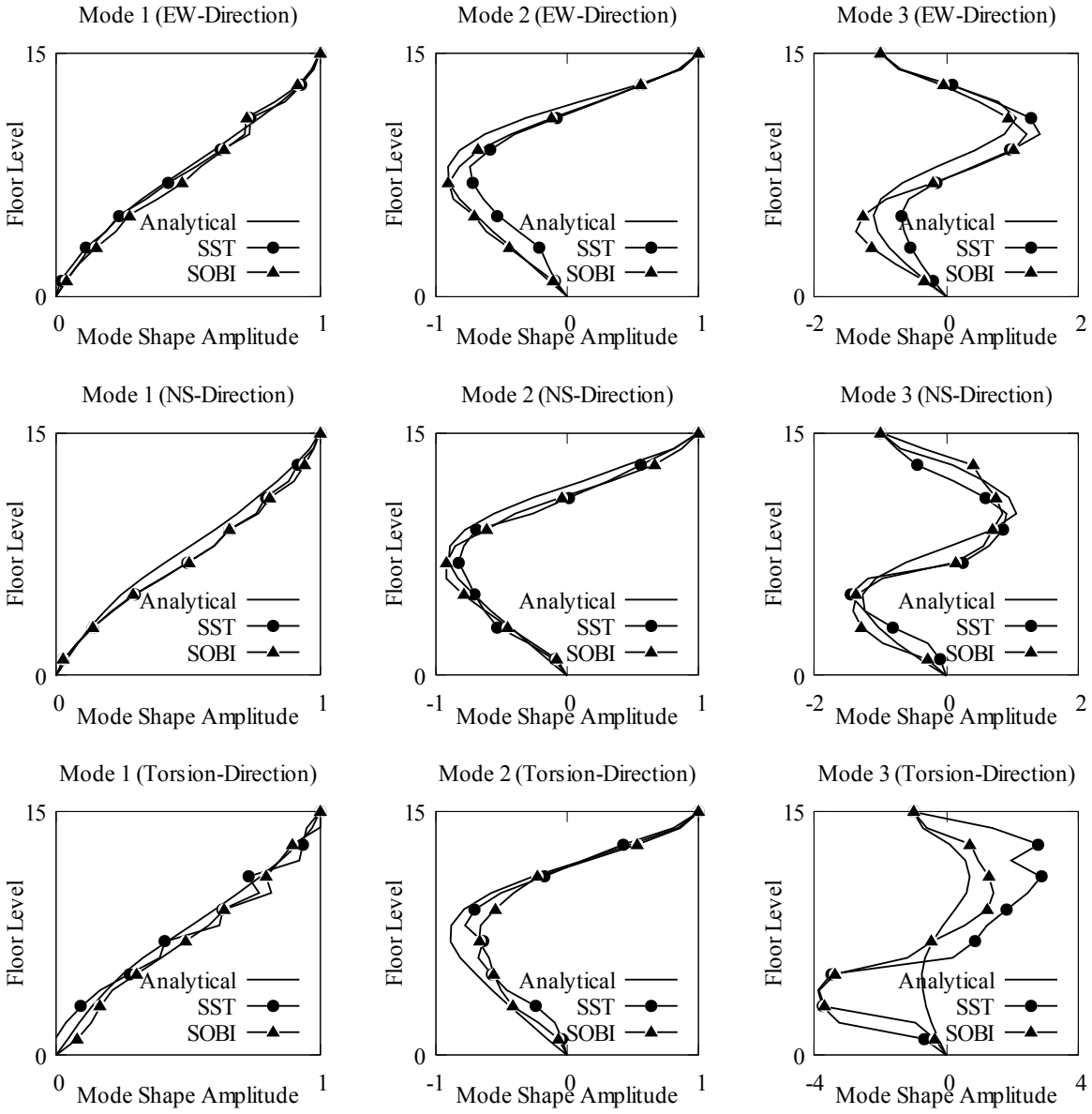

Fig. 4.11. Identified mode shapes for the Parkfield earthquake

Table 4.5. Modal assurance criterion (MAC) of UCLA Factor building from Parkfield earthquake

Mode	MAC1			MAC2		
	EW	NS	Tor	EW	NS	Tor
1	0.98	0.99	0.96	0.99	1.00	0.98
2	0.86	0.95	0.80	0.92	0.96	0.88
3	0.78	0.80	0.30	0.86	0.89	0.76

MAC1: FEM and SST estimates;

MAC2: SOBI and SST estimates

mode shapes from the vibration data. The mode shapes identified by SST- and SOBI-based procedures are in very good agreement and reinforce the validity of the simple mode shape estimation procedure proposed in this study. The SST identified modes shapes have good correlation with the analytical and SOBI identified shapes for all modes in each EW, NS, and torsional direction except for higher torsional mode. Poor quality of torsional modes may be because of insufficient energy in those modes in the dynamic response.

Estimation of Modal Damping

The modal damping is estimated by fitting the exponential decay function to the tail portion to estimated modal coordinates as proposed in Section 3.6.3. Figure 4.12 shows the damped exponential fit for the extracted tail data (normalized with respect to peak value) for the first three modes in each EW, NS and torsion direction identified by the SST procedure. A similar damped exponent fit for the tail data has also been obtained for sources identified via SOBI procedure. The modal damping estimates for sources identified by SST-based formulation are compared with those for SOBI and WMCC schemes (as reported in [37]) in Table 4.6. The estimates from different procedures are generally consistent with each other and estimated damping ratios are range bound considering that the modal damping is always an elusive parameter to estimate. For higher modes, the estimates of modal damping are generally much higher indicating the diminishing reliability of the identified modal parameters from identified sources with very small amplitudes. The SST identified results are in line with the results from other statistical BSS procedures like SOBI and WMCC. This shows that the non-statistical synchrosqueezed transform procedure provides an alternative to statistical based BSS procedure where, the implementation is not sensitive

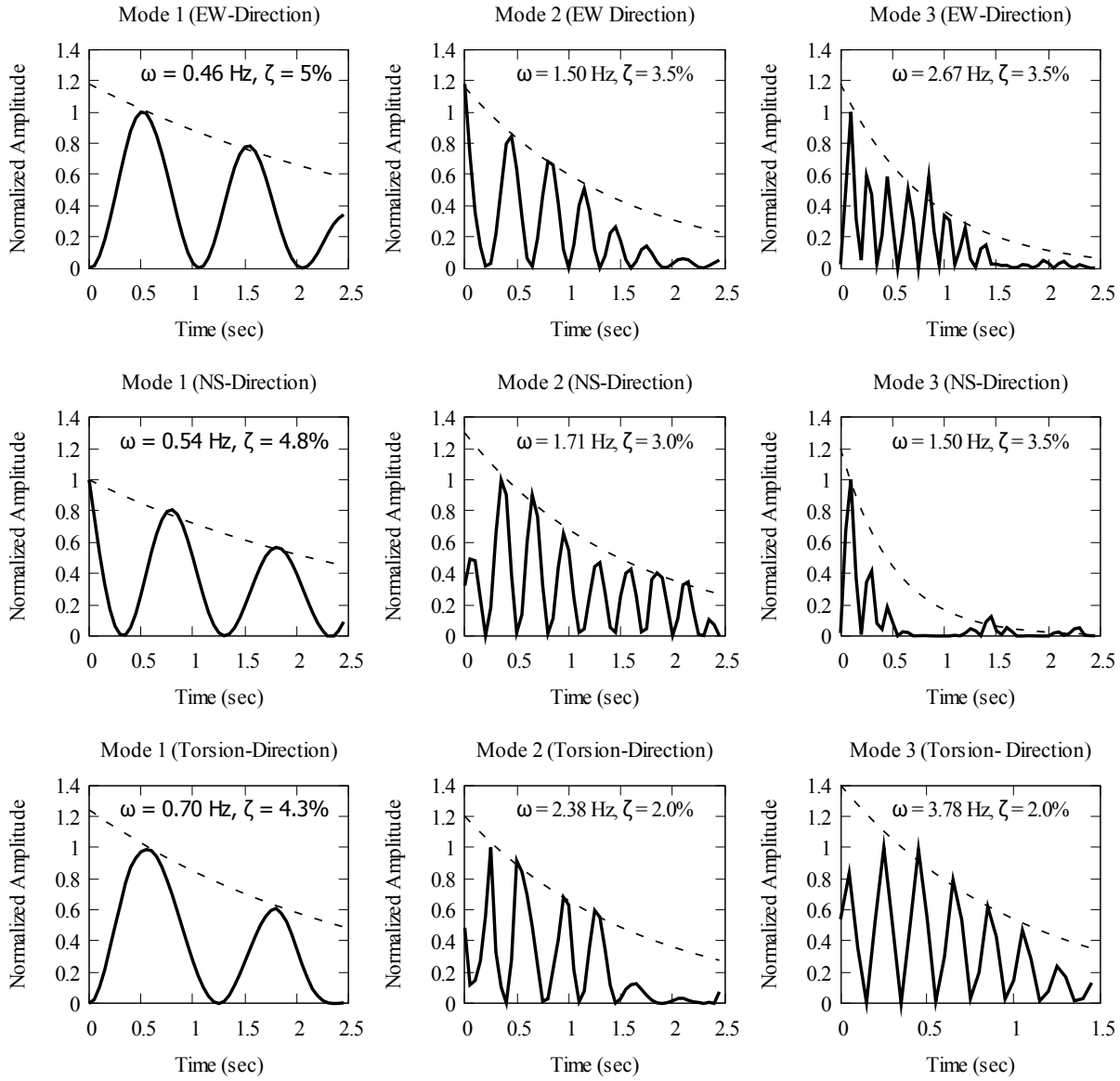

Fig. 4.12. Fitting of SST-based identified tail portion of sources with damped free vibration envelope

Table 4.6. Modal damping (%) of UCLA Factor building from Parkfield earthquake

Mode	SOBI			WMCC			SST		
	EW	NS	Tor	EW	NS	Tor	EW	NS	Tor
1	4.0	4.5	4.8	3.4	3.2	3.4	5.0	4.8	4.3
2	2.0	3.2	2.2	3.3	3.4	4.3	4.0	3.0	2.0
3	2.5	3.8	2.0	2.8	3.3	3.0	3.5	4.5	2.0

to the choice of operating parameters like the choice of time lag and the assumptions of Gaussianity, stationarity.

4.3 Numerical Study on UCLA Factor Building

In the preceding section, modal parameters are estimated by applying the SST based modal identification to UCLA Factor Building subjected to small amplitude Parkfield earthquake and compared the identification results with SOBI identified and available data from other researchers work. To validate the performance and to ascertain the robustness of SST based modal identification procedure UCLA Factor Building is further analysed numerically for different sets of earthquake ground motions. The performance of SST based modal identification to noisy measurements data is also examined. The dynamic response of the UCLA Factor Building finite element model has been computed for a suite of ground motions from Loma Prieta, Hector Mine and Northridge earthquakes. The details of the ground motion suite used for analysis is given in Table 4.7 and Fig. 4.13. The acceleration response obtained using Eq. (4.6) at each floor is considered as the vibration signature for modal identification purpose. The response along the EW axis at top floor for the Northridge event, its synchrosqueezed transform and the extracted harmonics are shown in Fig. 4.14. The four identified sources add up to 98% of the total energy of the measured total acceleration response. The modal frequencies are identified from the Fourier transform of these extracted components while the damping ratio can be estimated from the analysis of their tail portions.

4.3.1 Estimation of Mode Shapes

The mode shapes coefficients are estimated as the time average of instantaneous ratio (normalization) of SST identified sources with respect to nth level source component as given by Eq. (3.22). When UCLA Factor Building was analysed, for different suits of earthquakes, numerical instability was been observed in the identified mode shapes. Figure 4.15 shows the mode shapes for the Northridge event. The plot shows poor correlation between some of the analytical and SST identified mode shapes. Similarly for other earthquakes also some discrepancies in mode shapes have been observed whereas the frequency information in all cases are in line with analytical frequencies. The discrepancies in mode shapes are related to the sudden large amplitude at a particular floor level this may be due to the normalization procedure (i.e., normalization with respect to nth floor sources).

Table 4.7. Ground motions considered for numerical modal analysis

S. No.	Event Name, Date and Station	M_w	R (km)	PGA (g)	f_c (Hz)	Sampling Rate (sps)
1	Loma Prieta, Oct. 18, 1989, Hollister South & Pine	7.1	15	0.37 ($H1$), 0.18 ($H2$), 0.19 (V)	1.03	200
2	Northridge, Jan. 17, 1994, Simi Valley-Katherine Rd	6.7	48	0.80 ($H1$), 0.54 ($H2$), 0.40 (V)	2.04	100
3	Hector Mine, Oct. 16, 1999, Hector	7.1	27	0.27 ($H1$), 0.33 ($H2$), 0.14 (V)	3.44	100

(M_w: Moment magnitude, R: Epicentral distance, PGA: Peak ground acceleration, f_c: Characteristic frequency)

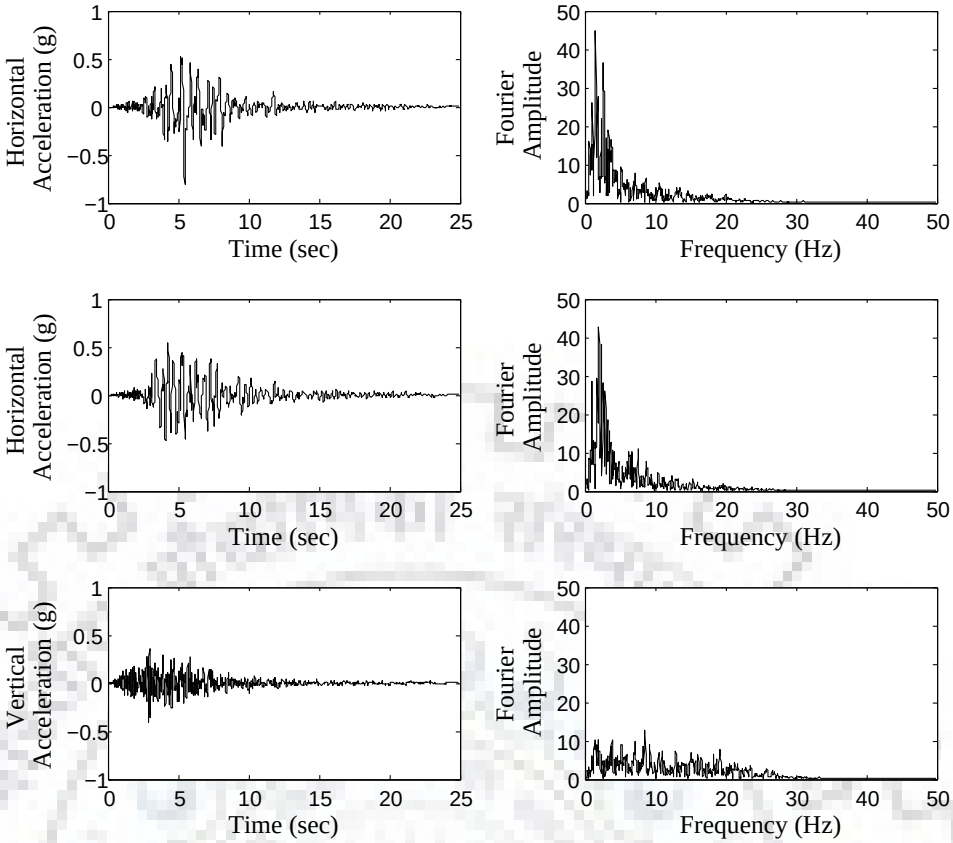

(a) Northridge

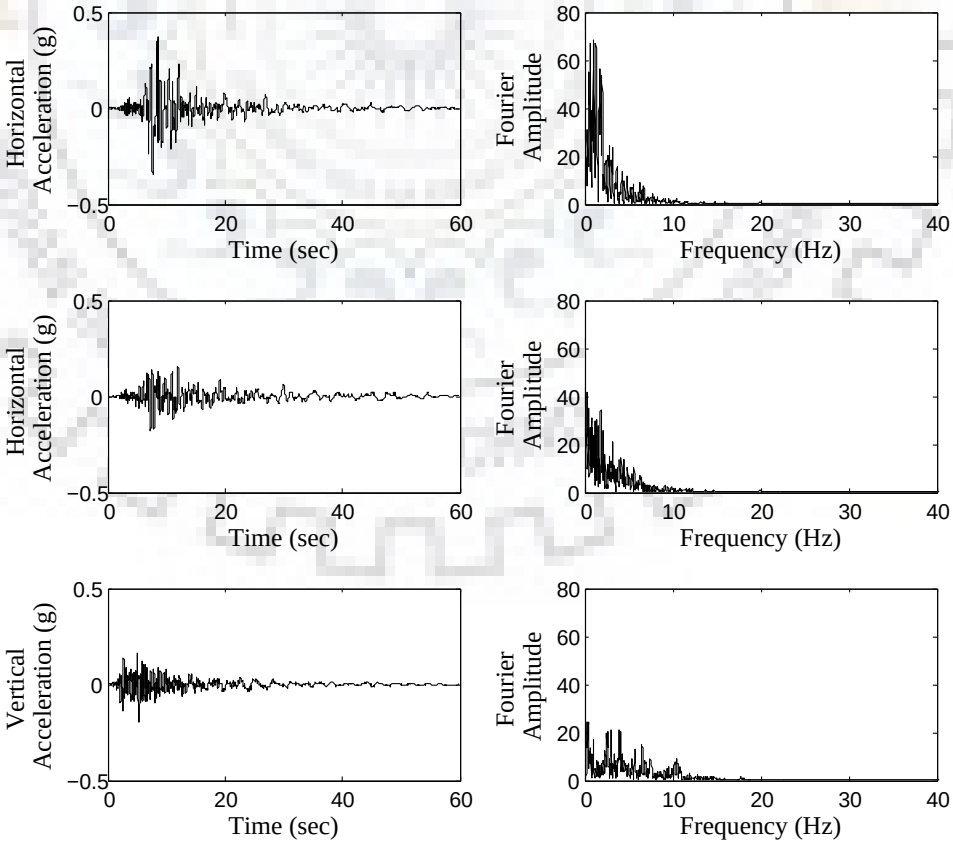

(b) Loma Prieta

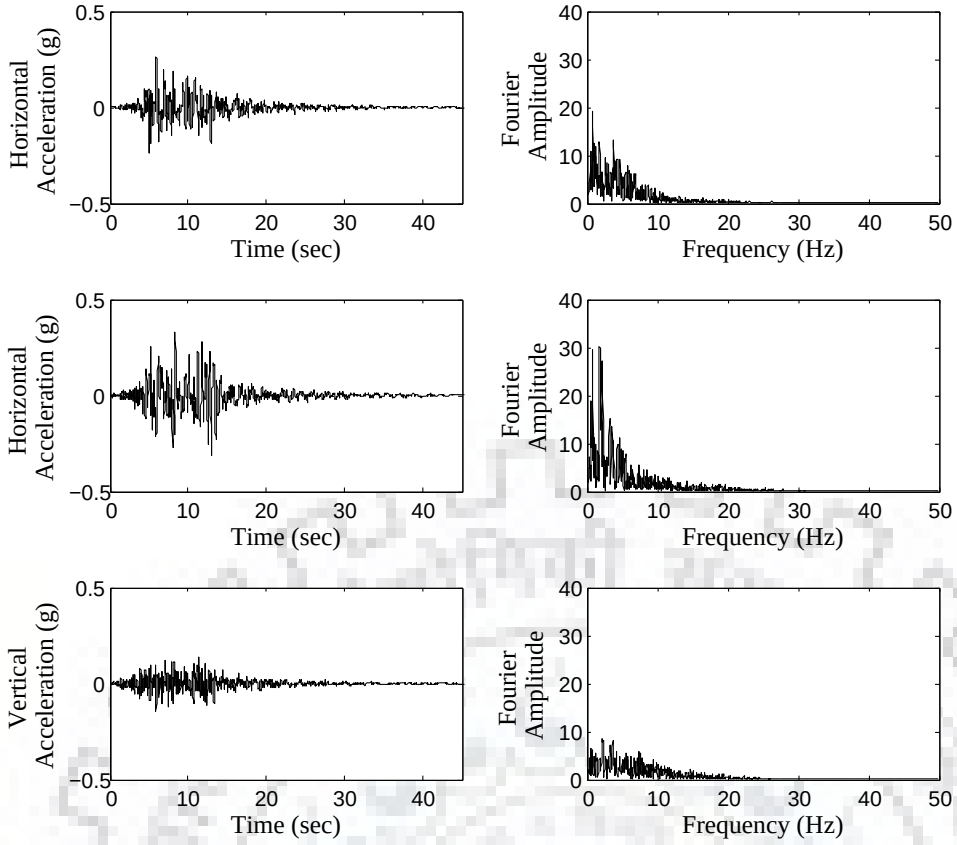

(c) Hector Mine

Fig. 4.13. Earthquake ground motion and Fourier spectrum

Table 4.8. Modal assurance criteria (MAC) values for different earthquake

Ground Motion	Mode 1			Mode 2			Mode 3		
	EW	NS	Tor	EW	NS	Tor	EW	NS	Tor
Loma Prieta	0.99	0.99	0.98	0.98	0.74	0.89	0.77	0.81	0.33
Northridge	0.99	0.99	0.99	0.87	0.99	0.99	0.93	0.72	0.09
Hector Mine	0.99	0.99	0.99	0.92	0.77	0.95	0.89	0.93	0.52

To avoid this computation related discrepancies in the identified results, mode shape estimation procedure is revised by considering normalization with respect to maximum energy component given by Eq. (3.23). The other modal parameters (natural frequency and modal damping) are estimated from post-processing of maximum energy source components as modal coordinates. The identified mode shapes are compared with those obtained from the calibrated finite element model of the UCLAFB are shown in Fig. 4.16 to Fig. 4.18.

A good agreement between the identified mode shapes and analytical mode shape has been observed. Their respective MAC values are listed in Table 4.8. The modal frequencies are identified from the Fourier transform of extracted maximum energy components. The identified modal frequencies are shown in Table 4.9. It is possible to identify up to three

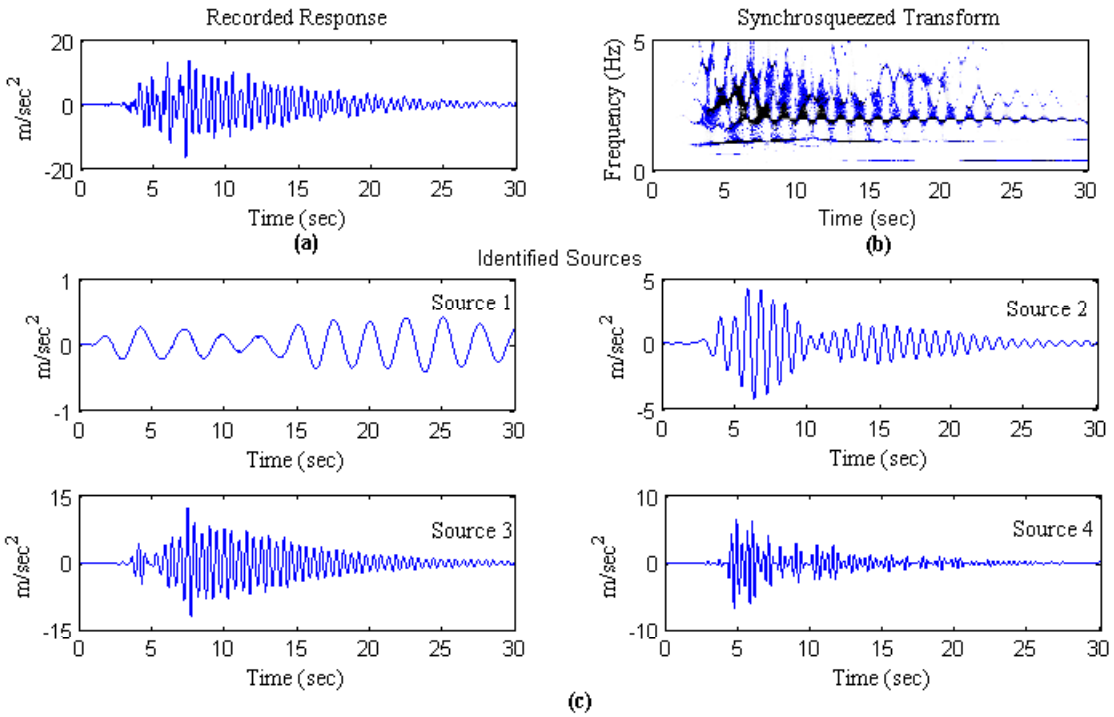

Fig. 4.14. Measured response at the top floor (EW-Direction), its synchrosqueezed transform and the extracted harmonic components (Northridge event)

Table 4.9. Natural frequencies (in Hz)

Ground Motion	Mode 1			Mode 2			Mode 3		
	EW	NS	Tor	EW	NS	Tor	EW	NS	Tor
Loma Prieta	0.38	0.40	0.55	1.13	1.25	1.66	1.91	2.11	2.81
Northridge	0.39	0.40	0.57	1.16	1.24	1.66	1.96	2.12	2.73
Hector Mine	0.40	0.39	0.56	1.16	1.23	1.96	1.96	2.12	2.85

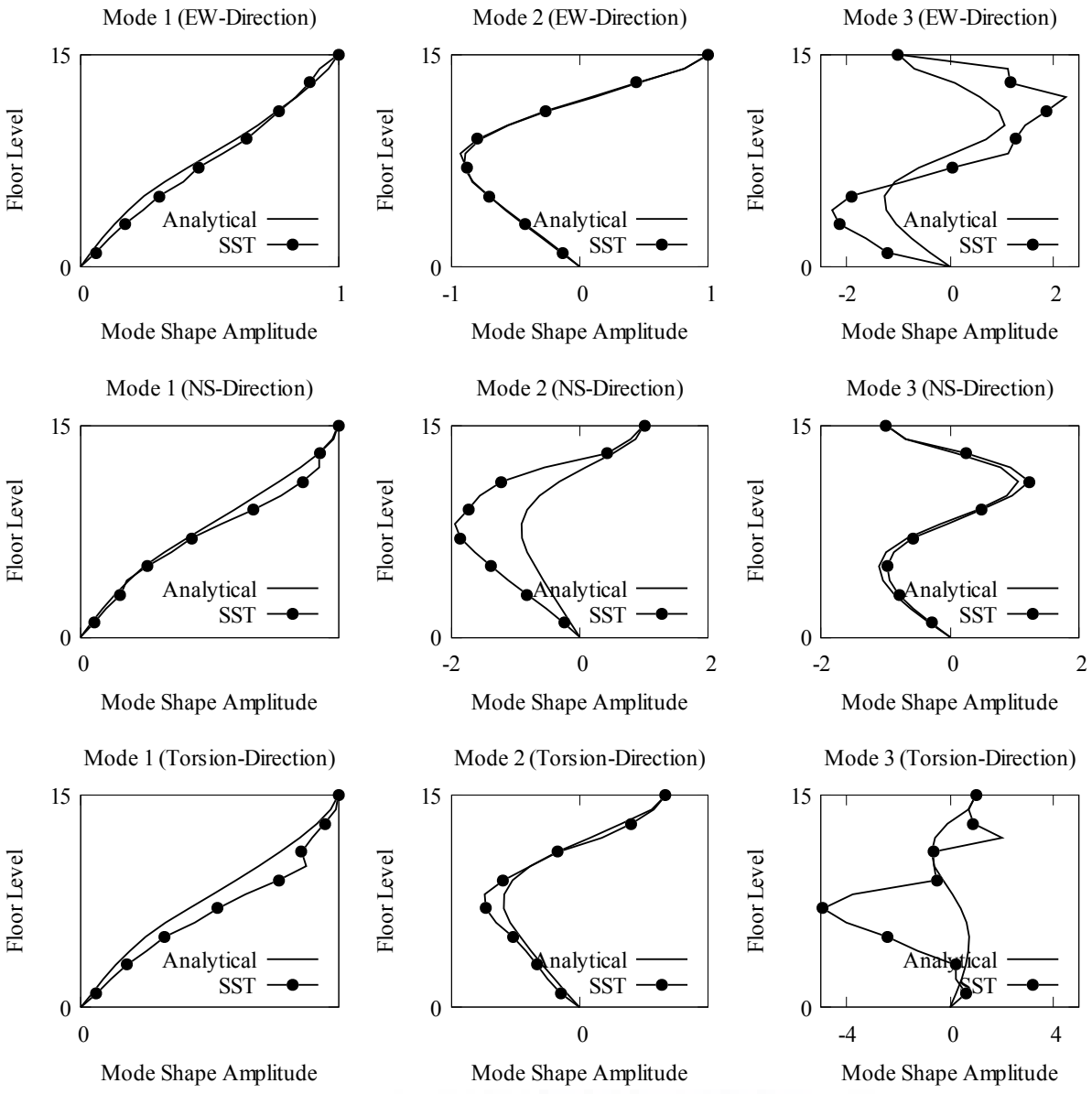

Fig. 4.15. Identified mode shapes in EW, NS and Torsion direction at respective floor levels with reference to top floor level from Northridge event

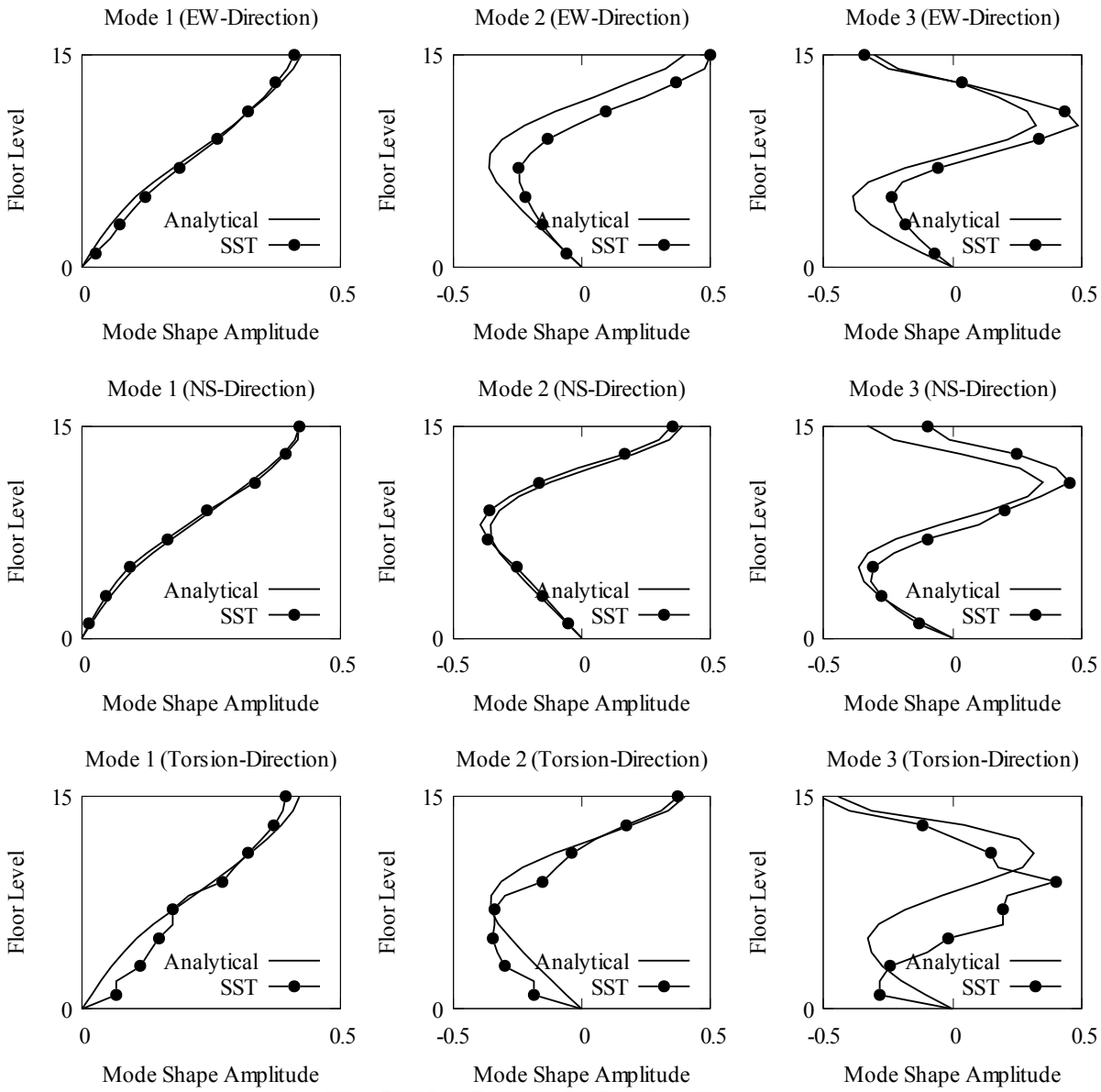

Fig. 4.16. Identified mode shapes in EW, NS and Torsion direction at respective floor levels from Loma Prieta event

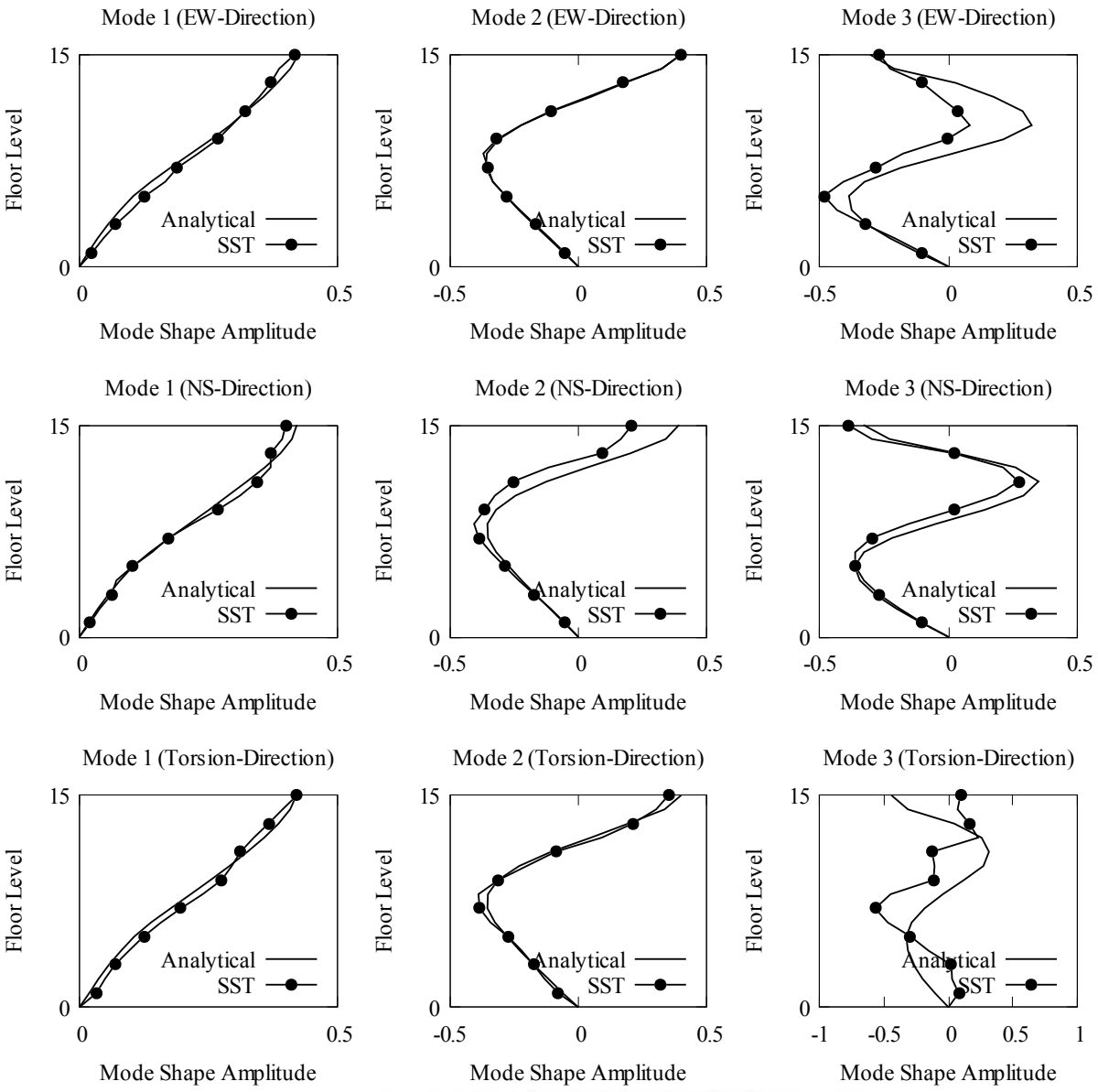

Fig. 4.17. Identified mode shapes in EW, NS and Torsion direction at respective floor levels from Northridge event

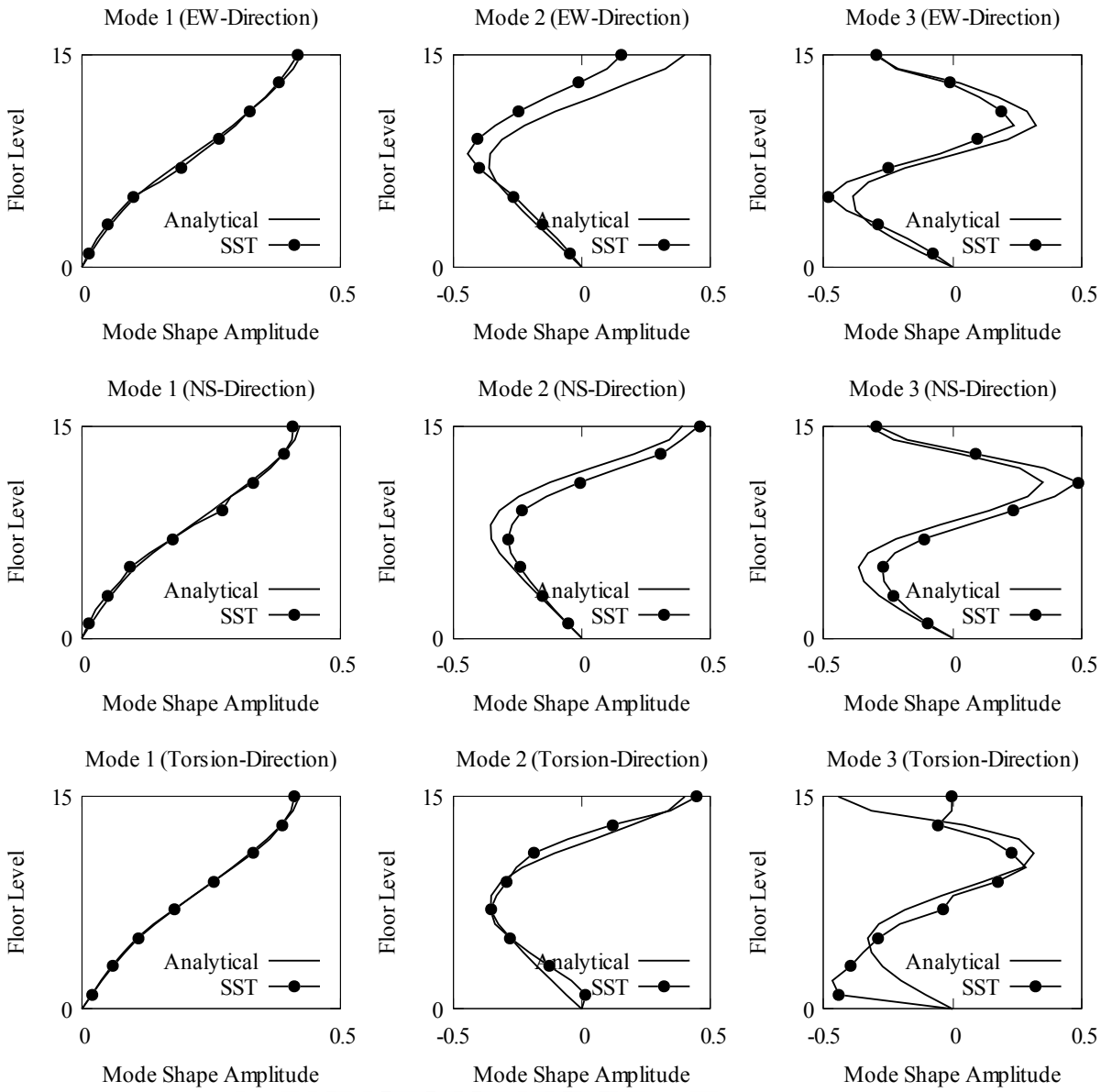

Fig. 4.18. Identified mode shapes in EW, NS and Torsion direction at respective floor levels from Hectormine event

Table 4.10. Modal assurance criteria (MAC) from synthetic Gaussian random noise

Mode 1			Mode 2			Mode 3			Mode 4		
EW	NS	Tor	EW	NS	Tor	EW	NS	Tor	EW	NS	Tor
1.00	1.00	1.00	0.95	0.99	0.94	0.87	0.96	0.56	0.78	0.72	0.26

modes in each NS and EW direction with high fidelity as indicated by the high MAC values. The vibration energy is smeared across a wider frequency band for higher frequencies, and it is difficult to isolate a single harmonic component from the synchrosqueezed transform as seen in Fig. 4.14. The estimated mode shapes for higher modes are therefore less strongly correlated with the mode shapes of analytical model. This is due to the lack of adequate energy in the ground motion in the requisite frequency band for exciting the higher modes of vibration. However, in torsion direction, only two modes are identified in a good correlation with analytical mode shapes. The third mode in torsion direction for all cases has shown poor correlation. The smaller value of MAC in torsion direction may be due to small energy content in torsional direction response.

To analyse the performance of proposed methodology UCLA Factor Building is re-analysed with white Gaussian noise at the sampling rate of 100 Hz for estimating higher modes. The mode shapes are estimated from the vibration response using Eq. (3.23). Sufficiently good correlation between the identified and analytical mode shape has been observed for first four modes in EW and NS direction and only first two modes in torsion direction. Figure 4.19 represents the mode shapes of UCLA Factor Building corresponding to synthetic white noise, and its MAC values are listed in Table (4.10).

4.3.2 Robustness to Noisy Data

The robustness of SST-based modal identification procedure for noisy measurements is verified by adding a Gaussian white noise to analytically computed acceleration time histories at each level for all example cases considered in this study to have a signal to noise ratio (SNR) of 13 dB. The mode shapes are identified for the noisy measurements and the modal assurance criterion computed for noisy data are given in Table 4.11. There is a significant performance degradation for identification of mode shapes beyond the first mode. The noisy measurements are then processed through a wavelet-based denoising procedure before performing the synchrosqueezed transform and subsequent modal identification. A

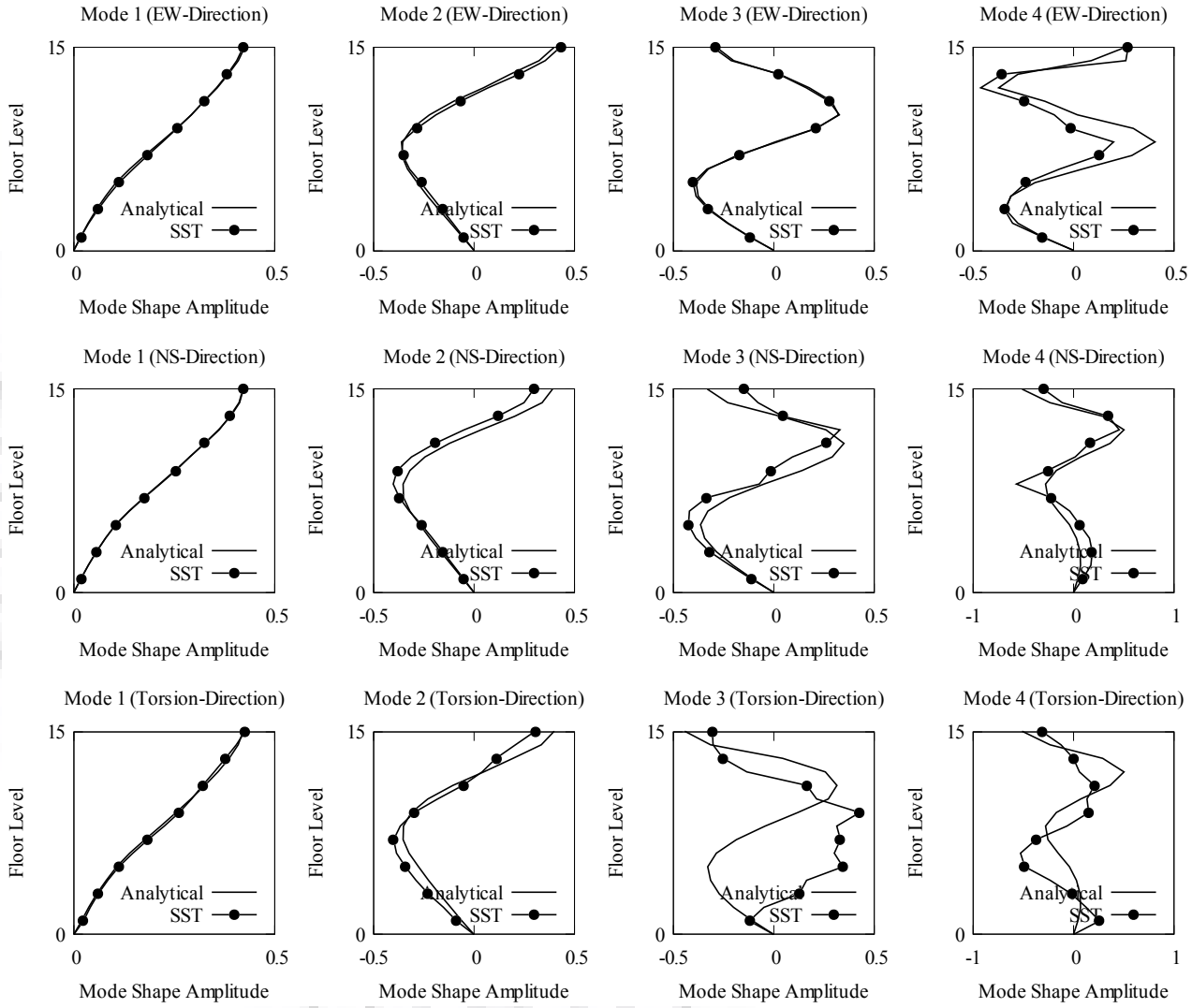

Fig. 4.19. Identified mode shapes in EW, NS and Torsion direction at respective floor levels for Gaussian random noise

major improvement in the quality of the estimated mode shapes after noise removal can be seen in the Table 4.11. The effect of noise is most significant in the Northridge case and the improvement after denoising is maximum in this case as well. The Northridge event is relative short duration event and a lower sampling rate produces fewer data points for discrete time processing of the signals. Fewer data points for processing generally lead to more errors in processing.

Table 4.11. Modal assurance criteria (MAC) values for mode shapes identified from noisy data and after denoising

Ground Motion	Mode	Noisy Data			Denoised Data		
		EW	NS	Tor	EW	NS	Tor
Loma Prieta	1	0.99	0.99	0.96	0.99	0.99	0.99
	2	0.85	0.98	0.25	0.95	0.9633	0.90
	3	0.97	0.98	0.01	0.97	0.97	0.18
Northridge	1	0.99	0.99	0.99	0.99	0.99	0.99
	2	0.80	0.54	0.21	0.87	0.91	0.89
	3	0.65	0.35	0.03	0.93	0.85	0.14
Hector Mine	1	0.99	0.99	0.99	1.00	0.99	0.99
	2	0.70	0.97	0.63	0.90	0.99	0.89
	3	0.57	0.83	0.37	0.90	0.94	0.01

4.4 Concluding Remarks

The performance of SST based modal identification is validated on small numerical model and complex real life building model. It has been observed that the results identified by simple SST based procedures are comparable with SOBI based identified results. The experiment results during small amplitude earthquake from fifteen storey UCLA Factor Building are used for modal identification. The modal contributions to structural response are directly extracted by using synchrosqueezed transform. The corresponding mode shape vectors are then obtained by the normalization of identified modal response from measured data at different floor levels with the one with maximum energy in that mode. A simple and efficient scheme for estimation of modal damping for earthquake excited systems is proposed based on free-vibration idealization of the tail portion of the response. The results are found to be in good agreement with those obtained from analytical model and from other

implementations of BSS modal identification. The robustness of the proposed procedure for modal identification with noisy data is studied and it is shown that a simple de-noising step enhances the fidelity of the modal identification.

Chapter 5

A Moving Window System for Seismic Damage Detection

To demonstrate the utility of SST based modal identification procedure, damage identification study is carried out in this chapter. Modal identification is performed in numbers of non-overlapping time intervals by using modal identification scheme proposed in Chapter 3. The time windows are selected based on the energy distribution of the signal in the time-frequency plane. As the window moves forward, the changes in modal parameters of the structure are tracked to detect changes in the state of structure. Numerical simulation studies are presented on UCLA Factor Building for different earthquake events to demonstrate the validity of the proposed method.

5.1 Background

Important civil infrastructure constitute critical lifeline facilities and their health greatly influences the recovery from a disaster. It is necessary to continuously monitor the health of these critical facilities to keep those operational. With the advancements in communication and sensor technologies coupled with easy availability of computing resources, various structural health monitoring schemes are increasingly being used for periodic health assessment of these large scale systems [31, 35, 10, 19]. Damage in any structural system is defined as a reduction in its load carrying capacity and is associated with stiffness degradation on account of changes in the material and/or geometric properties and boundary conditions. Primary reasons contributing to damage are poor maintenance, environmental conditions and extreme loading events. The damage, if not arrested in time, can grow to render structures unsuitable for occupation. Therefore, damage identification is an important part

of the preventive maintenance operations for enhancing the life of structures. There are generally four levels of damage identification, as defined by Rytter [90]: Level 1: damage detection, Level 2: damage detection and localization, Level 3: detection, localization, and quantification and the last Level 4: includes the prediction of the remaining life of the structure. The damage identification study in this thesis is limited to Level 1.

Vibration-based system identification techniques provide a convenient way to track changes in stiffness and damping properties via identification of modal parameters from the vibration signatures of structural system [32]. Of all modal parameters, namely, natural frequencies, mode shapes and damping ratios, frequencies are the easiest to identify from vibration records and consequently early attempts at structural health monitoring focused on tracking changes in the identified natural frequencies as indicator of damage [94]. However, natural frequencies of large structural systems are relatively insensitive to localized damages/effects and hence the success of natural frequency based procedure is limited to laboratory-scale structures with few damage locations. Since the local effects can be reflected in the estimated mode shapes, some measures such as modal assurance criterion (MAC), and coordinate modal assurance criterion (COMAC) have been proposed to track changes in mode shapes [2, 68, 110]. For bridge structures, the mode shape based damage detection procedures have been reported to be more robust in comparison with frequency based methods [95].The modes shapes based procedures have been also used for damage localization purpose [89, 36]. For detection of damage in beam-like structures, the mode shape curvature has been used [80]. The change in modal strain energy has also been used as an indicator for identifying damages [62, 31]. The mode shape based procedures require measurements from a dense network of sensors at different locations for robust estimation of mode shapes, or use some kind of interpolation to make-up for incomplete measurements [41, 98]. Tracking changes in physical parameters, such as, stiffness, or flexibility have also been considered for identification of damage. The difference in the stiffness matrix obtained from analytical model from the one constructed from modal properties (mode shapes and modal frequencies) is used as the measure for damage identification [40]. Because of the difficulty in estimating higher modes through vibration testing, the derived stiffness matrix is likely to be a poor approximation and consequently the use of a reduced rank approximation of flexibility matrix for damage detection has been proposed [79]. The changes in physical parameters of structural system can also be tracked by using model updating procedures. The model updating procedure deals with modifying the parameters of an analytical model through an optimization algorithm to minimize the differences in

the measured and computed responses [69, 83, 97, 122]. The updating procedures, if they converge, provide information about the locations as well as the severity of the damage. In this study the change in flexibility of the structure is tracked by using a rank-1 update reduced rank approximation along with the change in natural frequencies and mode shape of the structure.

5.2 Motivation

The primary issue in vibration based damage identification procedures is the dependence on prior calibrated analytical models and/or prior test data to serve as a benchmark for comparison. Many algorithms presume access to a detailed finite element model of the structure, while others presume that a data set from the undamaged structure is available [72]. Often, the lack of availability of this type of data can make a method impractical for certain applications [32]. These practical problems motivate the need for a method which extends the concepts damage identification with single event. This is accomplished by analysing a time series in different time windows, rather than the complete data. Modal parameters (frequencies and mode shapes) are identified in all time windows and the parameters corresponding to first window are used as reference parameters.

5.3 Moving Window Analysis

Structural health monitoring involves tracking of changes in the identified system parameters with respect to a reference set representing the healthy state of the system. Such a reference set of parameters may not be always available and in most of the past studies parameters corresponding to an analytical model of the system has been adopted as the reference set. However, analytical modeling of a complex structure is an onerous task, and an unvalidated and uncalibrated model may not be reliable. The modal parameters of a healthy structure may also be susceptible to seasonal variations due to environmental effects and comparison of identified parameters with an inappropriate reference set might be misleading. Since the damage in any structure during a strong earthquake is caused only during intense shaking following the arrival of S-wave, the structural response during the initial P-wave can be considered as the baseline for deriving the reference set for comparison of identified modal parameters to detect damage. The selection of appropriate time window is a crucial step in this exercise as a too small window may not have enough information

to identify modal parameters and a too large window might smear out any changes in the dynamic parameters. The selection of time windows is based on study of the distribution of energy of vibration record in the time-frequency plane for identifying time stretches of significant energy of similar frequency composition. Shiradhonkar and Shrikhande used the spectrogram to select time windows for parametric system identification [97]. We use the synchrosqueezed transform of the signal for selection of time windows because of its capacity to provide very sharp resolution in the time-frequency plane [27]. The response in different time windows is considered to correspond to an equivalent linear model. The objective is to measure the change in the state of the system by tracking the changes in the secant stiffness (reflected in modal parameters) of the system. The numerical study using time windows for damage detection is described in the next section.

5.4 Numerical Simulation

The UCLA Factor Building has been considered for numerical study on detection of damage caused due to strong earthquakes. The details about the UCLA Factor Building is already discussed in Chapter 4. In this study we have assumed the sub-surface condition as hard rock strata and finite element model is modelled using a fixed base foundation, therefore, the site characteristics effects are not accounted for. The UCLA Factor Building response is analyzed for three sets of ground motions corresponding to Northridge, Hector Mine, and Loma Prieta earthquakes respectively representing the near-field, intermediate distance and far-field events. The details of ground motions used for analysis are given in Table 5.1 and Fig. 5.1 [4].

Finite element model of the UCLA Factor Building has been developed in SAP 2000 and validated against the reported modal properties of this building. First nine modes correspond to natural frequencies ranging from 0.39 Hz to 2.74 Hz (see, Table 4.4). The non-linearity in the structure is modeled in terms of plastic hinges defined by FEMA 356 [33]. The total acceleration response is assumed to be the measured vibration signature of the building for further processing. Total acceleration in three in-place directions (two translations and one rotation) are obtained by assuming four uni-axial accelerometers installed at each floor using Eq. (4.5). The linear and nonlinear dynamic response of the UCLA Factor Building model is computed for these ground motions. A random, zero mean, Gaussian white noise is added to the computed acceleration response time histories to have a signal to noise ratio of about 13 dB to simulate noise of recording system and the wavelet

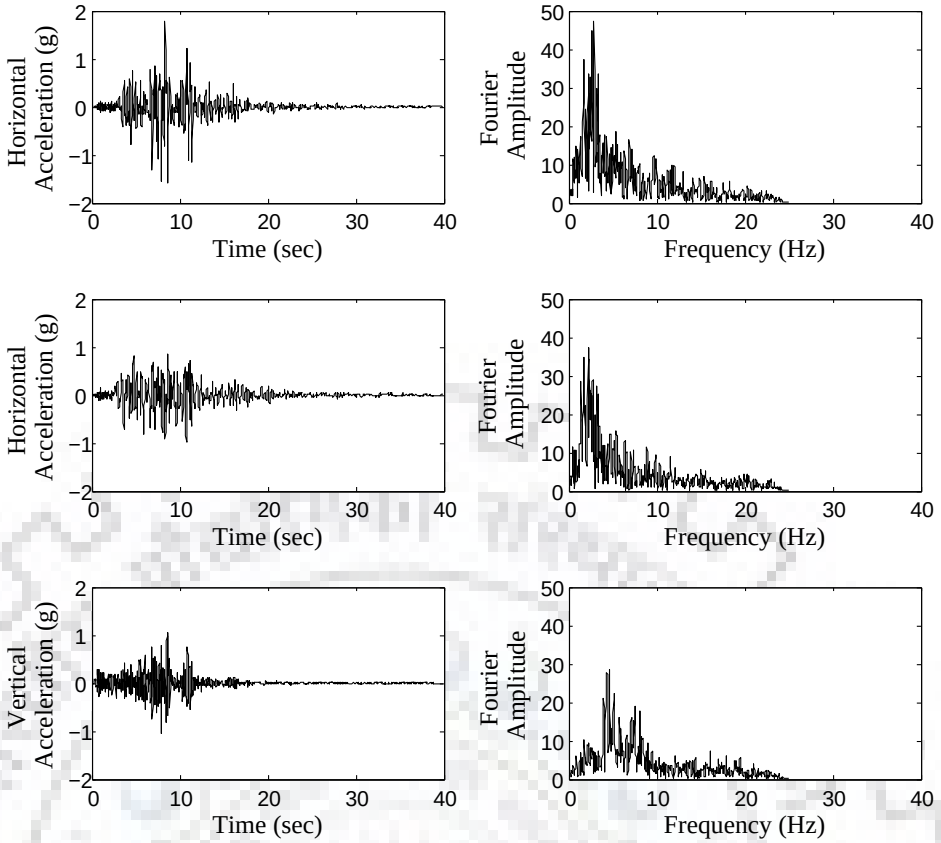

(a) Northridge

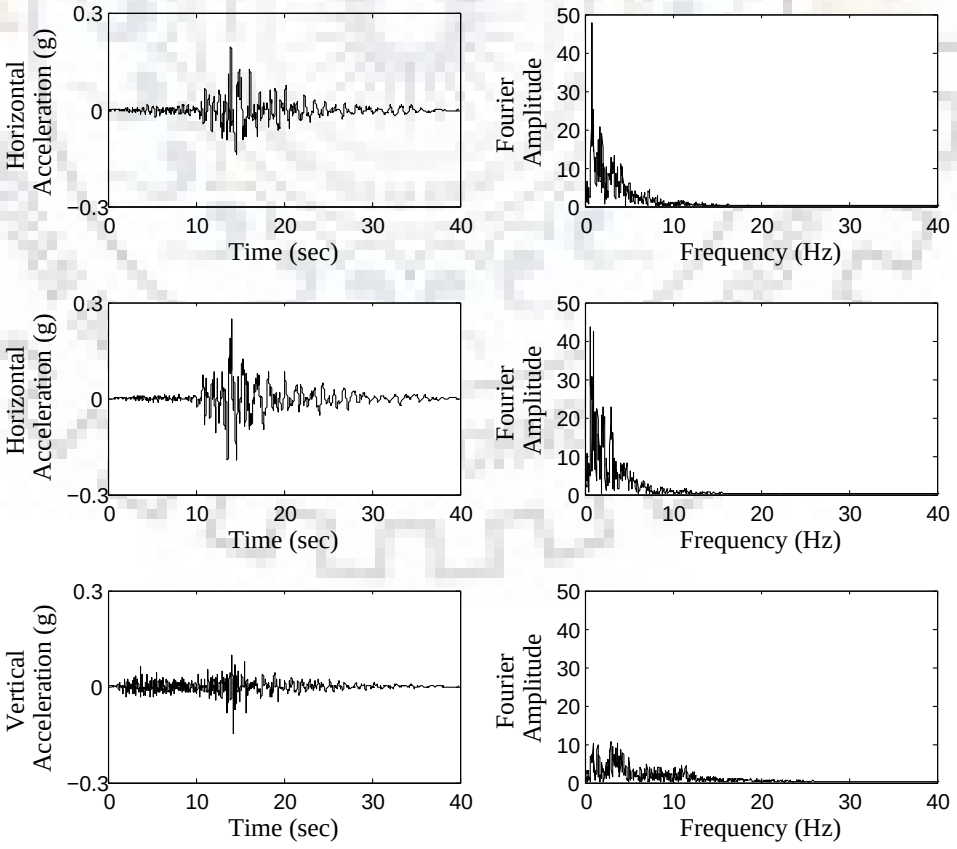

(b) Loma Prieta

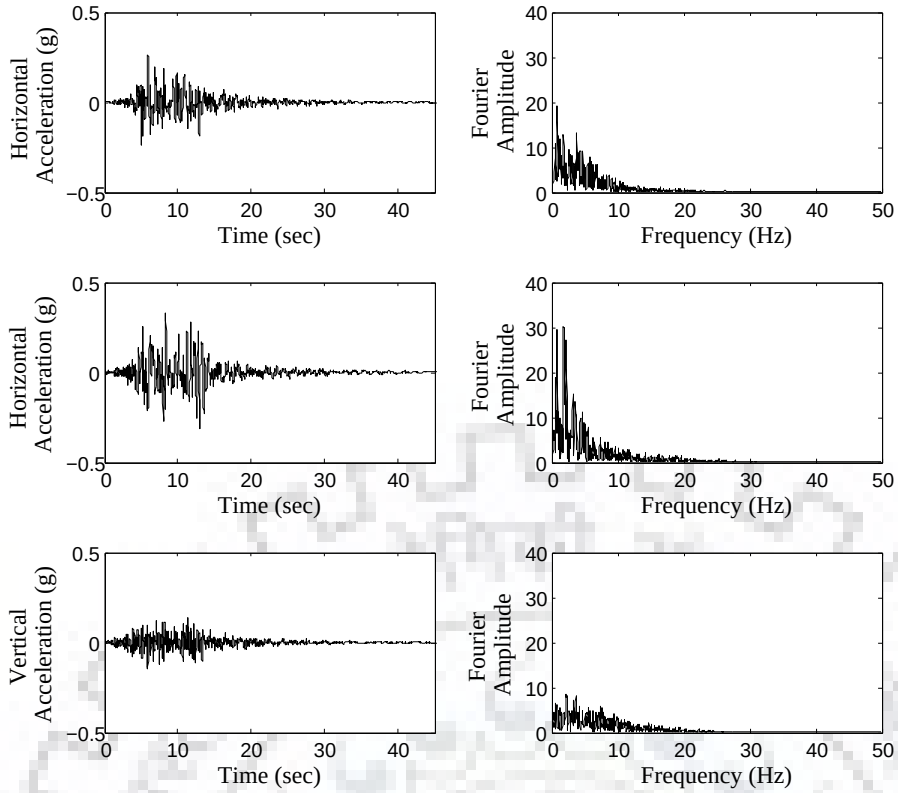

(c) Hector Mine

Fig. 5.1. Earthquake ground motion and corresponding Fourier spectrum for damage identification

Table 5.1. Ground motions considered for analysis

S. No.	Event Name, Date and Station	M_w	R (km)	PGA (g)	f_c (Hz)	Sampling Rate (sps)	Mechanism
1	Northridge, Jan. 17, 1994, Tarzana-Cedar Hill-A	6.7	7	1.8 $(H1)$, 1.00 $(H2)$, 1.04 (V)	2.9	50	Reverse
2	Hector Mine, Oct. 16, 1999, Hector	7.1	27	0.27 $(H1)$, 0.33 $(H2)$, 0.14 (V)	3.44	100	Strike slip
3	Loma Prieta, Oct. 18, 1989, Oakland-Title & Trust	7.1	91	0.19 $(H1)$, 0.25 $(H2)$, 0.15 (V)	0.79	200	Reverse oblique

M_w: Moment magnitude, R: Epicentral distance, PGA: Peak ground acceleration, f_c: Characteristic frequency

based denoising has been applied to noisy time histories before taking those up for modal identification. The linear dynamic response of the finite element model is first considered for validating modal identification from different time windows. The time windows are selected from the recorded response having maximum energy. The SST plots representing the time-frequency distribution of energy of the signal is used for selection of time windows as shown in Fig. 5.2 for the top floor response in EW, NS and Torsion direction for all events. Independent harmonic modal components extracted from these SST representation by using suitable band-pass filters and are shown next to each SST plots. The time windows are selected by examining the temporal distribution of energy in these components. We consider three time windows—W_1, W_2 and W_3—as the first, second and third window, respectively. The length of the data window is an important consideration and is selected by examining the temporal evolution of frequency content in the structural response time history using synchrosqueezed transform. We have observed that for robust estimation of parameters at least 256 sample points are required. In this study, time windows are selected to have at least 256 samples and more or less constant frequency line in the SST plot, except for Northridge case where we had to settle for smaller window owing to smaller sampling rate (50 sps). Smaller time windows for the Northridge earthquake are selected to capture the frequency variation. Selection of windows for each source is based on energy distribution of that source, therefore, the size and location of each time window is different for different components. Once the time windows are selected, next step is to validate the modal parameters identified from these time windows. The mode shapes are identified from the ratios of extracted harmonic sources in each time window and compared with the mode shapes obtained from free vibration analysis of finite element model via modal assurance criterion (MAC) [1]. The MAC matrix provides a graphical presentation of the correlation structure between different sets of vectors with darker shades representing stronger correlation. The MAC matrix between the analytically computed and SST identified mode shapes of UCLA Factor Building for all three earthquake events are shown in Fig. 5.3 and also summarized in Table 5.2.

A fairly good consistency has been observed between the analytically computed mode shapes and those identified from SST-based procedure for different time windows, except for higher torsional modes. Poor quality of torsional modes is because of insufficient energy in those modes in the computed dynamic response. We now take up the moving time window analysis of nonlinear response for damage detection.

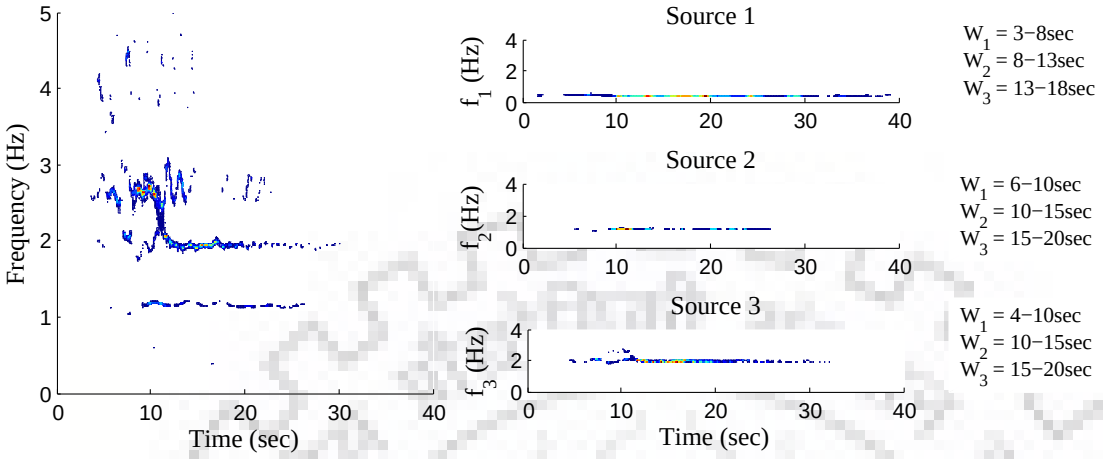

(a) Northridge-EW

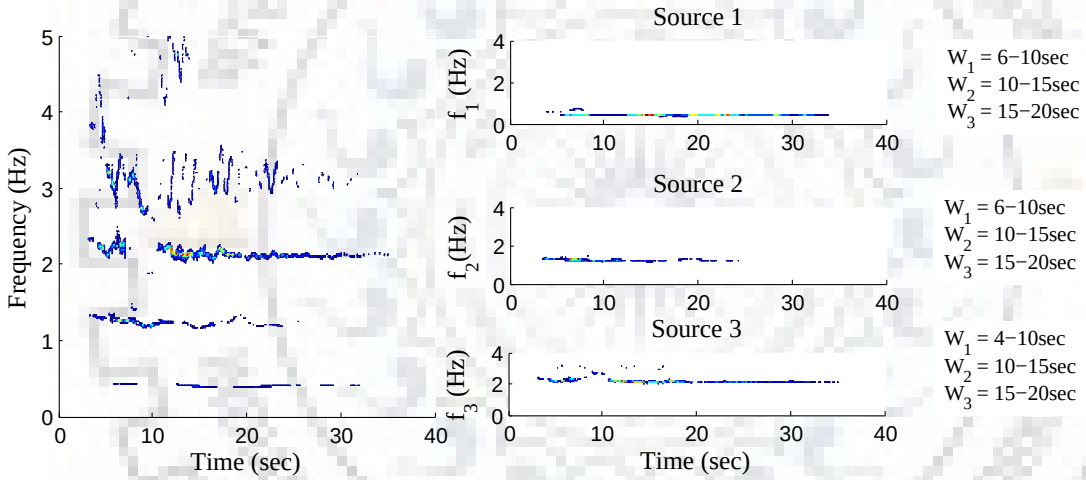

(b) Northridge-NS

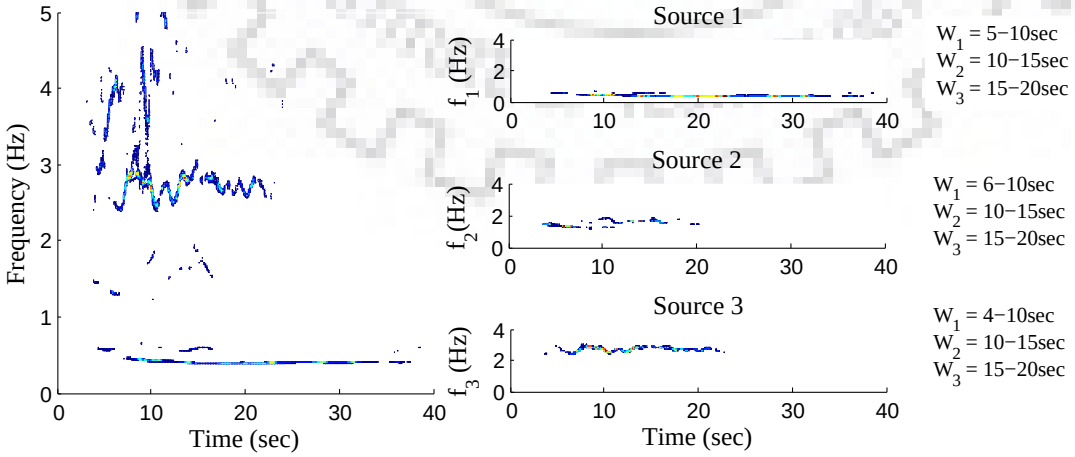

(c) Northridge-Torsion

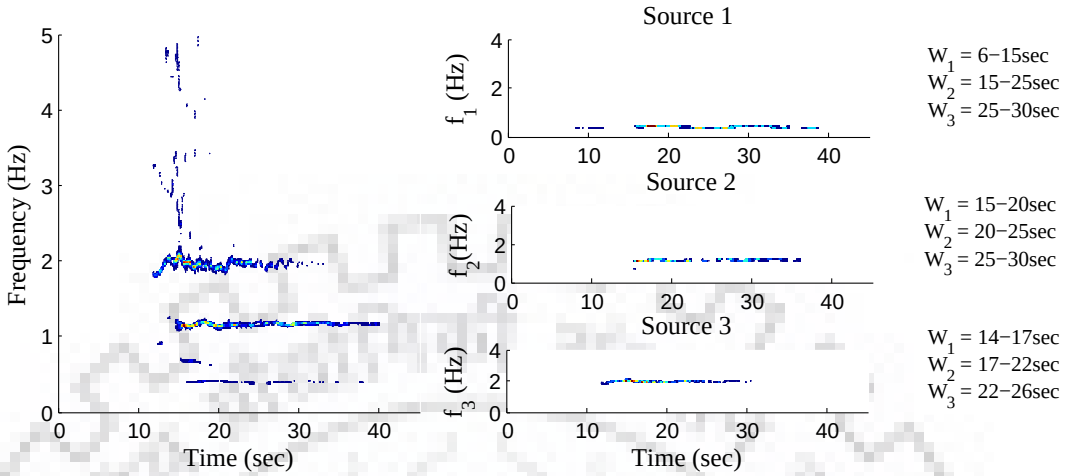

(d) Loma Prieta-EW

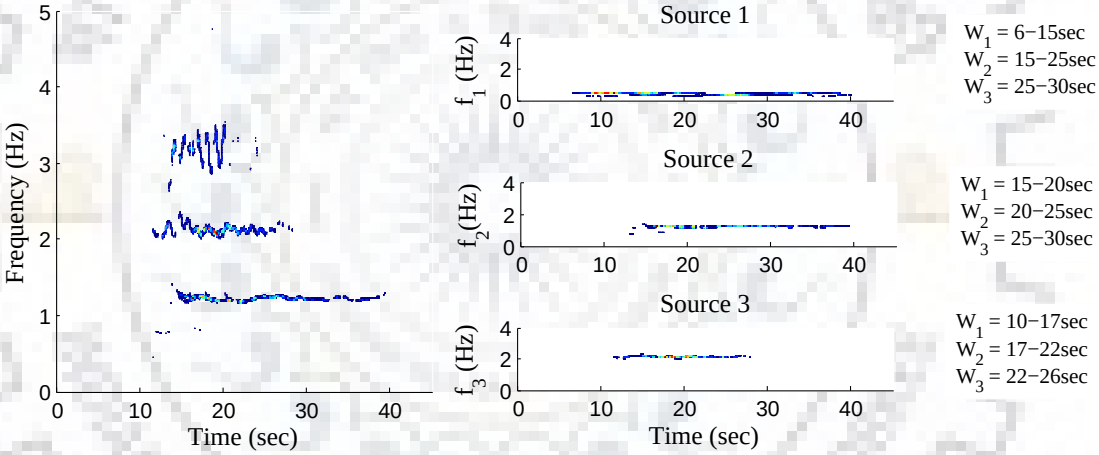

(e) Loma Prieta-NS

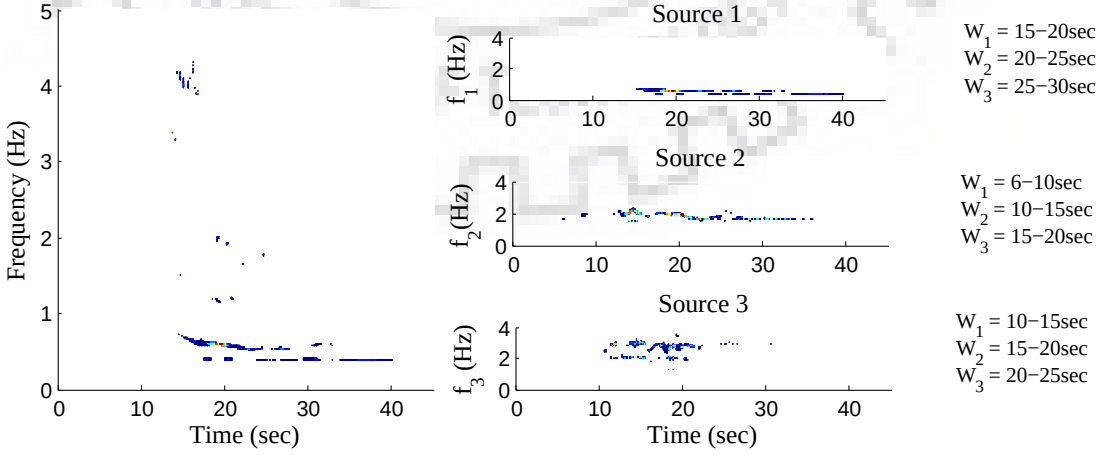

(f) Loma Prieta-Torsion

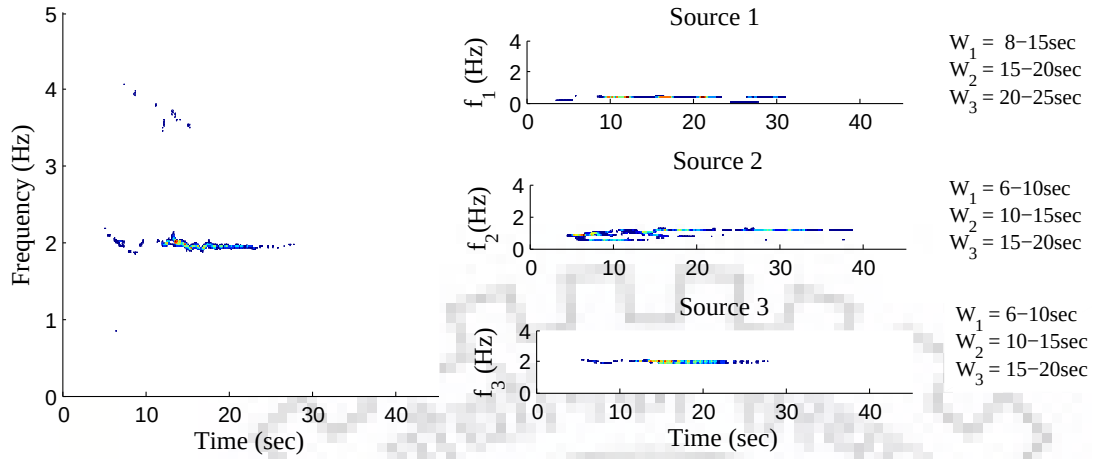

(g) Hector Mine-EW

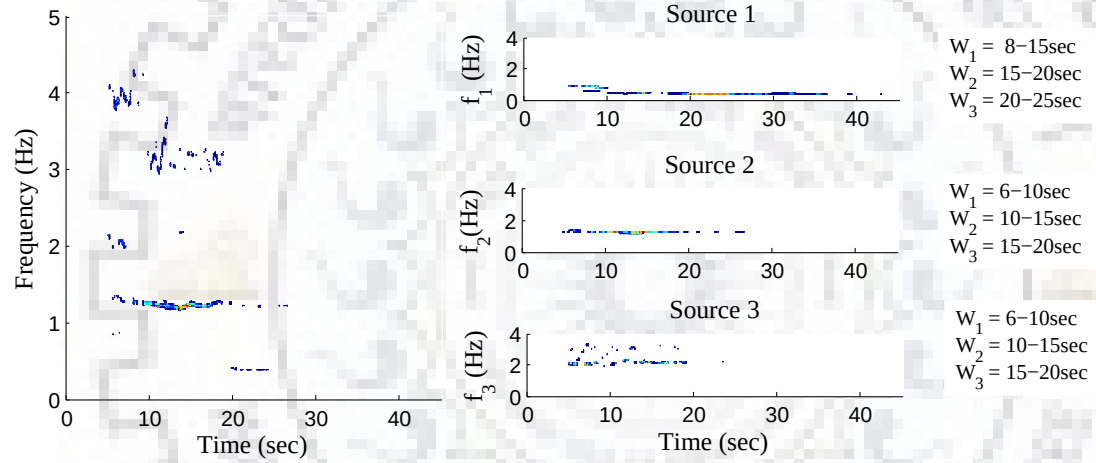

(h) Hector Mine-NS

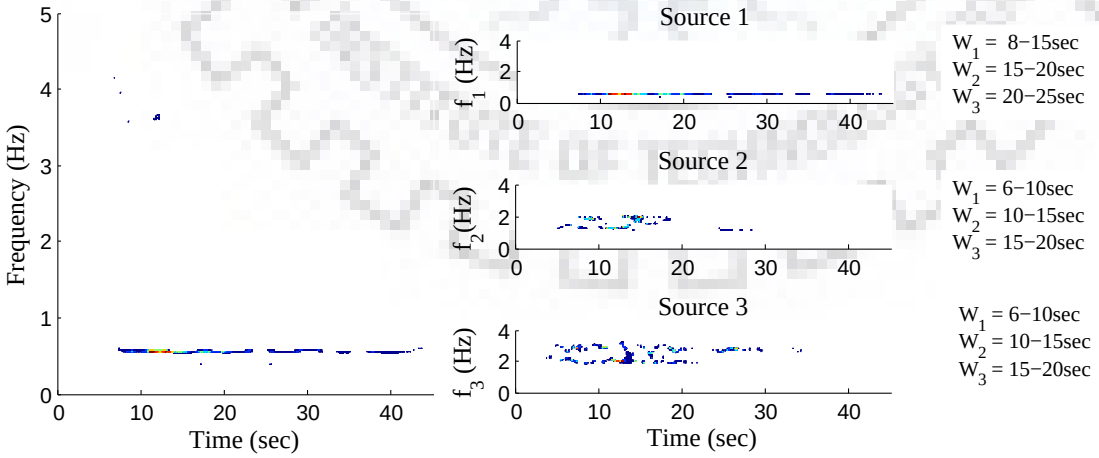

(i) Hector Mine-Torsion

Fig. 5.2. SST plot of linear dynamic response in EW, NS and torsion direction at top floor of UCLAFB along with selected time windows—all earthquake event

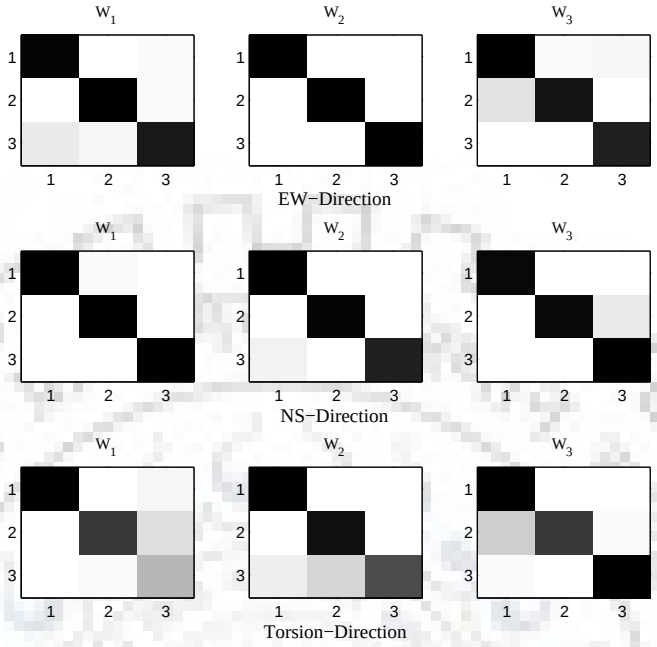

(a) Northridge

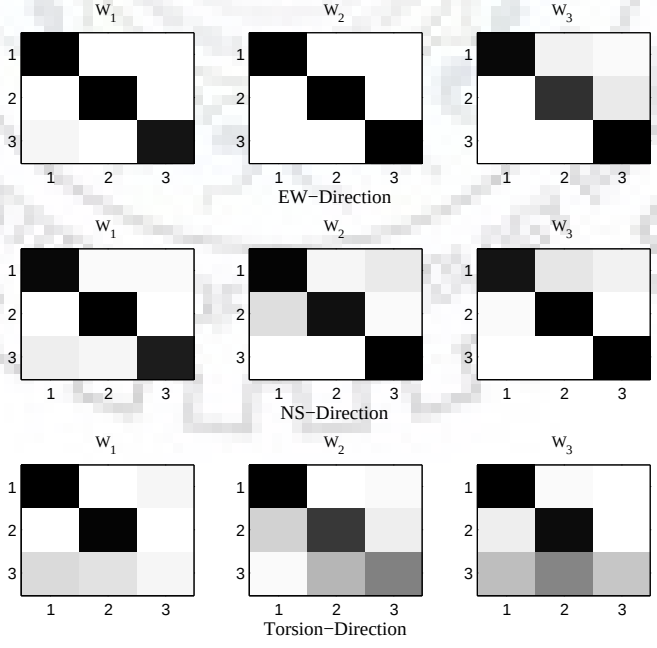

(b) Loma Prieta

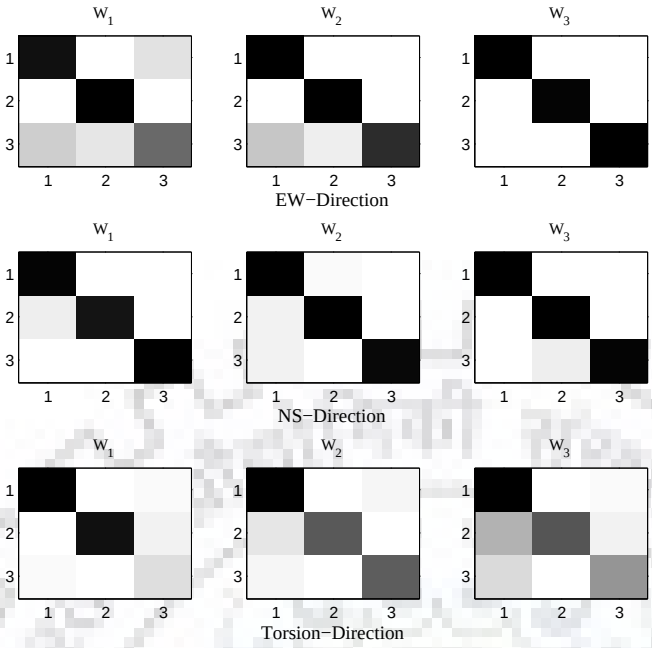

(c) Hector Mine

Fig. 5.3. MAC matrix between analytically computed and estimated mode shapes in different time windows (linear analysis) (X-axis: SST identified mode shapes and Y-axis: analytical mode shapes)

Table 5.2. Modal assurance criteria (MAC) values for mode shapes in different time windows

Ground Motion	Mode	Window 1			Window 2			Window 3		
		EW	NS	Tor	EW	NS	Tor	EW	NS	Tor
Northridge	1	0.95	0.97	0.99	0.99	0.99	0.98	0.94	0.96	0.99
	2	0.97	0.91	0.77	0.98	0.98	0.91	0.86	0.95	0.77
	3	0.87	0.98	0.28	0.99	0.85	0.68	0.82	0.99	0.98
Loma Prieta	1	0.95	0.98	0.99	0.93	0.99	0.99	0.90	0.95	0.96
	2	0.99	0.97	0.97	0.88	0.99	0.77	0.98	0.80	0.92
	3	0.87	0.90	0.04	0.95	0.99	0.49	0.96	0.99	0.23
Hector Mine	1	0.91	0.97	0.99	0.97	0.92	0.99	0.98	0.99	0.99
	2	0.97	0.91	0.92	0.97	0.92	0.64	0.97	0.99	0.65
	3	0.68	0.99	0.12	0.80	0.89	0.63	0.99	0.96	0.45

5.5 Damage Detection

The nonlinear behaviour is modelled by the formation of plastic hinges and consequently reflects the stiffness degradation on account of damage during a strong ground shaking. The nonlinear dynamic response of the UCLA Factor Building finite element model has been computed. Appropriate time windows for modal identification have been identified on the basis of time-frequency distribution of energy in each harmonic source in SST plot. The details about the SST plots and time windows of top floor response in EW, NS and Torsion direction from non-linear analysis for all earthquake events are shown in Fig. 5.4. Since it is proposed to use the modal parameters identified from the first time window as the reference set for comparison to detect damage, it is necessary to test their suitability for this purpose. Therefore, the identified modal parameters for the first time windows are compared with the modal parameters of the linear analytical model. Fig. 5.5 shows the MAC matrices analytical mode shapes and the identified modes shapes from first time windows. The numeric MAC values are reported in Table 5.3.

Table 5.3. Modal assurance criteria (MAC) values between analytical mode shapes and W_1 estimates for different earthquake

Ground Motion	Mode	EW	NS	Torsion
Northridge	1	0.93	0.90	0.99
	2	0.97	0.73	0.97
	3	0.88	0.97	0.16
Loma Prieta	1	0.92	0.93	0.99
	2	0.99	0.99	0.75
	3	0.87	0.84	0.66
Hector Mine	1	0.93	0.97	0.99
	2	0.97	0.91	0.92
	3	0.96	0.99	0.17

Reasonably high consistency has been observed for the first three modes in EW and NS directions and two torsional modes for all ground motions considered. It might be recalled that the identified torsional modes are of suspect quality due to inadequate energy in the torsional response. The consistency of the modal parameters identified from the first time window with the modal parameters of the linear system support our hypothesis that the first time window parameters can be considered as the reference set to track changes for

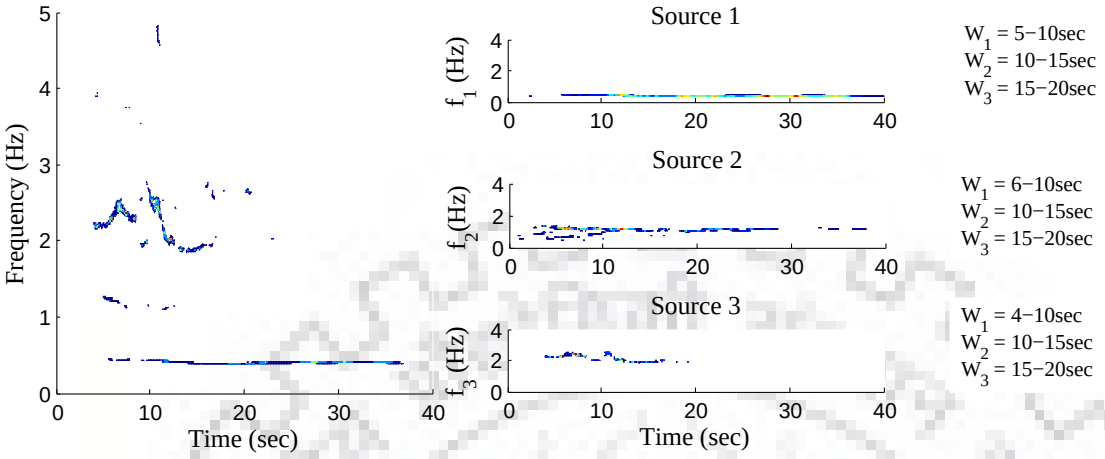

(d) Northridge-EW

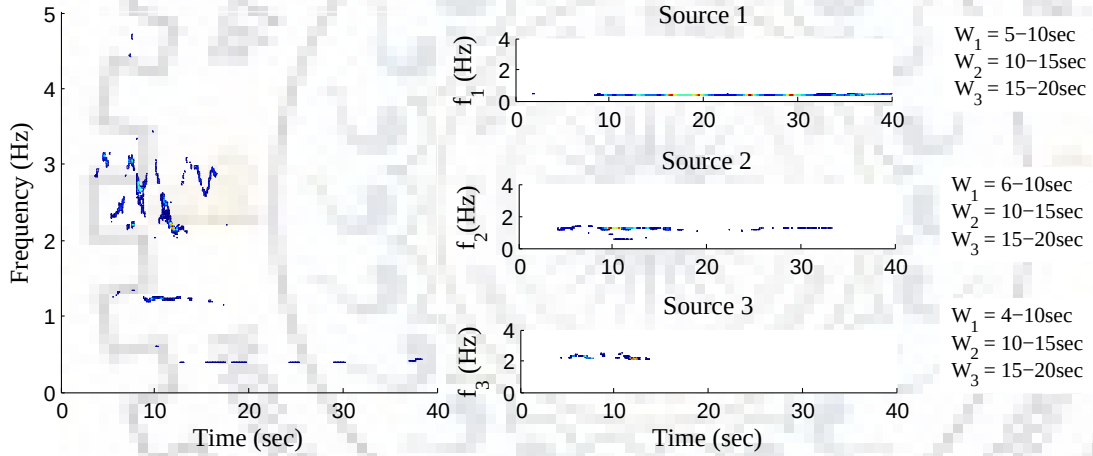

(e) Northridge-NS

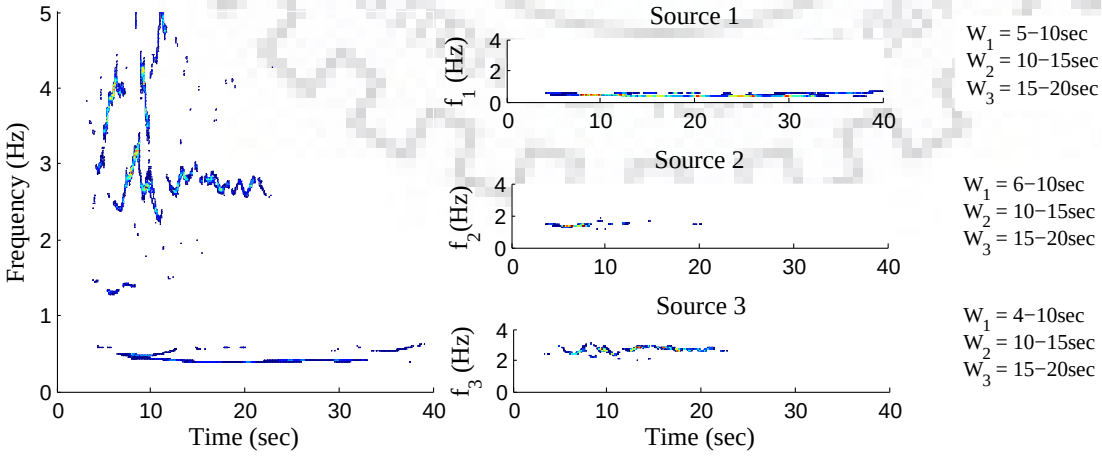

(f) Northridge-Torsion

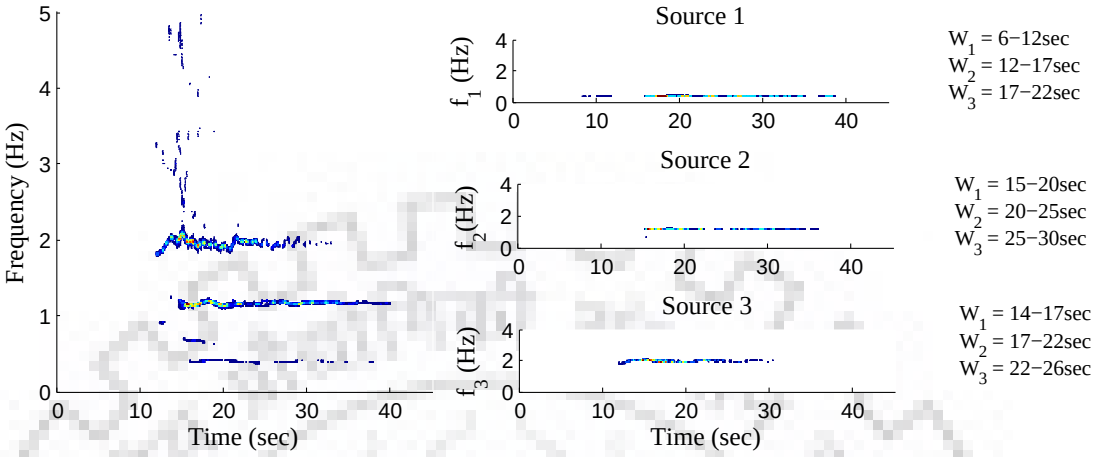

(g) Loma Prieta-EW

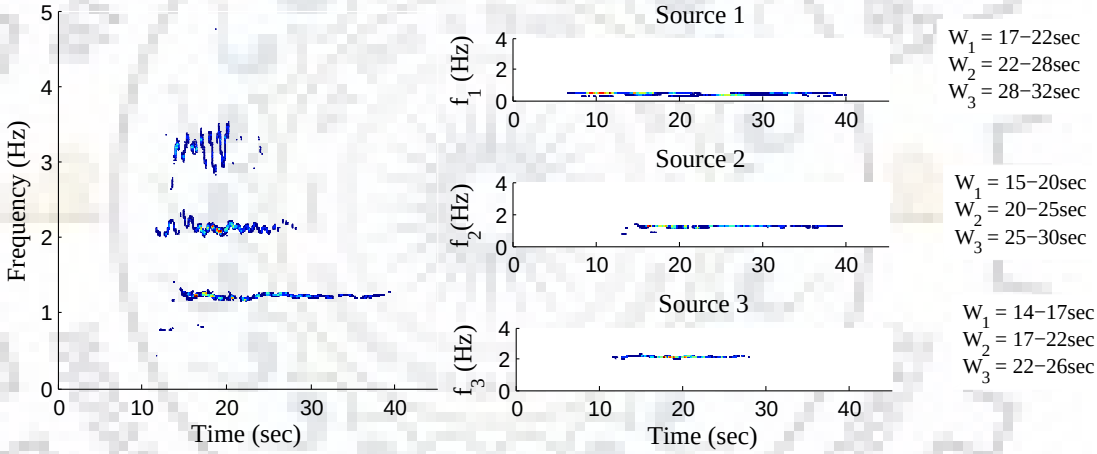

(h) Loma Prieta-NS

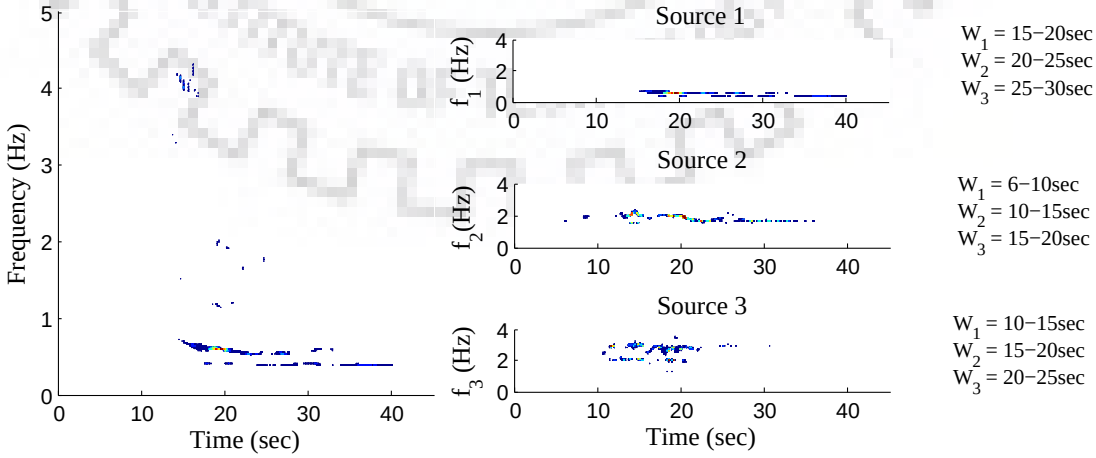

(i) Loma Prieta-Torsion

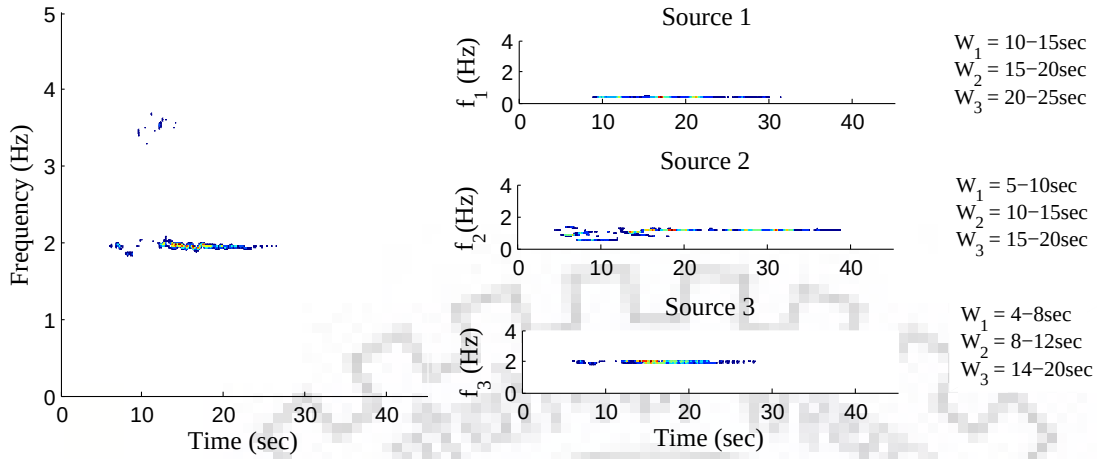

(j) Hector Mine-EW

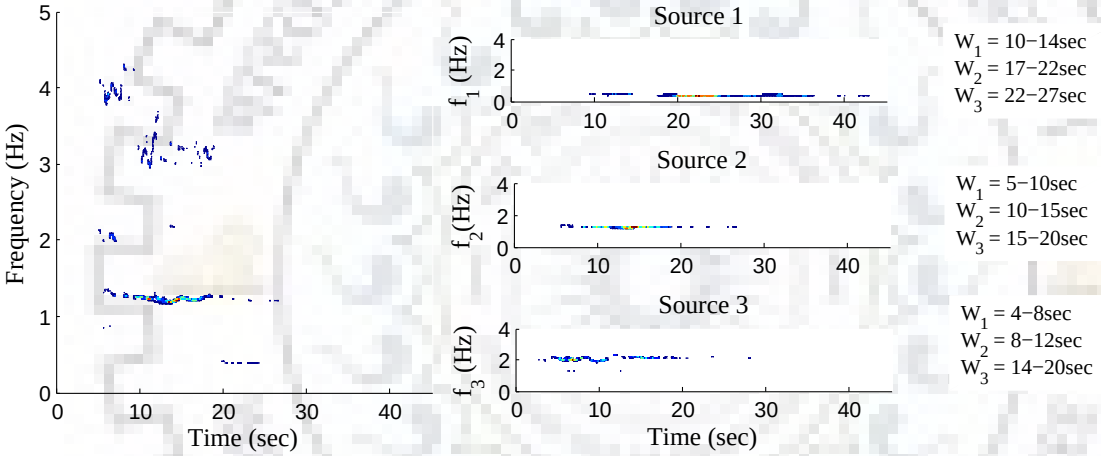

(k) Hector Mine-NS

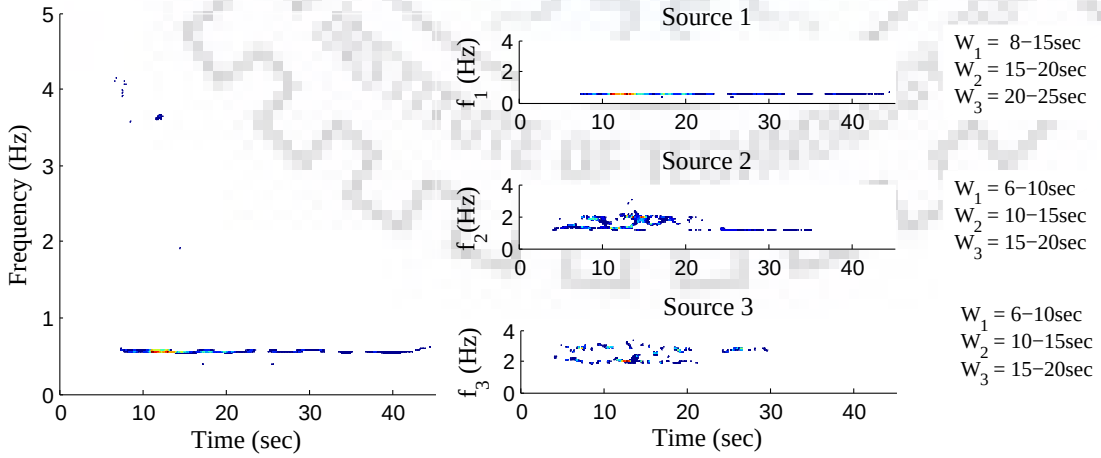

(l) Hector Mine-Torsion

Fig. 5.4. SST plot of nonlinear dynamic response in EW, NS and torsion direction at top floor of UCLAFB along with selected time windows—all earthquake event

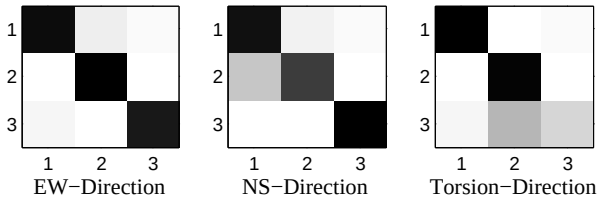

(a) Northridge

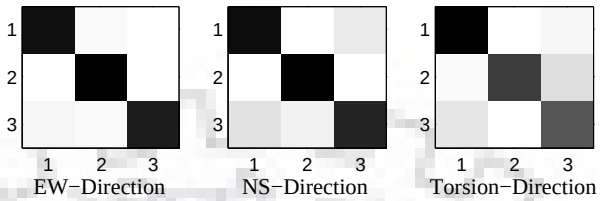

(b) Loma Prieta

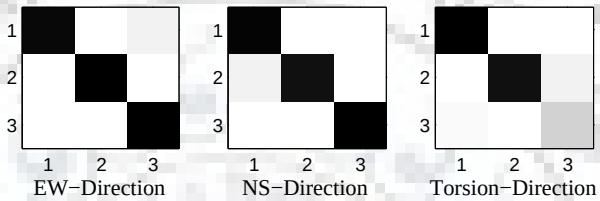

(c) Hector Mine

Fig. 5.5. MAC matrix between mode shapes obtained from W_1 and analytical mode shapes (X-axis: SST identified mode shapes and Y-axis: analytical mode shapes)

damage detection.

5.5.1 Changes in Natural Frequencies and Mode Shapes

Any damage to the structural system is associated with the degradation of its stiffness and considering the mass to be invariant, this softening effect should reflect in the change (decrease) in the natural frequencies. Tracking changes in the system natural frequencies is the one of the earliest procedures used for structural health monitoring. The natural frequencies have been estimated from the SST sources in all time windows. Natural frequencies identified in different time windows are given in Table 5.4. The percentage decrease in natural frequencies in windows W_2 and W_3 with respect to W_1 are shown in Fig. 5.6. It is observed that while the natural frequencies decrease with the formation of plastic hinges, different modes are affected differently by the earthquake ground motions. The near field Northridge event has significant influence on the first two modes with reduction in frequencies in the range of 10–20% while the effect is considerably less pronounced in the case of far field Loma Prieta event. This is consistent with the very few hinge formations (less than 5%) in the case of Loma Prieta shaking. The intermediate distance event of Hector Mine seems to

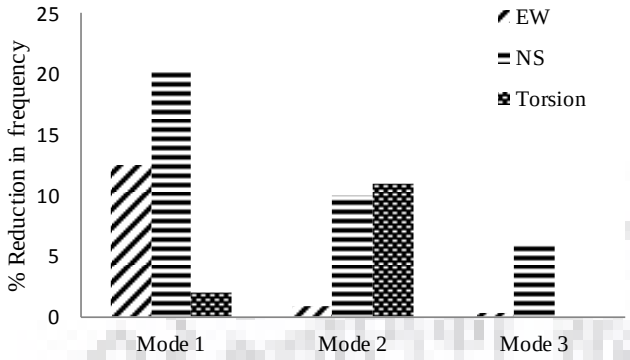

(a) Northridge

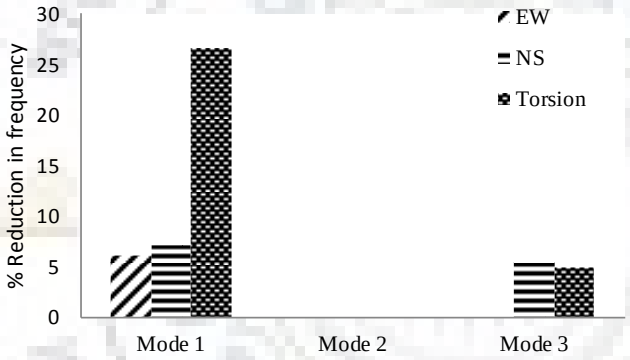

(b) Loma Prieta

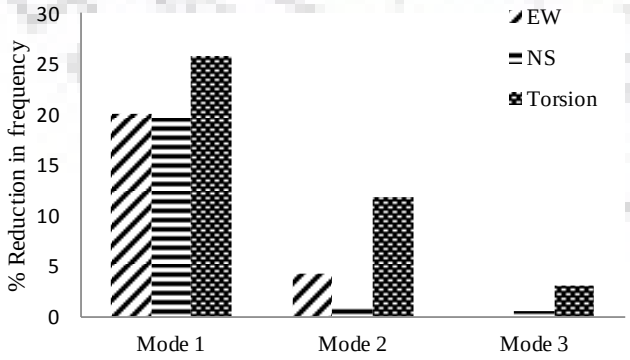

(c) Hector Mine

Reduction in frequencies in W_2 with respect to W_1

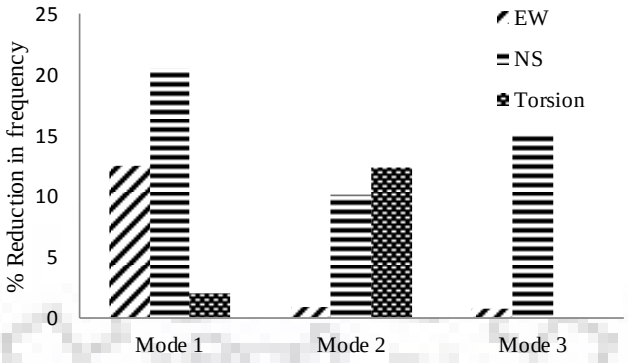

(d) Northridge

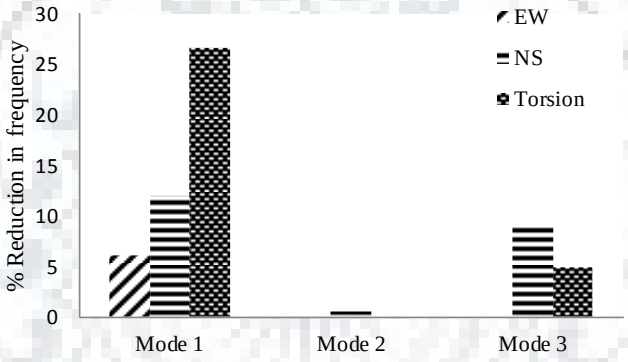

(e) Loma Prieta

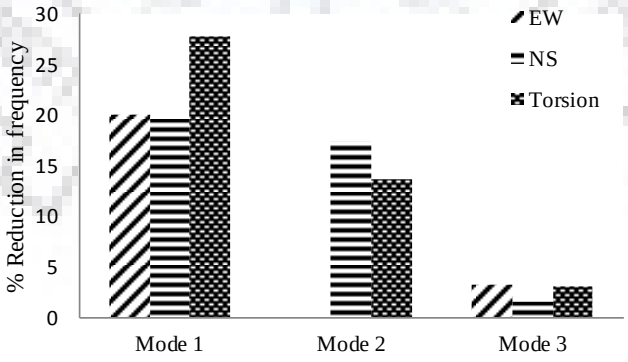

(f) Hector Mine

Reduction in frequencies in W_3 with respect to W_1

Fig. 5.6. Reduction in natural frequencies

Table 5.4. Estimated natural frequencies (in Hz) in first three time windows for different earthquake

Ground Motion	Mode	Window 1			Window 2			Window 3		
		EW	NS	Tor	EW	NS	Tor	EW	NS	Tor
Northridge	1	0.45	0.49	0.50	0.39	0.39	0.49	0.39	0.39	0.49
	2	1.19	1.32	1.49	1.18	1.19	1.33	1.18	1.19	1.29
	3	1.96	2.63	2.99	1.95	2.48	2.99	1.94	2.24	2.83
Loma Prieta	1	0.39	0.42	0.59	0.37	0.39	0.44	0.37	0.37	0.44
	2	1.19	1.19	1.19	1.19	1.19	1.19	1.19	1.19	1.19
	3	2.00	2.33	2.79	1.99	2.19	2.66	1.99	2.11	2.66
Hector Mine	1	0.49	0.49	0.66	0.39	0.39	0.49	0.39	0.39	0.49
	2	1.28	1.19	1.33	1.23	1.18	1.17	1.27	0.99	1.15
	3	2.24	1.99	2.83	2.24	1.98	2.75	2.17	1.96	2.75

have similar effect as that of the near field Northridge event as far as reduction in natural frequencies is concerned.

Natural frequencies are global parameters and are not very sensitive to the changes due to local softening effects. These local effects are better captured by the mode shapes and we now track the changes in identified mode shapes for damage detection. The mode shapes estimated from the SST sources from W_2 and W_3 are compared with the W_1 estimates and the correlations are presented as MAC matrices in Fig. 5.7 while the numeric MAC values are tabulated in Table 5.5. There is a significant change in mode shapes for the near field Northridge event while the mode shapes in windows W_2 and W_3 appear to be better correlated with the reference mode shapes in the first time window W_1. The results for the intermediate distance event of Hector Mine seem to fall somewhere in between the near field and far field cases. This pattern is consistent with the extent of damage in the structure due to these ground motions. In this study it has been observed that if the response have insignificant energy in parts of the interval, mode shape estimation is severely affected which leads to poor correlation. In general damage affects the higher modes of the structure and the lower modes are not much affected so a very small MAC values in lower modes is due to insignificant energy in the time window being considered. To validate this hypothesis, we considered a white noise excitation whose frequency content does not change with time. The SST plot of white noise excitation is shown in Fig. 5.8. Figures 5.9-5.10 show the SST

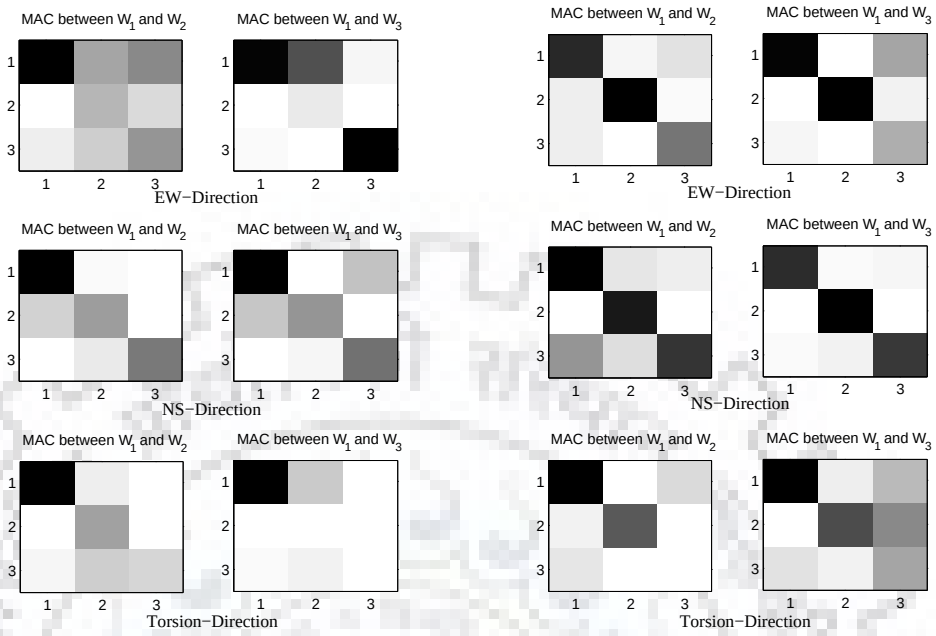

(a) Northridge

(b) Loma Prieta

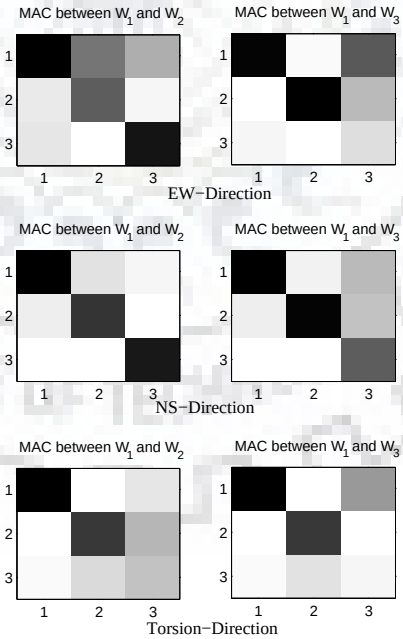

(c) Hector Mine

Fig. 5.7. MAC matrices for mode shapes from windows W_2 and W_3 with the reference state W_1 (X-axis: SST identified mode shapes and Y-axis: analytical mode shapes)

Table 5.5. Modal assurance criteria (MAC) values for mode shapes from windows W_2 and W_3 with the reference state W_1

Ground Motion	Mode	MAC1			MAC2		
		EW	NS	Tor	EW	NS	Tor
Northridge	1	0.89	0.87	0.99	0.91	0.88	0.95
	2	0.26	0.33	0.63	0.072	0.36	0.67
	3	0.36	0.45	0.01	0.94	0.49	0.33
Loma Prieta	1	0.71	0.96	1.00	0.93	0.78	0.98
	2	0.85	0.85	0.36	0.96	0.96	0.01
	3	0.46	0.76	0.16	0.30	0.74	0.01
Hector Mine	1	0.79	0.96	0.99	0.88	0.96	0.98
	2	0.50	0.75	0.76	0.90	0.95	0.75
	3	0.72	0.86	0.23	0.13	0.60	0.03

MAC1: MAC value between W_1 and W_2, MAC2: MAC value between W_1 and W_3

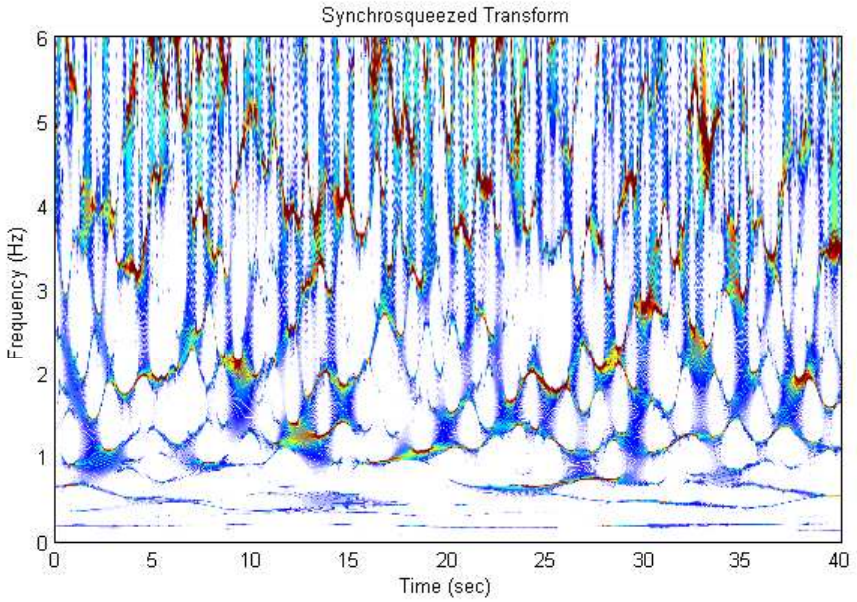

Fig. 5.8. Synchrosqueezed transform of White noise excitation

plot of e top floor response from linear and nonlinear analysis in EW direction. A constant energy line throughout is visible which results in good quality estimation of mode shapes. In fact, it is possible to extract up to four modes for white noise excitation case. The MAC2 value in case of Northridge earthquake EW component is much severe than the NS component. The energy of the signal in EW direction is maximum in the frequency band close to the second and third mode as shown in the SST plot of earthquake EW component

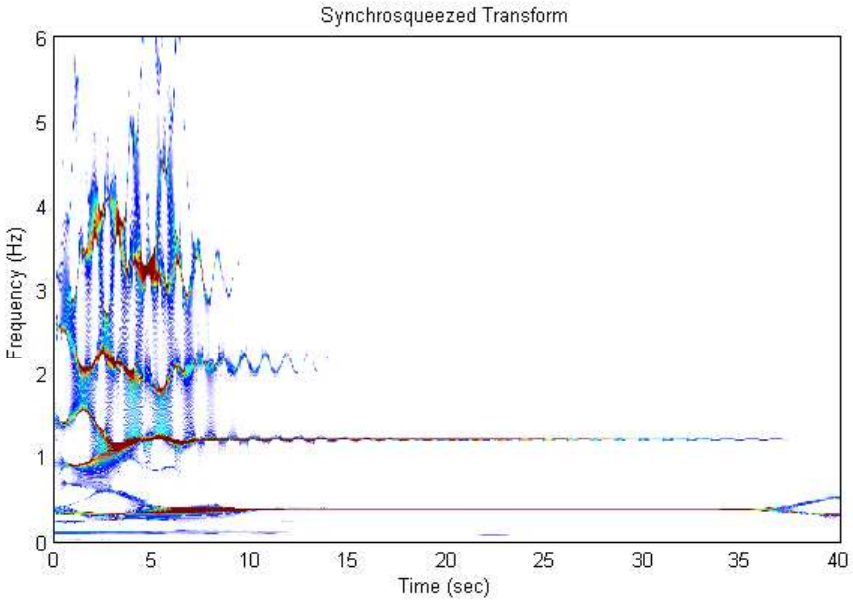

Fig. 5.9. Synchrosqueezed transform of linear response EW component (White noise excitation)

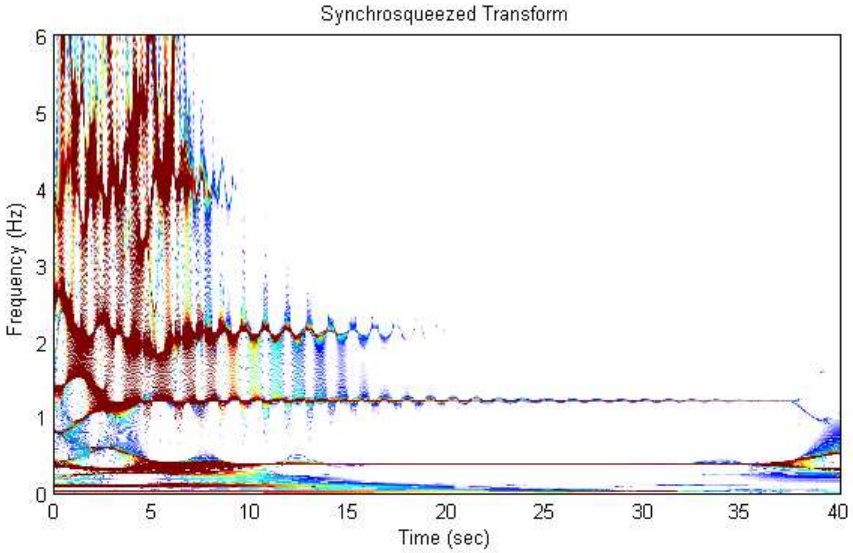

Fig. 5.10. Synchrosqueezed transform of nonlinear response EW component (White noise excitation)

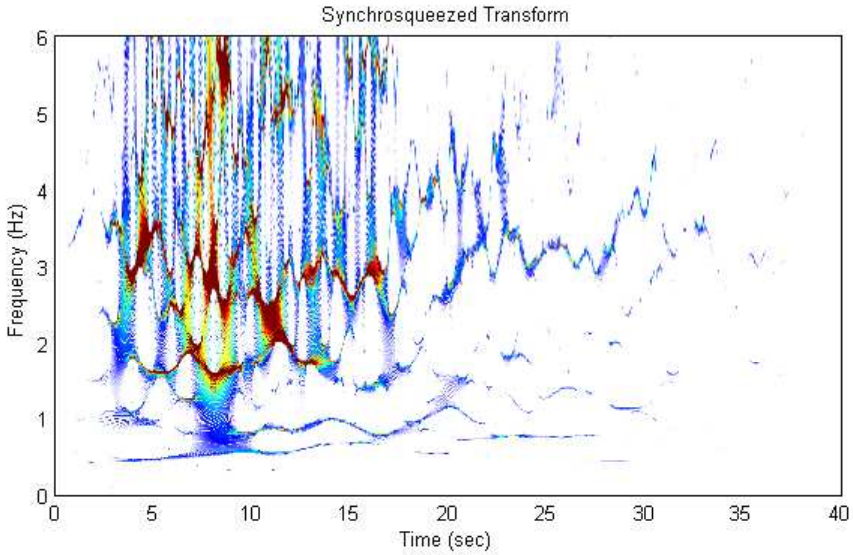

Fig. 5.11. Synchrosqueezed transform of Northridge ground motion EW component

as shown in Fig. 5.11. The damage in the structure is due to both second and third modes (the mode participation factor (as computed in SAP2000) of second and third modes in EW direction are 0.27 and 0.19 , respectively). In the third window (W3 $\in [15, 20]$) for the second source, the excitation as well as the response have insignificant energy in parts of the interval which adversely affects the mode estimation and this leads to poor correlation with the mode shape estimate from the first window.

5.5.2 Changes in Flexibility

The structural stiffness and flexibility matrices can be reconstructed with the help of mass matrix, mode shapes and natural frequencies as:

$$\mathbf{K} = \mathbf{M}\mathbf{\Phi}\mathbf{\Lambda}\mathbf{\Phi}^{-1} \quad \text{and} \quad \mathbf{F} = \mathbf{K}^{-1} = \mathbf{\Phi}\mathbf{\Lambda}^{-1}\mathbf{\Phi}^{-1}\mathbf{M}^{-1} \ . \tag{5.1}$$

While the stiffness is proportional to the eigenvalues ($\mathbf{\Lambda}$), flexibility is inversely proportional to those and hence a reasonably good reduced rank approximation of system flexibility matrix can be constructed by using only a few lower order modes which can be identified from the vibration records. Such estimates of flexibility matrices in different time windows can provide some indication of the damage in the system manifesting as increasing flexibility (or, stiffness degradation). Assuming mass orthonormal mode shapes, i.e., $\mathbf{\Phi}^T \boldsymbol{M} \mathbf{\Phi} = \mathbf{I}$, the inverse of the mode shape matrix is easily obtained as $\mathbf{\Phi}^{-1} = \mathbf{\Phi}^T\mathbf{M}$. The flexibility matrix can be constructed as the rank-1 update using mode shapes and natural frequencies as:

$$\mathbf{F} = \mathbf{\Phi}\mathbf{\Lambda}^{-1}\mathbf{\Phi}^T = \sum_{i=1}^{n} \frac{1}{\omega_i^2} \boldsymbol{\phi}_i \boldsymbol{\phi}_i^T \tag{5.2}$$

Table 5.6. Frobenius norm of reduced rank approximation for flexibility

Ground Motion	EW			NS			Torsion		
	W_1	W_2	W_3	W_1	W_2	W_3	W_1	W_2	W_3
Northridge	0.10	0.17	0.17	0.11	0.16	0.16	0.10	0.10	0.10
Loma Prieta	0.16	0.18	0.16	0.14	0.16	0.18	0.11	0.13	0.13
Hector Mine	0.10	0.16	0.16	0.10	0.16	0.16	0.10	0.10	0.10

A reduced rank approximation of the flexibility matrix can be constructed by limiting the sum in Eq. (5.2) to the number of modes identified from the vibration records. However the primary contribution to flexibility comes from the first mode for which a decrease in frequency is detected in all subsequent windows owing to the formation of hinges. We consider the Frobenius norm [100] for tracking the changes in the system flexibility over different time windows. The Frobenius norm is the the measure of absolute value of a matrix and is estimated as:

$$\|\mathbf{F}\| = \left(\sum_{i=1}^{m} \sum_{j=1}^{n} |f_{ij}|^2 \right)^{1/2} \tag{5.3}$$

and is tabulated in Table 5.6 for the reduced rank approximations of flexibility matrices in different time windows for different ground motions. The percentage increase in system flexibility in time windows W_2 and W_3 with respect to the window W_1 is shown in Fig. 5.12. The largest increase in the Frobenius norm has been estimated for the near field Northridge event where the numbers of hinges formed in the structure are also maximum and it is smallest for the far field Loma Prieta event where the number of hinges formed is minimum as shown in Fig. 5.13. The mass orthonormal mode shapes influences the identified flexibility matrix to a scale factor, the relative changes of the flexibility matrix will be constant. Therefore, the damage parameters identified in different time windows will not be affected by the choice of normalization process of mode shapes.

5.6 Concluding Remarks

A moving time window procedure to track the changes in structural system is proposed for the purpose of damage detection. The structural system is characterized by the modal properties identified by using a SST based blind identification technique which facilitates a sharp resolution in both time and frequency domain to isolate the modal response components. The vibration-based structural health monitoring procedures always require parameters of a

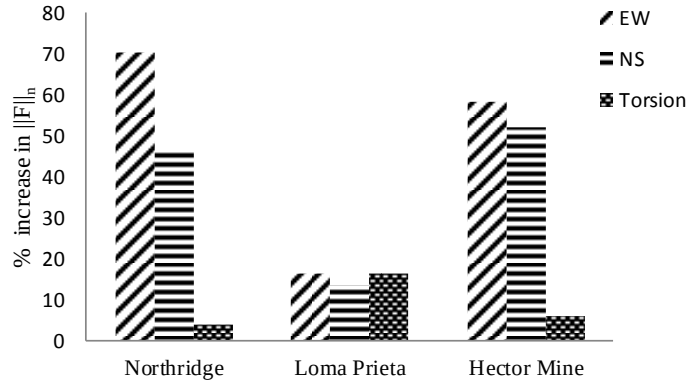

(a) Window 1 vs Window 2

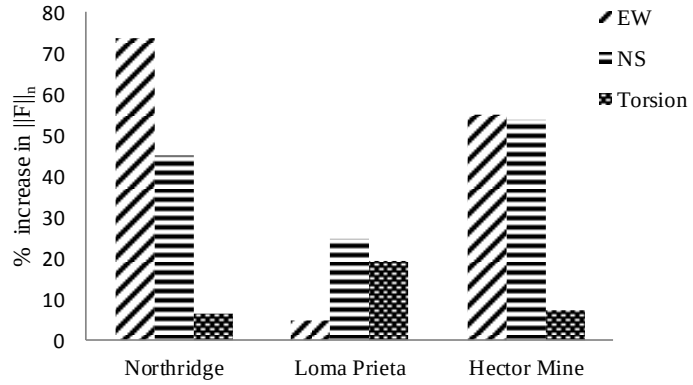

(b) Window 1 vs Window 3

Fig. 5.12. Increase in system flexibility

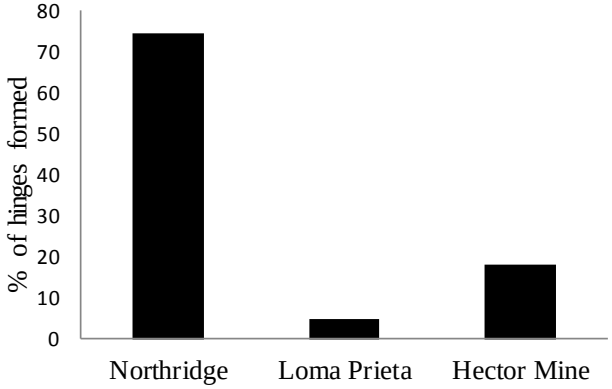

Fig. 5.13. Hinge formation in the structural members of UCLAFB model

reference undamaged state of the structure. It is shown that the reference state parameters can be estimated from the initial segment of the vibration records. The system parameters can be identified from different time windows of the vibration signatures. The selection of appropriate time windows is facilitated by the synchrosqueezed transform to study the distribution of energy in the time-frequency plane. The modal parameters estimated in the first window corresponding to the undamaged state of the building is compared with the parameters estimated in subsequent windows for damage detection. Changes in natural frequency, mode shapes and system flexibility have been shown to be good identifiers of the damage.

Chapter 6

Conclusions and Recommendations

The problem of output-only modal identification has been addressed in this thesis to provide a non-statistical framework for blind source separation using a time-frequency characterisation tool, namely, the synchrosqueezed transform. The proposed formulation leads to a robust and elegant modal parameter estimation procedure which can be used for damage detection. The significant contributions of this research work are summarized as follows:

1. While the governing equations for the earthquake response are formulated in terms of motion relative to the base motion, the response measurements are invariably total accelerations. The blind source separation formulation of representing observed system response as a mixture of independent sources is extended for the base excitation case.

2. A new blind identification scheme has been developed using time-frequency based synchrosqueezed transform. The sources identified from synchrosqueezed transform show high fidelity with the modal responses.

3. A robust non-statistical framework has been developed for estimating the mode shapes from ratios of the identified sources for lightly damped systems.

4. A simple and efficient scheme for approximate estimation of modal damping for earthquake excited systems is proposed based on the free-vibration modeling of the tail portion of the response.

5. The vibration-based damage detection process always requires reference parameters to serve as a benchmark for comparison. To eliminate this pre-requisite, vibration signatures are analysed in moving time windows where modal parameters identified in first window are considered as reference parameters.

6.1 Conclusions

The following conclusions are drawn from this thesis:

1. For earthquake excited structures, the accelerometers record the total acceleration at a point, comprising of structural vibrations as well as the ground acceleration. Therefore the measured response data (total acceleration) cannot be expressed directly in terms of modal response. In this study we propose a BSS formulation for base excited, lightly damped structures based on measurements of total accelerations which also enhances the participation of higher modes—an important factor for structural health monitoring applications.

2. The SST provides the sharp resolution of the signal in time-frequency plane and facilitates the separation of different harmonics. When SST is applied to the vibration measurements, the estimated sources are the measure of modal responses to their true strength and not within a scaling factor as in case of statistical BSS techniques (ICA, SOBI, CP, and derivatives). This allows for a simplified procedure for estimation of modes shapes by the normalizing of identified modal response from measured data at different floor levels with maximum energy component in that mode. The maximum energy source components is the measure of modal coordinates. The other two modal parameters namely, natural frequencies and modal damping are identified through post processing of modal coordinates. The proposed method performed well for small and a large class of structural system identification problems.

3. A simplified procedure is proposed for estimation of modal damping ratio by examining the tail data. The tail portion of the earthquake response is dominated by the free vibration and therefore by fitting the tail data with exponential decay function damping coefficients are obtained.

4. Moving time window based damage identification procedure is proposed. The modal properties are identified using SST based blind identification technique. The vibration-based structural health monitoring procedures always require parameters of a reference undamaged state of the structure which, if available, may not be reliable. The reference state parameters are estimated from the initial time window of the vibration records. The synchrosqueezed transform representation of time series is taken in account for selection of appropriate time windows. The modal parameters identified from the initial time window are compared with the modal parameters estimated in

subsequent windows. The variation in natural frequencies, mode shapes and system flexibility have been shown as ideal damage detection parameters.

6.2 Recommendations for Future Work

This thesis makes contribution to the development of output-only modal identification methodologies using time-frequency based synchrosqueezed transform and also its application to structural health monitoring. The following seem useful leads for further exploration:

1. In the proposed work, mode shapes are obtained using the vibration response measurement on all floor. It is not practically possible to monitor each degree of freedom and the effect of missing response from a few degrees of freedom should be studied.

2. Presently, very few BSS procedures are equipped to analyse structures with complex modes. Formulation for handling complex modes should be developed for cases with supplemental damping, soil-structure interaction, etc.

3. The proposed study is focused towards the earthquake excited buildings. The methodology needs to be extended to other important structural types.

4. In this work the damage detection study is carried out in moving time window. The study needs to further extended for damage quantification.

Appendix A

Wavelet-based Modified Cross-correlation

Modified cross-correlation (MCC) and wavelet-based modified cross-correlation (WMCC) procedure are the extension of second order blind identification (SOBI) [37, 38]. The SOBI procedure was initially extended to MCC by Hazra *et* al. [38] to deal with noisy measurements as well as to simplify the damping identification process by using auto and cross-correlation of the measured data as the inputs, rather than the actual measurement data of the system. The auto and cross-correlation of the measurement data are obtained using the concepts of the NExT algorithm. The MCC procedure was further extended to WMCC by using stationary wavelet transform (SWT) to improve the separability of the sources and to deal with non-stationary measurement data. The WMCC is different from the traditional SOBI procedure in two ways. First, the wavelet coefficients obtained through the stationary wavelet transform (SWT) of the correlation of measurements are used instead of the measurements directly; secondly, the non-stationary nature of the sources is handled through the use of several time-lagged non-overlapping windows. Starting with basic BSS problem statement given as:

$$\mathbf{x}(t) = \mathbf{A}\mathbf{s}(t) \tag{A.1}$$

where, $\boldsymbol{x}(t)$ is the measurement data, $\mathbf{A}$ the mixing matrix and $\mathbf{s}(t)$ is the source signals. Considering the orthogonal wavelet decomposition of the sources, each source signal in terms of its decomposition coefficients:

$$s_i^j(t) = \sum_k c_{ki}^j \psi_k^j(t) \quad \text{i=1,2,...,m} \tag{A.2}$$

Where, j represents the scale parameter or dilation parameter, k represents the shift index, and i represents source index. c_{ki}^j are the decomposition coefficients, and $\psi(t)$ is the selected

wavelet. Similarly, each component of the measurements $\mathbf{x}$ can be expressed as:

$$x_i^j(t) = \sum_k f_{ki}^j \psi_k^j(t) \quad \text{i=1,2,...,m} \tag{A.3}$$

Where, i is the sensor index, and f_{ki}^j represents the decomposition coefficients. Substituting A.2 and A.3 in the basic BSS equation A.1 by considering the wavelet coefficients at lth shift of sensor sources and then applying the orthogonality condition for wavelet:

$$\mathbf{f_l} = \mathbf{A}\mathbf{c_l} \tag{A.4}$$

where $\mathbf{A}$ is $m \times m$ size mixing matrix with m sources, and m sensor responses. The vector obtained from the lth coefficients of the mixtures and sources are $\mathbf{f_l}$ and $\mathbf{c_l}$ respectively.

The second step involved in the formulation is the estimation of autocorrelation matrices of the wavelet coefficients of the sources c_{kl}^j, and the responses f_{kl}^j using SWT. The covariance matrices in terms of of wavelet coefficients are defined given as

$$R_s(\tau) = E\left[\sum_l c_l^j \psi_l^j(t)) \sum_i c_{i+\tau}^j \psi_i^j(t+\tau)\right] \tau \neq 0 \tag{A.5}$$

and

$$R_x(\tau) = E\left[\sum_l f_l^j \psi_l^j(t)) \sum_i f_{i+\tau}^j \psi_i^j(t+\tau)\right] \quad \tau \neq 0 \tag{A.6}$$

using orthogonality properties of the wavelet:

$$\begin{aligned} R_s(\tau) = R_{ws}(\tau) = E\left[c_l^j c_{l+\tau}^j\right] \\ R_x(\tau) = R_{ws}(\tau) = E\left[f_l^j f_{l+\tau}^j\right] \end{aligned} \tag{A.7}$$

Now multiplying Eq. (A.4) both sides by f_{p+l} and taking the expectation operator on both sides, the equation is modified as:

$$E\left\{f_l f_{l+p}^l\right\} = \mathbf{A} E\left\{c_l c_{l+p}^T\right\} \mathbf{A^T} \tag{A.8}$$

where, p is an index with same meaning as τ. Using Eq. (A.7) and Eq. (A.8) the covariance matrix of response and sources are simplified as:

$$\mathbf{R}_{wx}(p) = \mathbf{A}\mathbf{R}_{ws}(p)\mathbf{A^T} \tag{A.9}$$

Now the Eq. (A.9) is the form similar to the SOBI and the procedure of estimation of mixing matrix and sources are same as for SOBI procedure *i.e.* the whitening, orthogonalization followed by unitary transform. Whitening is a linear transformation expressed as:

$$\bar{\mathbf{x}}(k) = \mathbf{Q}\mathbf{x}(k) = \mathbf{\Lambda}_x^{-\frac{1}{2}} \mathbf{V}_x^T \mathbf{x}(k) \tag{A.10}$$

where, $\mathbf{V}_x$ and $\mathbf{\Lambda}_x$ are the eigenvector and eigenvalue of the covariance matrix of $\mathbf{x}$. The next step is the orthogonalization, to diagonalize the time lagged covariance matrix to get:

$$\hat{\mathbf{R}}_{w\bar{x}}(p) = \mathbf{QAR}_{ws}(p)\mathbf{A}^T\mathbf{Q}^T \tag{A.11}$$

If the sources are assumed to be uncorrelated and scaled to have a unit variance, the product $\mathbf{QA}$ is a unitary matrix. the problem now becomes one of diagonalizing the matrix $\hat{\mathbf{R}}_{w\bar{x}}(p)$ resulting in the unitary matrix, $\mathbf{U} = \mathbf{QA}$. The mixing matrix can be then estimated from the relationship between whitening matrix and the estimated unitary matrix. The independent sources can be subsequently estimated from the measured data and pseudo-inverse of the mixing matrix.

Bibliography

[1] R.J. Allemang. The modal assurance criterion–twenty years of use and abuse. *Sound and Vibration*, 37(8):14–23, 2003.

[2] R.J. Allemang and D.L. Brown. A correlation coefficient for modal vector analysis. In *Proceedings of the 1st International Modal Analysis Conference*, volume 1, pages 110–116. Orlando: Union College Press, 1982.

[3] K.F. Alvin, A.N. Robertson, G.W. Reich, and K.C. Park. Structural system identification: from reality to models. *Computers & structures*, 81(12):1149–1176, 2003.

[4] T.D. Ancheta, R.B. Darragh, J.P. Stewart, E. Seyhan, W.J. Silva, B.S.J Chiou, K.E. Wooddell, R.W. Graves, A.R. Kottke, D.M. Boore, T. Kishida, and J.L. Donahue. PEER NGA-West2 Database. Technical Report PEER 2013/03, Pacific Earthquake Engineering Research Center, University of California Berkeley, U.S.A., 2013.

[5] J. Antoni, R. Castiglione, and L. Garibaldi. Interpretation and generalization of complexity pursuit for the blind separation of modal contributions. *Mechanical Systems and Signal Processing*, 85:773–788, 2017.

[6] J. Antoni, L. Garibaldi, S. Marchesiello, and M. Sidhamed. New separation techniques for output-only modal analysis. *Shock and Vibration*, 11(3-4):227–242, 2004.

[7] J.L. Beck. Bayesian system identification based on probability logic. *Structural Control and Health Monitoring*, 17(7):825–847, 2010.

[8] A. Belouchrani, K. Abed-Meraim, J.F. Cardoso, and E. Moulines. A blind source separation technique using second-order statistics. *IEEE Transactions on Signal Processing*, 45(2):434–444, 1997.

[9] J.S. Bendat and A.G. Piersol. Engineering applications of correlation and spectral analysis. *Wiley-Interscience, New York, 315 p.*, 1980.

[10] S. Bhalla and C. Kiong Soh. Structural impedance based damage diagnosis by piezo-transducers. *Earthquake Engineering & Structural Dynamics*, 32(12):1897–1916, 2003.

[11] E. Brevdo, N.S. Fuckar, G. Thakur, and H.T. Wu. The synchrosqueezing algorithm: a robust analysis tool for signals with time-varying spectrum. *Computing Research Repository - CORR*, abs/1105.0010, 2011.

[12] P.T. Brewick and A.W. Smyth. Increasing the efficiency and efficacy of second-order blind identification (SOBI) methods. *Structural Control and Health Monitoring*, 24(6), 2017.

[13] R. Brincker, A. De Stefano, and B. Piombo. Ambient data to analyze the dynamic behavior of bridges: A first comparison between different techniques. In *Proceedings-SPIE the International Society for Optical Engineering*, pages 477–482. SPIE International Society for Optical, 1996.

[14] R. Brincker, L. Zhang, and P. Andersen. Modal identification from ambient responses using frequency domain decomposition. In *Proceedings of IMAC 18th, the International Modal Analysis Conference*, page 625–630, San Antonio, Texas, 2000.

[15] R. Brincker, L. Zhang, and P. Andersen. Modal identification of output-only systems using frequency domain decomposition. *Smart Materials and Structures*, 10(3):441, 2001.

[16] D.L. Brown, R.J. Allemang, R. Zimmerman, and M. Mergeay. Parameter estimation techniques for modal analysis. 1979.

[17] J.F. Cardoso. Blind signal separation: statistical principles. *Proceedings of the IEEE*, 86(10):2009–2025, 1998.

[18] M. Celebi. Seismic instrumentation of buildings (with emphasis on federal buildings). Technical Report No. 0-7460-68170, United States Geological Survey, 2002.

[19] M.N. Chatzis, E.N. Chatzi, and A.W. Smyth. An experimental validation of time domain system identification methods with fusion of heterogeneous data. *Earthquake Engineering & Structural Dynamics*, 44(4):523–547, 2015.

[20] A.K. Chopra. *Dynamics of structures: Theory and applications to earthquake engineering*. Pearson Education, Inc., 5th edition, 2017.

[21] H.A. Cole. On-line failure detection and damping measurement of aerospace structures by random decrement signatures. Technical Report NASA CR-2205, Nelson Engineering and Research Institute, Mountain View, California, 1973.

[22] H.A. Cole. On-the-line analysis of random vibrations. In *9th Structural Dynamics and Materials Conference*, page 288, Palm Springs, California, April 1968.

[23] P. Comon. Independent component analysis, a new concept? *Signal Processing*, 36(3):287–314, 1994.

[24] R. Crawford and H.S. Ward. Determination of the natural periods of buildings. *Bulletin of the Seismological Society of America*, 54(6A):1743–1756, 1964.

[25] A.K. Datta, M. Shrikhande, and D.K Paul. On the optimal location of sensors in multi-storeyed buildings. *Journal of Earthquake Engineering*, 6(01):17–30, 2002.

[26] I. Daubechies. *Ten Lectures on Wavelets*, volume 61. Society for Industrial and Applied Mathematics, 1992.

[27] I. Daubechies, J. Lu, and H.T. Wu. Synchrosqueezed wavelet transforms:An empirical mode decomposition-like tool. *Applied and Computational Harmonic Analysis*, 30(2):243–261, 2011.

[28] I. Daubechies and S. Maes. A nonlinear squeezing of the continuous wavelet transform based on auditory nerve models. *Wavelets in Medicine and Biology*, pages 527–546, 1996.

[29] S.W. Doebling, C.R. Farrar, M.B. Prime, and D.W. Shevitz. Damage identification and health monitoring of structural and mechanical systems from changes in their vibration characteristics: A literature review. Technical Report LA–13070-MS, Los Alamos National Laboratory, 1996.

[30] D.J. Ewins. *Modal Testing: Theory, Practice, and Application.* Research Studies Press, Hertfordshire, England, 2000.

[31] C.R. Farrar and S.W. Doebling. *Damage Detection and Evaluation II*, pages 345–378. Springer Netherlands, Dordrecht, 1999.

[32] C.R. Farrar and S.W. Doebling. An overview of modal-based damage identification methods. In *EUROMECH 365 International Workshop: DAMAS 97, Structural*

Damage Assessment Using Advanced Signal Processing Procedures, pages 269–278, Sheffield, UK, June, 1997.

[33] FEMA-356. Pre-standard and commentary for the seismic rehabilitation of buildings. *Federal Emergency Management Agency*, 2000.

[34] Z. Feng, X. Chen, and M. Liang. Iterative generalized synchrosqueezing transform for fault diagnosis of wind turbine planetary gearbox under nonstationary conditions. *Mechanical Systems and Signal Processing*, 52:360–375, 2015.

[35] A. Ghobarah, H. Abou-Elfath, and A. Biddah. Response-based damage assessment of structures. *Earthquake Engineering & Structural Dynamics*, 28(1):79–104, 1999.

[36] G. Ghosh and S. Ray-Chaudhuri. Location sensitivity of fundamental and higher mode shapes in localization of damage within a building. *Journal of Sound and Vibration*, 365:244–259, 2016.

[37] B. Hazra and S. Narasimhan. Wavelet-based blind identification of the UCLA Factor building using ambient and earthquake responses. *Smart Materials and Structures*, 19(2):025005, 2009.

[38] B. Hazra, A.J. Roffel, S. Narasimhan, and M.D. Pandey. Modified cross-correlation method for the blind identification of structures. *Journal of Engineering Mechanics*, 136(7):889–897, 2010.

[39] B. Hazra, A. Sadhu, A.J. Roffel, P.E. Paquet, and S. Narasimhan. Underdetermined blind identification of structures by using the modified cross-correlation method. *Journal of Engineering Mechanics*, 138(4):327–337, 2012.

[40] J. He and D.J. Ewins. Analytical stiffness matrix correction using measured vibration modes. *International Journal of Analytical and Experimental Modal Analysis*, 1(3):1–9, 1986.

[41] G. Hegde and R. Sinha. A technique for placing few sensors on a building for complete modal identification. *Mechanics of Advanced Materials and Structures*, 16(3):248–259, 2009.

[42] J. Herault and C. Jutten. Space or time adaptive signal processing by neural network models. In John S. Denker, editor, *Neural Networks for Computing*, volume 151, pages 206–211. AIP Publishing, 1986.

[43] R.H. Herrera, J. Han, and M. Van der Baan. Applications of the synchrosqueezing transform in seismic time-frequency analysis. *Geophysics*, 79(3):55–64, 2014.

[44] N.E. Huang, Z. Shen, S.R. Long, M.C. Wu, H.H. Shih, Q. Zheng, N.C. Yen, C.C. Tung, and H.H. Liu. The empirical mode decomposition and the hilbert spectrum for nonlinear and non-stationary time series analysis. In *Proceedings of the Royal Society of London A: Mathematical, Physical and Engineering Sciences*, volume 454, pages 903–995. The Royal Society, 1998.

[45] A. Hyvärinen. Complexity pursuit: Separating interesting components from time series. *Neural Computation*, 13(4):883–898, 2001.

[46] A. Hyvärinen and E. Oja. Independent component analysis: algorithms and applications. *Neural Networks*, 13(4-5):411–430, 2000.

[47] D. Iatsenko, P.V.E. McClintock, and A. Stefanovska. Linear and synchrosqueezed time–frequency representations revisited: Overview, standards of use, resolution, reconstruction, concentration, and algorithms. *Digital Signal Processing*, 42:1–26, 2015.

[48] S.R. Ibrahim. The experimental determination of vibration parameters from time responses. *The Shock and Vibration Bulletin.*, 46(5):187–196, 1976.

[49] S.R. Ibrahim. A method for the direct identification of vibration parameters from the free response. *The Shock and Vibration Bulletin*, 47:183, 1977.

[50] S.R. Ibrahim. Random decrement technique for modal identification of structures. *Journal of Spacecraft and Rockets*, 14(11):696–700, 1977.

[51] H. Imai, C.B. Yun, O. Maruyama, and M. Shinozuka. Fundamentals of system identification in structural dynamics. *Probabilistic Engineering Mechanics*, 4(4):162–173, 1989.

[52] G.H. James III, T.G. Carne, and J.P. Lauffer. The natural excitation technique (NExT) for modal parameter extraction from operating wind turbines. Technical Report SAND- 92-1666, Sandia National Labs., Albuquerque, NM (United States), 1993.

[53] J.N. Juang and R.S. Pappa. An eigensystem realization algorithm for modal parameter identification and model reduction. *Journal of Guidance, Control, and Dynamics*, 8(5):620–627, 1985.

[54] C. Jutten and J. Herault. Blind separation of sources, part I: An adaptive algorithm based on neuromimetic architecture. *Signal Processing*, 24(1):1–10, 1991.

[55] D.C. Kammer. Sensor placement for on-orbit modal identification and correlation of large space structures. *Journal of Guidance, Control, and Dynamics*, 14(2):251–259, 1991.

[56] J. Karhunen, A. Hyvarinen, R. Vigário, J. Hurri, and E. Oja. Applications of neural blind separation to signal and image processing. In *Acoustics, Speech, and Signal Processing, ICASSP-97*, volume 1, pages 131–134. IEEE, 1997.

[57] G. Kerschen, J. Golinval, A.F. Vakakis, and L.A. Bergman. The method of proper orthogonal decomposition for dynamical characterization and order reduction of mechanical systems: an overview. *Nonlinear Dynamics*, 41(1-3):147–169, 2005.

[58] G. Kerschen, F. Poncelet, and J.C. Golinval. Physical interpretation of independent component analysis in structural dynamics. *Mechanical Systems and Signal Processing*, 21(4):1561–1575, 2007.

[59] T. Kijewski and A. Kareem. Wavelet transforms for system identification in civil engineering. *Computer-Aided Civil and Infrastructure Engineering*, 18(5):339–355, 2003.

[60] T. Kijewski-Correa and A. Kareem. Efficacy of hilbert and wavelet transforms for time-frequency analysis. *Journal of Engineering Mechanics*, 132(10):1037–1049, 2006.

[61] T. Kijewski-Correa and A. Kareem. Performance of wavelet transform and empirical mode decomposition in extracting signals embedded in noise. *Journal of Engineering Mechanics*, 133(7):849–852, 2007.

[62] J.T. Kim and N. Stubbs. Model-uncertainty impact and damage-detection accuracy in plate girder. *Journal of Structural Engineering*, 121(10):1409–1417, 1995.

[63] P. Kisilev, M. Zibulevsky, and Y.Y. Zeevi. A multiscale framework for blind separation of linearly mixed signals. *Journal of Machine Learning Research*, 4(Dec):1339–1363, 2003.

[64] F. Kozin and H.G. Natke. System identification techniques. *Structural Safety*, 3(3-4):269–316, 1986.

[65] J. Lardies and S. Gouttebroze. Identification of modal parameters using the wavelet transform. *International Journal of Mechanical Sciences*, 44(11):2263–2283, 2002.

[66] C. Li and M. Liang. A generalized synchrosqueezing transform for enhancing signal time–frequency representation. *Signal Processing*, 92(9):2264–2274, 2012.

[67] C. Li and M. Liang. Time–frequency signal analysis for gearbox fault diagnosis using a generalized synchrosqueezing transform. *Mechanical Systems and Signal Processing*, 26:205–217, 2012.

[68] N.A.J. Lieven and D.J. Ewins. Spatial correlation of mode shapes, the coordinate modal assurance criterion (COMAC). In *Proceedings of the 6th International Modal Analysis Conference*, volume 1, pages 690–695, Orlando, FL, February 1988.

[69] T.W. Lim. Structural damage detection using constrained eigenstructure assignment. *Journal of Guidance Control and Dynamics*, 18(3):411–418, 1995.

[70] L. Ljung. System identification. In A. Procházka, J. Uhlíř, P.W.J. Rayner, and N.G. Kingsbury, editors, *Signal Analysis and Prediction*, pages 163–173. Birkhäuser Boston, Boston, MA, 1998.

[71] N.M.M. Maia. *Extraction of valid modal properties from measured data in structural vibrations*. PhD thesis, Imperial College London (University of London), 1988.

[72] L. Majumder and C.S. Manohar. A time-domain approach for damage detection in beam structures using vibration data with a moving oscillator as an excitation source. *Journal of Sound and Vibration*, 268(4):699–716, 2003.

[73] S. Makeig, A.J. Bell, T.P. Jung, and T.J. Sejnowski. Independent component analysis of electroencephalographic data. In *Advances in Neural Information Processing Systems*, pages 145–151, 1996.

[74] S.I. McNeill. An analytic formulation for blind modal identification. *Journal of Vibration and Control*, 18(14):2111–2121, 2011.

[75] S.I. McNeill and D.C. Zimmerman. A framework for blind modal identification using joint approximate diagonalization. *Mechanical Systems and Signal Processing*, 22(7):1526–1548, 2008.

[76] M. Mihalec, J. Slavič, and M. Boltežar. Synchrosqueezed wavelet transform for damping identification. *Mechanical Systems and Signal Processing*, 80:324–334, 2016.

[77] L.A Montejo and A.L Vidot-Vega. Synchrosqueezed wavelet transform for frequency and damping identification from noisy signals. *Smart Structures and Systems*, 9(5):441–459, 2012.

[78] H.A. Nasrellah and C.S. Manohar. Finite element method based monte carlo filters for structural system identification. *Probabilistic Engineering Mechanics*, 26(2):294–307, 2011.

[79] A.K. Pandey and M. Biswas. Damage detection in structures using changes in flexibility. *Journal of Sound and Vibration*, 169(1):3–17, 1994.

[80] A.K. Pandey, M. Biswas, and M.M. Samman. Damage detection from changes in curvature mode shapes. *Journal of Sound and Vibration*, 145(2):321–332, 1991.

[81] B. Peeters and G. De Roeck. Stochastic system identification for operational modal analysis: a review. *Journal of Dynamic Systems, Measurement, and Control*, 123(4):659–667, 2001.

[82] R. Peled, S. Braun, and M. Zacksenhouse. A blind deconvolution separation of multiple sources, with application to bearing diagnostics. *Mechanical Systems and Signal Processing*, 19(6):1181–1195, 2005.

[83] P.V. Pokharkar and M. Shrikhande. Structural health monitoring via stiffness update. *ISET Journal of Earthquake Technology*, 47(1):47–60, 2010.

[84] F. Poncelet. *Experimental Modal Analysis using Blind Source Separation Techniques*. PhD thesis, University of Liége, Place du 20 Août 7, 4000 Liége, Belgium, May 2010.

[85] F. Poncelet, G. Kerschen, J. C. Golinval, and D. Verhelst. Output-only modal analysis using blind source separation techniques. *Mechanical Systems and Signal Processing*, 21(6):2335–2358, 2007.

[86] N.H. Pontoppidan, S. Sigurdsson, and J. Larsen. Condition monitoring with mean field independent components analysis. *Mechanical Systems and Signal Processing*, 19(6):1337–1347, 2005.

[87] T.D. Popescu. Blind separation of vibration signals and source change detection–application to machine monitoring. *Applied Mathematical Modelling*, 34(11):3408–3421, 2010.

[88] C. Rainieri, G. Fabbrocino, and E. Cosenza. Some remarks on experimental estimation of damping for seismic design of civil constructions. *Shock and Vibration*, 17(4, 5):383–395, 2010.

[89] K. Roy and S. Ray-Chaudhuri. Fundamental mode shape and its derivatives in structural damage localization. *Journal of Sound and Vibration*, 332(21):5584–5593, 2013.

[90] A. Rytter. *Vibrational based inspection of civil engineering structures*. PhD thesis, Deptartment of Building Technology and Structural Engineering, Aalborg University, Denmark, April 1993.

[91] A. Sadhu and B. Hazra. A novel damage detection algorithm using time-series analysis-based blind source separation. *Shock and Vibration*, 20:423–438, 2013.

[92] A. Sadhu, B. Hazra, and S. Narasimhan. Blind identification of earthquake-excited structures. *Smart Materials and Structures*, 21(4):1–12, 2012.

[93] A. Sadhu, S. Narasimhan, and J. Antoni. A review of output-only structural mode identification literature employing blind source separation methods. *Mechanical Systems and Signal Processing*, 94:415–431, 2017.

[94] O.S. Salawu. Detection of structural damage through changes in frequency: a review. *Engineering Structures*, 19(9):718–723, 1997.

[95] O.S. Salawu and C. Williams. Bridge assessment using forced-vibration testing. *Journal of Structural Engineering*, 121(2):161–173, 1995.

[96] SAP 2000. *CSI Analysis Reference Manual*. Computers and Structures, Inc., Berkeley, California, USA, 2016.

[97] S.R. Shiradhonkar and M. Shrikhande. Seismic damage detection in a building frame via finite element model updating. *Computers & Structures*, 89(23–24):2425–2438, 2011.

[98] M. Shrikhande. Reconstruction of missing response data for identification of higher modes. *Earthquakes and Structures*, 2(4):323–336, 2011.

[99] M. Shrikhande. Reconstruction of missing response data for identification of higher modes. *Earthquakes and Structures*, 2(4):323–336, 2011.

[100] M. Shrikhande. *Finite Element Method and Computational Structural Dynamics*. PHI Learning Pvt. Ltd., New Delhi, 2014.

[101] D. Skolnik, Y. Lei, E. Yu, and J.W. Wallace. Identification, model updating, and response prediction of an instrumented 15-story steel-frame building. *Earthquake Spectra*, 22(3):781–802, 2006.

[102] F.R. Spitznogle and A.H. Quazi. Representation and analysis of time-limited signals using a complex exponential algorithm. *The Journal of the Acoustical Society of America*, 47(5A):1150–1155, 1970.

[103] W.J. Staszewski. Identification of damping in MDOF systems using time-scale decomposition. *Journal of Sound and Vibration*, 203(2):283–305, 1997.

[104] J.V. Stone. Blind source separation using temporal predictability. *Neural Computation*, 13(7):1559–1574, 2001.

[105] V.S. Sundar and C.S. Manohar. Random vibration testing with controlled samples. *Structural Control and Health Monitoring*, 21(10):1269–1283, 2014.

[106] G. Thakur, E. Brevdo, N.S. Fučkar, and H.T. Wu. The synchrosqueezing algorithm for time-varying spectral analysis: Robustness properties and new paleoclimate applications. *Signal Processing*, 93(5):1079–1094, 2013.

[107] M.D. Trifunac. Comparisons between ambient and forced vibration experiments. *Earthquake Engineering & Structural Dynamics*, 1(2):133–150, 1972.

[108] P. Van Overschee and B.L. De Moor. *Subspace Identification for Linear Systems: Theory– Implementation– Applications*. Springer Science & Business Media, 2012.

[109] H. Vold, J. Kundrat, G. Rocklin, and R. Russell. A multi-input modal estimation algorithm for mini-computers. *SAE Technical Paper*, (No.- 820194), 1982.

[110] W.M. West. Illustration of the use of modal assurance criterion to detect structural changes in an orbiter test specimen. In *Proceedings of 4th International Modal Analysis Conference*, volume 1, pages 1–6, Los Angeles, CA, 1986.

[111] H.T. Wu, P. Flandrin, and I. Daubechies. One or two frequencies? The synchrosqueezing answers. *Advances in Adaptive Data Analysis*, 03(01–02):29–39, 2011.

[112] J.N. Yang and Y. Lei. Identification of natural frequencies and damping ratios of linear structures via Hilbert transform and empirical mode decomposition. In *Proceedings of International Conference on Intelligent Systems and Control*, pages 310–315. Anaheim, 1999.

[113] J.N. Yang, Y. Lei, S. Pan, and N. Huang. System identification of linear structures based on Hilbert–Huang spectral analysis. Part 1: Normal modes. *Earthquake Engineering & Structural Dynamics*, 32(9):1443–1467, 2003.

[114] J.N. Yang, Y. Lei, S. Pan, and N. Huang. System identification of linear structures based on Hilbert–Huang spectral analysis. Part 2: Complex modes. *Earthquake Engineering & Structural Dynamics*, 32(10):1533–1554, 2003.

[115] Y. Yang and S. Nagarajaiah. Time-frequency blind source separation using independent component analysis for output-only modal identification of highly damped structures. *Journal of Structural Engineering*, 139(10):1780–1793, 2012.

[116] Y. Yang and S. Nagarajaiah. Blind modal identification of output-only structures in time-domain based on complexity pursuit. *Earthquake Engineering & Structural Dynamics*, 42(13):1885–1905, 2013.

[117] Y. Yang and S. Nagarajaiah. Structural damage identification via a combination of blind feature extraction and sparse representation classification. *Mechanical Systems and Signal Processing*, 45(1):1–23, 2014.

[118] Y. Yang and S. Nagarajaiah. Output-only modal identification by compressed sensing: Non-uniform low-rate random sampling. *Mechanical Systems and Signal Processing*, 56:15–34, 2015.

[119] C. Zang, M.I. Friswell, and M. Imregun. Structural damage detection using independent component analysis. *Structural Health Monitoring*, 3(1):69–83, 2004.

[120] W. Zhou and D. Chelidze. Blind source separation based vibration mode identification. *Mechanical Systems and Signal Processing*, 21(8):3072–3087, 2007.

[121] M.l. Zibulevsky and B. A. Pearlmutter. Blind source separation by sparse decomposition. In *Wavelet Applications VII*, volume 4056, pages 165–175. International Society for Optics and Photonics, 2000.

[122] D.C. Zimmerman and S.W. Smith. *Model refinement and damage location for intelligent structures*. Springer, Dordrecht, 1992.

List of Publications

International Journal

1. Kaloni, S. and Shrikhande, M. Output only system identification based on synchrosqueezed transform, Proceedia Engineering, 199, 1002-1007, 2017.

2. Kaloni, S. and Shrikhande, M. Blind Source Modal Identification via Synchrosqueezed Transform. (under review)

3. Kaloni, S. and Shrikhande, M. Estimation of Normal Modes via Synchrosqueezed Transform. (under review)

4. Kaloni, S. and Shrikhande, M. A Moving Window System for Seismic Damage Detection. (under review)

Conference

1. Kaloni, S. and Shrikhande, M., Damage detection in structural system via blind source separation, in Proceedings of 16^{th} World Conference in Earthquake Engineering January 9-13, 2017 Santiago Chile.

2. Kaloni, S. and Shrikhande, M., Blind source separation based system identification of earthquake excited structures, in Proceedings of 8^{th} ISSS National Conference on MEMS, Smart Materials, Structures and Systems, September 28–30, 2016, Indian Institute of Technology Kanpur, 2016.

3. Kaloni, S. and Shrikhande, M., Seismic Damage Detection Using Blind Source Separation. (to be presented in 16th Synposium on Earthquake Engineering).